Vav1 Controls the Stability and Function of SLP-76 Containing Signaling Microclusters

A thesis submitted by

Nicholas Sylvain

In partial fulfillment of the requirements for the degree of

Doctor of Philosophy in

Immunology

Tufts University

Sackler School of Graduate Biomedical Sciences

April 5, 2011

Advisor: Stephen C. Bunnell, Ph.D.

1 Abstract

Generation of productive immune responses requires T cell activation and differentiation into various effector and helper subsets. T cell activation is mediated by signaling events that originate at the T cell receptor (TCR) and result in the phosphorylation of several critical adapter and effector molecules. These early signaling events result in the formation of multisubunit structures known as SLP-76-containing signaling microclusters (SLP-76 MC). These SLP-76 MC are the structures responsible for T cell signaling; their formation and persistence are closely linked with productive T cell signaling. I propose that SLP-76 MC perform two functions to facilitate T cell activation. First, they act as a central 'hub' where enzymes contact and act upon their substrates. Recruiting these proteins to a common location increases access to substrates and the efficiency with which they are activated. Second, they act as molecular adhesion points that connect the T cell receptor to the cytoskeleton. Interaction with the cytoskeletal machinery increases the efficiency with which SLP-76 MC are formed and provides a mechanism to explain the centralized movement of SLP-76 MC. To gain further insight into the structure and function of SLP-76 MC, I have analyzed a critical component of the microcluster: the Rho family guanine-nucleotide exchange factor (GEF) Vav1.

Here, I show that Vav1 is recruited to the N-terminal tyrosines of SLP-76 and is required for the structural stability of the microcluster. Vav1 possesses a C-terminal cassette composed of Src homology (SH) domains that directs recruitment into SLP-76 MC and contributes to multivalent interactions that are required for microcluster persistence.

However, these domains are insufficient to mediate microcluster persistence, indicating that the N-terminal domains of Vav1 also make structural contributions. Consistent with a model in which the microcluster is a hub of enzymatic activity, Vav1 recruitment to SLP-76 MC is required for its phosphorylation and activation. In turn, Vav1 also acts on downstream GTPases within microclusters. The enzymatic GEF activity of Vav1, while not required for structural stabilization of microclusters, acts as a downstream effector required for full T cell activation. In addition, I show that the N-terminal domains, which are associated with regulating the enzymatic activity of Vav1, are required to link Vav1 to the translocation machinery of the cell and allow SLP-76 MC to act as attachment points between the TCR and cytoskeleton. I conclude that Vav1 mediates T cell activation by increasing SLP-76 MC persistence and function through multiple non-catalytic scaffolding interactions. Analysis of this critical SLP-76 MC component has revealed novel aspects of how SLP-76 MC mediate T cell activation.

2 List of Figures

3 List of Abbreviations

ADAP	Adhesion and Degranulation promoting Adaptor Protein
APC	Antigen Presenting Cell
CH	Calponin Homology
CRAC	Calcium Release Activated Calcium channel
CTL	Cytotoxic T lymphocyte
CTLA-4	Cytotoxic T-lymphocyte antigen
DAG	Diacylglycerol
Dbl	Diffuse B cell Leukemia
DH	Dbl Homology
DSP	Dithiobis[succinimidyl propionate]
EGFP	Enhanced Green Fluorescent Protein
GADS	GRB2 related Adapter Downstream of SHC
GEF	Guanine Nucleotide Exchange Factor
GRB2	Growth factor Receptor Bound protein 2
IP3	Inositol trisphosphate
ITAM	Immunoreceptor Tyrosine Activation Motif
ITK	IL-2 Inducible T cell Kinase
LAT	Linker of Activation in T cells
MC	Microcluster
MOT	Maximum Over Time
MTOC	Microtubule Organizing Center
mCFP	Monomeric Cyan Fluorescent Protein
mYFP	Monomeric Yellow Fluorescent Protein
NFAT	Nuclear Factor of Activated T cells
PH	Pleckstrin Homology
PI3K	Phosphatidylinositol 3 Kinase
PIP	Phosphatidyl Inositol Phosphate
PKC	Protein Kinase C
PLC	Phospholipase C
PMA	Phorbol 12-Myristate 13-Acetate
pMHC	Peptide-Major Histocompatibility Complex
PTEN	Phosphatase and Tensin Homologue
ROI	Region of interest
scFv	single chain variable fragment
SH	Src Homology
SHIP	SH2-domain containing Inositol pholyphosphate 5’ Phosphatase
SLP-76	SH2-containing Lymphocyte Protein of 76 kDa
SMAC	Supra-Molecular Activation Complex
TCR	T Cell Receptor
WB	Western Blot
ZAP-70	Zeta-Associated Protein of 70 kDa

Table of Contents

Vav1 Controls the Stability and Function of SLP-76 Containing Signaling Microclusters

4 Introduction

T cells of the immune system play a critical role in mediating host defense against pathogens. During the course of an immune response, the T cell will receive a variety of signals from the environment that will determine its activation status and function. The signaling machinery within the T cell is essential for interpreting signals from the environment and converting signals of varying affinity into discrete functional outcomes. Elucidating the molecular mechanisms that control T cell signaling and activation is critical to our understanding of the immune system.

4.1 T Cell Activation in the Immune Response

4.1.1 T cell activation

Circulating naïve T cells must first become activated in order to participate in the immune response. This activation is required for the many effector subtypes, such as $CD8^+$ cytotoxic T lymphocytes (CTLs), $CD4^+$ T helper (Th) cells, and pro-inflammatory Th17 cells, to coordinate immune responses. In addition, long-lived memory T cells are also generated, which confer protection from subsequent challenge with the same antigen [Wange and Samelson 1996]. In a physiological setting, T cell activation is accomplished by the interaction of the T cell with an antigen-presenting cell (APC) in secondary lymphoid organs. These APCs present foreign and self-peptides in the context of endogenous Major Histocompatibility (MHC) molecules. Upon recognizing its cognate peptide in the context of MHC (pMHC), the T cell receptor (TCR) binds and initiates a cascade of signaling events. TCR-mediated signals are critical for T cell

activation and induce multiple phosphorylation events that result in the generation of second messengers (discussed in detail in Section 4.6). These early signaling events lead to transcription factor activation and the transcription of genes required for proliferation and cytokine production. In addition, activation induces many changes in T cell behavior that do not depend on transcription factors, such as altering cell polarity, morphology, and migration. In the absence of appropriate T cell activation, immunodeficiency can result, indicating the critical role that these events play in the maintenance of host health.

4.1.2 Balance of signaling in health and disease

Signaling events initiated at the TCR are critical for the generation of productive immune responses that protect the host from pathogens. However, termination of T cell signaling is also required to prevent damage to the host. Uncontrolled immune responses can result in a myriad of autoimmune diseases, while ineffective signaling results in immunodeficiency [Goodnow, Sprent et al. 2005]. For this reason, a balance of T cell activation and inhibition must be maintained and several mechanisms exist to down modulate T cell responses. At the cell surface, inhibitory receptors and TCR internalization both contribute to the down modulation of TCR signaling. The inhibitory receptor cytotoxic T-lymphocyte antigen-4 (CTLA-4) is expressed on the cell surface following TCR stimulation and competes with the costimulatory receptor CD28 for B7 ligands expressed on the surface of an APC [Rudd, Taylor et al. 2009]. In addition, TCR internalization and degradation is increased following TCR ligation and also serves to decrease T cell activation. Within the cell, activation of the TCR also triggers many mechanisms that will down modulate the TCR-induced activation [Acuto, Di Bartolo et al. 2008]. These mechanisms include dephosphorylation by phosphatases,

phosphorylation on inhibitory sites by kinases [Singer and Koretzky 2002; Veillette, Latour et al. 2002], or activation of ubiquitin ligases that can lead to protein degradation [Balagopalan, Barr et al. 2007]. However, these inhibitory mechanisms are not only active following T cell stimulation. Experiments which block inhibitors (phosphatases) with pharmacological agents result in activation of the T cell [Secrist, Burns et al. 1993]. This result suggests that inhibitory processes are always at work in a resting cell to counteract the basal activity of pro-activating kinases. In this way, T cell activation can be thought of as a shift in the homeostasis of a resting T cell.

4.2 T Cell Signaling in Development and Activation

4.2.1 TCR Ligation Drives T Cell Signaling

T cell activation is critically dependent upon ligation of the TCR. The salient feature of TCR interaction with pMHC is the half-life of the interaction between these molecules, which determines the fate of the T cell [Davis, Boniface et al. 1998]. The kinetic proofreading model (discussed in Section 4.7.1) suggests that the signaling machinery involved in ligand discrimination senses differences in TCR-pMHC dwell time of as little as 1 second [McKeithan 1995; Rabinowitz, Beeson et al. 1996]. Indeed, subtle differences in TCR-pMHC recognition result in distinct functional outcomes [Sloan-Lancaster and Allen 1996], indicating the importance of the dwell time of the TCR-pMHC complex.

Though the TCR must discriminate between foreign peptides, it must also be tolerant to self-peptides presented on endogenous MHC in order to minimize autoimmune reactions. Each T cell expresses a unique, antigen-specific TCR on its surface that is generated by

rearrangements at the DNA level. Though this process generates an immense array of specificities, it also introduces the possibility that the TCR will respond to self-peptide. Therefore, the T cell must maintain a delicate balance of recognizing endogenous MHC without being autoreactive to self-peptides presented within MHC molecules. In essence, the TCR must distinguish between self and non-self peptide ligands. This is accomplished by selection processes that occur in the thymus. Positive selection provides pro-survival signals to those T cells which possess TCRs that are weakly reactive to endogenous MHC molecules. In contrast, those T cells that react too strongly with self-peptides are deleted in the process of negative selection. These processes ensure that the surviving T cells are capable of recognizing self-MHC, while at the same time being minimally self-reactive.

4.2.2 Differential thresholds for TCR signaling throughout development

The same TCR molecule mediates both development and activation of the T cell. However, the outcome of stimulation with agonist (activating) or antagonist (non-activating) TCR ligands changes throughout the development of the T cell. Agonist peptides induce activation in mature T cells whereas they induce apoptosis in developing thymocytes [Hogquist, Jameson et al. 1994]. In addition, weak agonist peptides for double positive thymocytes lose their potential for stimulation as the T cell develops [Lucas, Stefanova et al. 1999]. These data indicate that there are different thresholds for signaling that are mediated by the developmental stage of the T cell. The signaling machinery within the cell determines the outcome of TCR ligation at various times in development. One critical component of this signaling machinery is the kinase ZAP-70

(Zeta-Associated Protein of 70 kDa), which becomes differentially activated at distinct stages of T cell maturity [Negishi, Motoyama et al. 1995].

4.3 Signaling occurs in the context of the immunological synapse

Biochemical assays have provided a wealth of information regarding the events of T cell signaling. However, these techniques provide limited spatial and temporal information regarding the behavior of molecules in individual, living cells. Imaging studies allow us to monitor events in real time and provide a useful complement to classical biochemical experiments.

4.3.1 Formation if the immunological synapse

Signaling in T cell development and activation requires contact between the T cell and an antigen presenting cell (APC). T cells must engage and communicate with APCs to convert external cues into discrete outcomes. The tight junction formed at the interface of a T cell and APC is known as the immunological synapse (IS) [Paul and Seder 1994]. T cell adhesion to the APC and immunological synapse formation are required to initiate and sustain T cell activation [Billadeau, Nolz et al. 2007].

Upon entering a lymph node, T cells will undergo a series of brief encounters with antigen-presenting dendritic cells (DCs), scanning for its cognate pMHC [Mempel, Henrickson et al. 2004]. Naïve T cells move rapidly through the lymph node, with a maximum speed of ~25 μm/min [Miller, Wei et al. 2003]. As these initial encounters are very brief, T cells must quickly scan the many pMHC molecules presented by the DC. The interaction of the TCR is extremely sensitive to its cognate pMHC and T cells can

coordinate responses to as few as 10 pMHC molecules [Irvine, Purbhoo et al. 2002]. If the TCR contacts its cognate pMHC molecule, the cell arrests and forms a more stable contact with the APC, resulting in the formation of the immunological synapse [Fooksman, Vardhana et al. 2009].

This tight contact between the T cell and APC provides a mechanism by which the T cell can scan and respond to pMHC on the APC. This adhesion is important for the T cell to receive costimulatory signals in addition to signals received through the TCR. In addition, imaging studies revealed that the T cell polarizes toward the antigen-presenting B cell [Kupfer and Dennert 1984]. This polarization orients the cell to allow for the directional secretion of cytokines or cytotoxic granules [Kupfer, Mosmann et al. 1991; Stinchcombe, Majorovits et al. 2006]. In addition, the cytoskeletal proteins involved in establishing cell polarity provide the framework for the recruitment of molecules that mediate adhesion or to transduce signals that are necessary for T cell proliferation and activation [Billadeau, Nolz et al. 2007]. Imaging studies that strive for accuracy must emulate this TCR:APC interaction, while making compromises that facilitate the visualization of TCR signaling.

4.3.2 Structure of the Supra-Molecular Activation Complex

Early imaging studies using murine CD4+ T cells and a B cell lymphoma as an APC revealed that signaling proteins rearrange within the immunological synapse to form a 'bulls-eye' structure known as a Supra-Molecular Activation Complex (SMAC) [Monks, Freiberg et al. 1998]. This highly ordered structure is composed of the central SMAC (cSMAC), which is enriched in TCR. Integrin and adhesion proteins surround this

region, forming the peripheral SMAC (pSMAC). A diagram of the SMAC structure is shown in Figure 1. Due to the highly ordered nature of the SMAC structure, it was originally hypothesized that this structure was required for T cell signaling. However, several lines of evidence suggest that the SMAC is not required for all aspects of T cell activation and may instead be a mechanism to down-regulate signals emanating from the TCR. First, fixed APCs are capable of stimulating T cells [Allen and Unanue 1984]. Such fixed APCs could not undergo the necessary cytoskeletal rearrangements to form the SMAC structure. Second, CD4 cells can become activated in the absence of SMAC formation [Balamuth, Leitenberg et al. 2001] and the kinetics of T cell activation do not match the kinetics of SMAC formation [Lee, Holdorf et al. 2002]. In addition, imaging studies using murine T cells and antigen-presenting dendritic cells (DCs) did not observe the formation of the canonical SMAC structure. Instead, upon contacting DCs, the majority of T cells formed multifocal synapses which were competent to induce calcium elevations [Brossard, Feuillet et al. 2005]. Third, single chain antibodies specific for MHC perturb continued signaling, but do not affect SMAC structure of T cells stimulated on lipid bilayers containing pMHC [Varma, Campi et al. 2006]. Fourth, several signaling proteins are internalized in the cSMAC in a ubiquitin-dependent manner [Balagopalan, Barr et al. 2007; Barr, Balagopalan et al. 2006] and the cSMAC is enriched in markers of lysosomal degradation [Varma, Campi et al. 2006]. Finally, augmented signaling responses were observed in systems in which SMAC formation was prevented. These systems include 1) cells deficient in CD2AP, a molecule required for receptor segregation into the SMAC structure, 2) preventing SMAC formation by using a physical barrier, and 3) preventing SMAC formation through the use of costimulatory ligands [Lee, Dinner et

al. 2003; Mossman, Campi et al. 2005; Nguyen, Sylvain et al. 2008]. These many pieces of evidence suggest that the SMAC is not required for every aspect of T cell signaling and may in fact be a structure that down modulates TCR signaling. Whether or not the SMAC structure forms, the immunological synapse serves as the active interface between the T cell and APC and creates polarity within the T cell, which mediates directed secretion of cytokines or cytotoxic granules [Yokosuka and Saito 2009].

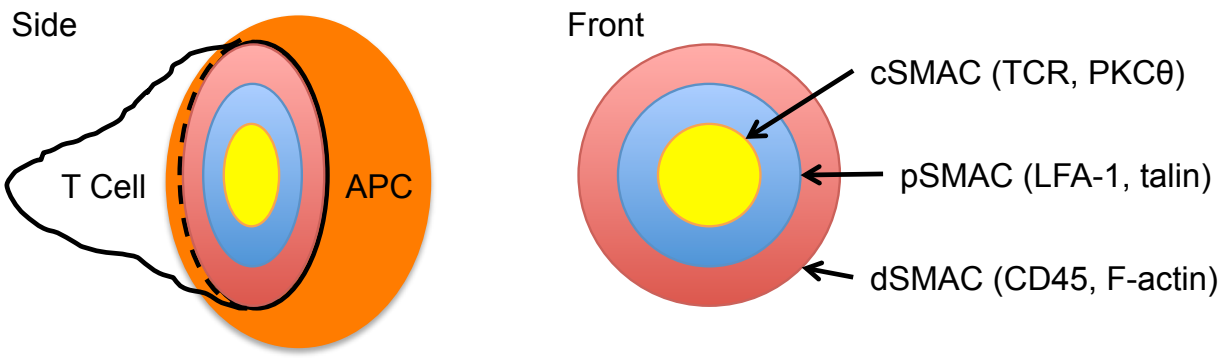

Figure 1: Supramolecular organization of the Immune Synapse (IS)

Side and front views of an Immune Synapse (IS) formed between a T cell and APC. In a mature synapse, three distinct supramolecular activation complexes (SMACs) are formed. The central SMAC (cSMAC – yellow) is enriched in TCR molecules as well as PKCθ. The peripheral SMAC (pSMAC – blue) contains adhesion molecules such as LFA-1. Finally the distal SMAC (dSMAC – red) is rich in F-actin and CD45. Although this is a highly ordered structure, evidence suggests that the SMAC is not required for T cell activation, contrary to the nomenclature. Figure adapted from [Dustin 2008].

4.4 The shifting paradigm: Signaling Microclusters

4.4.1 TCR Microclusters form in multifocal synapses

The discovery of multifocal immune synapses challenges the model that cSMAC formation is required for T cell activation. These immune synapses form multiple small, TCR-rich contacts which are distributed throughout the contact between a T cell and APC [Krummel and Davis 2002]. In addition, these TCR-rich zones are formed within areas of close adhesion between the T cell and either an artificial stimulatory surface or an APC [Grakoui, Bromley et al. 1999; Krummel, Sjaastad et al. 2000]. Analogous TCR rich structures have been observed across different artificial stimulatory surfaces as well as in T cell-APC conjugates [Campi, Varma et al. 2005; Lee, Holdorf et al. 2002; Yokosuka, Sakata-Sogawa et al. 2005]. These structures were found to be highly enriched in phosphotyrosine and to associate with the kinase ZAP-70, suggesting their importance in TCR-induced signal transduction.

Several lines of evidence suggest that the dispersed, TCR-rich clusters formed within multifocal synapses are competent to induce T cell activation. First, these TCR microclusters formed prior to the consolidation of the cSMAC and were competent to induce calcium elevations [Bunnell, Hong et al. 2002]. In addition, critical events for T cell activation, such as LAT (Linker of Activation in T cells) phosphorylation, DAG (diacyl glycerol) production, and calcium flux were observed to occur within the window of time dictated by individual pMHC recognition events [Bunnell, Hong et al. 2002; Huse, Klein et al. 2007]. Furthermore, inhibition of actin polymerization blocked the formation of new microclusters without disrupting the structure of the cSMAC.

However, when microcluster formation was prevented in this manner, calcium signaling was also inhibited [Varma, Campi et al. 2006]. These data showed that signaling microclusters are the structures responsible for initiating and maintaining TCR signaling, not the cSMAC.

4.4.2 SLP-76 MC are the sites of TCR signaling

Biochemical studies have established that the formation of a signaling complex containing LAT, Gads (Grb2 related Adapter downstream of SHC), and SLP-76 (SH2-domain containing Lymphocyte Protein of 76 kDa) is important to transduce TCR signals. Imaging studies have confirmed that each of these proteins is rapidly and continuously recruited into peripheral microclusters comparable in size to TCR microclusters [Bunnell, Hong et al. 2002; Bunnell, Singer et al. 2006]. Furthermore, the initiation of calcium elevations ~15 s following TCR microcluster formation [Bunnell, Hong et al. 2002] indicates that these proteins must be activated in a comparable time frame because they are required to generate calcium flux. In contrast to the SMAC, the formation of microclusters containing the adapter SLP-76 (SLP-76 MC) is temporally correlated with markers of T cell activation such as calcium flux.

Several lines of evidence suggest that SLP-76 MC are the structures responsible for TCR-mediated signaling. First, they form adjacent to the TCR [Douglass and Vale 2005; Nguyen, Sylvain et al. 2008; Yokosuka, Sakata-Sogawa et al. 2005]. Second, they are enriched in phosphotyrosine induced following TCR ligation [Bunnell, Hong et al. 2002; Nguyen, Sylvain et al. 2008]. Third, their formation and persistence are perfectly correlated with T cell activation [Bunnell, Singer et al. 2006; Yokosuka, Sakata-Sogawa

et al. 2005]. These many lines of evidence strongly suggest that SLP-76 MC are the structures that drive TCR-mediated signaling.

Upon contacting a stimulatory surface, SLP-76 microclusters form throughout the zone of contact. In various imaging systems, SLP-76 MC that form in the periphery display centripetal movement in the plane of contact between the cell and stimulatory surface. The SLP-76 MC accumulate in the center of the contact to form a structure reminiscent of the TCR-rich cSMAC. The significance and exact mechanism for this movement remain unknown. However, halting the inward movement of SLP-76 MC with a physical barrier increases intracellular calcium flux [Mossman, Campi et al. 2005]. In addition, the enzymatic activity of Cbl, a ubiquitin ligase which antagonizes TCR signaling, was required for their inward movement and internalization [Balagopalan, Barr et al. 2007], indicating that movement may be a mechanism of down-regulating T cell signaling. Furthermore, ligation of costimulatory integrin receptors prevents the inward movement and retains SLP-76 MC in the periphery, where they remain enriched in phosphotyrosine for longer periods of time [Nguyen, Sylvain et al. 2008]. This study also revealed that SLP-76 MC are formed adjacent to the TCR, in close proximity to their upstream kinase. The inward movement of SLP-76 MC could therefore be a mechanism to move microcluster components away from their upstream kinases, thereby down regulating T cell signaling. Although microcluster movement and persistence track together and are predictive of effective signaling, the results described above indicate that movement cannot be required for activation. Instead, microcluster movement is correlated with events that are important for activation. One such event could be the tethering of

microcluster components to the actin meshworks, since the formation of microclusters require dynamic actin rearrangements and costimulatory signals which slow retrograde actin flow also slow the inward flow of microclusters [Nguyen, Sylvain et al. 2008; Varma, Campi et al. 2006]. The formation of SLP-76 MC within zones of tight adhesion (multifocal synapses) is shown in Figure 2.

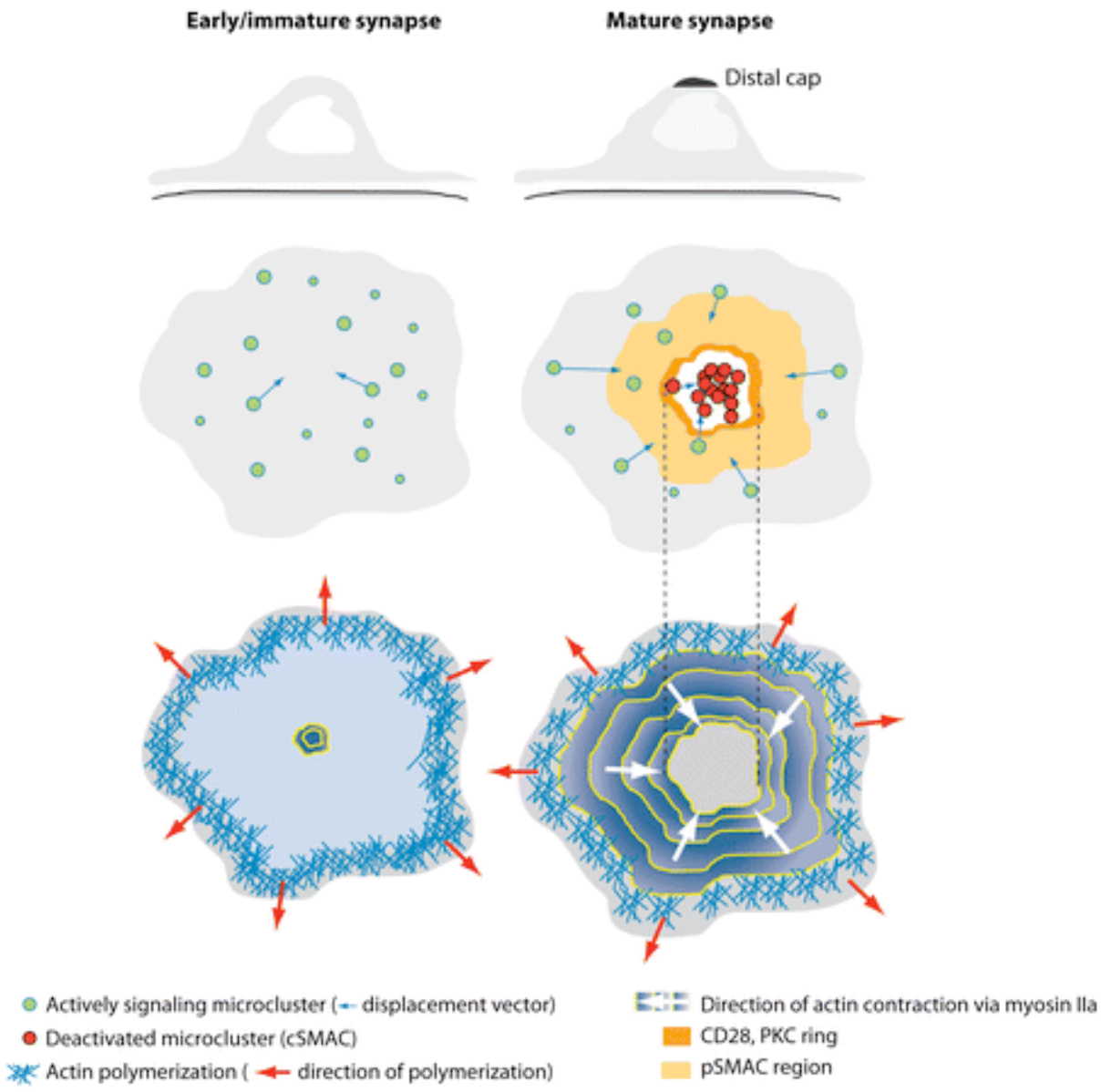

Figure 2: Signaling microcluster formation within multifocal synapses

In the early synapse, actin polymerization radiates outward from the center of the contact. Signaling microclusters that are competent to transduce signals form throughout the contact within zones of tight adhesion and migrate toward the center of the cell contact. In the mature synapse, these microclusters become inactivated and form the cSMAC structure. New microclusters are continuously formed in the periphery and migrate toward the center of the contact. **Top panels**: side view of a T cell responding to a stimulatory surface. **Middle and bottom panels**: en face view of the multifocal synapse. Figure adapted from [Fooksman, Vardhana et al. 2009].

4.5 Model Systems for Imaging T cell Activation

Signal transduction relies on the dynamic interaction of many adapters and effectors. These interactions lead to critical post-translational modifications, such as phosphorylation, that are required for signal transmission. Biochemical experiments have elucidated many aspects of the cell signaling machinery. In addition, live cell imaging assays are able to capture dynamic interactions in real time and are a useful complement to classic biochemical experiments. Using these tools to complement one another elucidates the earliest events of T cell signaling.

4.5.1 The Jurkat Model system

The Jurkat human leukemic model system has proven to be an invaluable tool for elucidating the mechanism of T cell signaling since the 1980s [Abraham and Weiss 2004]. Studies involving Jurkat T cells have examined the structure of the TCR:CD3 complex, calcium flux, and protein tyrosine kinases [Meuer, Fitzgerald et al. 1983]. Jurkat T cells are deficient in two lipid phosphatases, phosphatase and tensin homologue (PTEN) and SH2-domain-containing inositol polyphosphate 5' phosphatase (SHIP) [Astoul, Edmunds et al. 2001; Shan, Czar et al. 2000; Wang, Gjorloff-Wingren et al. 2000]. The loss of PTEN leads to constitutive activation of the PI3K pathway and the accumulation of PIP3 within the cell, which can complicate studying proteins within this pathway, such as AKT or ITK. However, the use of Jurkat T cells carries a number of advantages. Jurkat cells are relatively easy to culture and transfect and a number of mutant cell lines have been derived which are defective in a wide variety of signaling proteins have been created and characterized. Of particular interest to our work is the generation of a Vav1 deficient Jurkat cell line by targeted gene disruption [Cao, Janssen

et al. 2002]. In addition, disruptions of many signaling proteins can lead to blocks in T cell development, which hinders study of the functions of these proteins in mature T cells. The ability to perform knockdown of specific proteins eliminates the risk that the absence of these proteins may have triggered compensatory mechanisms in an *in vivo* system. Most importantly, these cells display remarkable, well-established predictive power. Many of our advances in TCR signaling were established in the Jurkat model system and they continue to be useful in dissecting T cell signaling pathways [Abraham and Weiss 2004]. Like *in vivo* mouse systems, the Jurkat model system is a useful tool for assaying TCR signal transduction.

4.5.2 Different stimulatory systems yield similar results with respect to microcluster behavior

Direct cell-cell contact between a T cell and an APC is a critical feature of T cell activation *in vivo*. However, the interaction of a T cell with an APC is a highly dynamic process, which is extremely difficult to capture in real time at high resolution. For this reason, many current live-cell imaging assays employ an artificial stimulatory surface, which simulates an APC. These model systems restrict the T cell contact to a two-dimensional plane that is both easily imaged using various types of microscopy and allows for the capture of high resolution (200 nm) images of the T cell interface in the *xy* plane. In addition, the user determines the composition of the stimulatory surface, allowing the contributions of various molecules to be observed. Two main model systems are currently in use: the lipid bilayer system and the antibody coated coverglass system. These systems are compared and contrasted below.

In the planar bilayer model, a synthetic phospholipid bilayer, which represents the surface of a eukaryotic cell, is deposited on a silica surface. Surface molecules such as pMHC and ICAM-1 are anchored in a lipid bilayer through glycosylphosphatidylinositol (GPI) linkage. These molecules replicate aspects of the *in vivo* immunological synapse, including integrin ligands and peptide presentation in the context of MHC. Although this system allows mobility of the molecules within the lipid bilayer, it does not fully replicate the conditions present in a physiological setting. This is because surface molecules are not freely diffusible within the plasma membrane, but are tethered to the actin cytoskeleton [Chen, Chen et al. 2007; Treanor, Depoil et al. 2010]. In addition, not every protein present on the surface of an APC is present in the lipid bilayer. For these reasons, the segregation of signaling molecules within the immunological synapse may not reflect the physiological setting.

The studies performed in this thesis employ the antibody coated coverglass system. In this system, anti-TCR antibodies are non-covalently immobilized on the coverglass and stimulate the TCR of responding T cells. The coverglass may also be coated with integrin ligands or antibodies against other T cell surface proteins. This system carries the additional advantage that it is easy to set up and requires minimal preparation. Like the planar bilayer system, this system also has drawbacks. Although many ligands within the surface of the APC are tethered to the actin cytoskeleton [Chen, Chen et al. 2007; Rozdzial, Pleiman et al. 1998], they are mobile during the course of the T cell:APC interaction. The antibody coated coverglass system is unable to replicate this mobility, as the stimulatory ligands are immobilized on the coverglass. Finally, the affinity of anti-

TCR antibodies for the TCR is greater than that of pMHC. Therefore, issues of ligand affinity cannot be addressed in this system.

Both model systems carry the caveat that they do not replicate the physiological T cell:APC interaction with perfect accuracy. The coverglass and planar bilayer model systems differ in the mobility of their stimulatory ligands; those in the coverglass system are immobilized to the surface and those in the planar bilayer system are freely diffusible in two dimensions. This represents two extremes of mobility of molecules within the immunological synapse. The conditions found within the physiological T cell:APC interface most likely fall between these two systems. The TCR is able to move within the plasma membrane, though it is not freely diffusible, as the TCR is also tethered to the actin cytoskeleton [Rozdzial, Pleiman et al. 1998]. Both these model systems restrict the T cell:APC interface to a two-dimensional plane that is easily amenable to real-time live cell imaging. Despite the differences in the affinity and mobility of the TCR ligands employed in each case, many similarities exist in these two systems. Independent labs working with different model systems have arrived at the same conclusions regarding: the formation of distinct TCR and ZAP-70 containing microclusters [Bunnell, Hong et al. 2002; Campi, Varma et al. 2005], the exclusion of the phosphatase CD45 from TCR microclusters [Bunnell, Hong et al. 2002; Varma, Campi et al. 2006], the speed with which scaffolds and effectors are recruited to the microcluster [Bunnell, Hong et al. 2002; Huse, Klein et al. 2007], the ligand densities required to support microcluster formation [Nguyen, Sylvain et al. 2008; Varma, Campi et al. 2006; Yokosuka, Sakata-Sogawa et al. 2005], the segregation of microclusters containing TCR and ZAP-70 from those

containing CD2, LAT, and SLP-76 [Douglass and Vale 2005; Kaizuka, Douglass et al. 2009; Lillemeier, Pfeiffer et al. 2006; Nguyen, Sylvain et al. 2008; Yokosuka, Sakata-Sogawa et al. 2005], and the speed and directional movement of molecules within the immunological synapse [Liu, Purbhoo et al. 2010; Nguyen, Sylvain et al. 2008; Yokosuka, Sakata-Sogawa et al. 2005]. Based on these extensive similarities, there is no reason to dismiss either model system based on its past predictive power. Although the ligand size and half-life of interaction with the TCR play important roles in T cell activation, these imaging data indicate that the mobility, affinity, and size of the TCR ligand play small roles at the level of the microcluster. A diagram of the imaging system used in this work is shown in Figure 3.

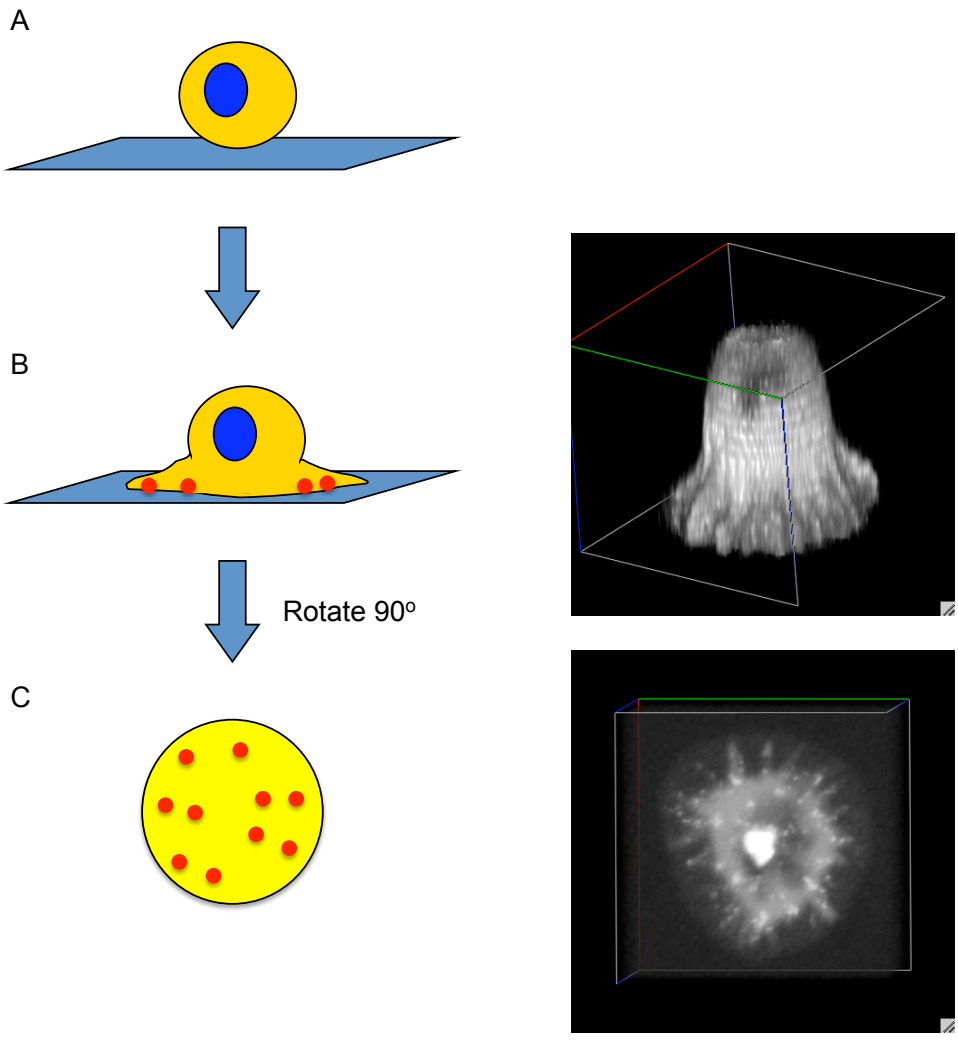

Figure 3: Planar stimulatory imaging assay

Jurkat T cells are stimulated on glass coverslips coated with 3 µg/ml anti-CD3ε antibodies (OKT3). This stimulatory surface approximates the surface of an APC and restricts the interaction with the T cell to a 2-dimensional plane amenable to imaging studies. For each step in this process, a simplified cartoon diagram is shown on the left and a 3D reconstruction of a Jurkat T cell expressing YFP-tagged SLP-76 (SLP-76.YFP) is shown on the right. **A -** Upon contacting the stimulatory surface, the cell will adhere and spread. **B -** SLP-76 MC (red dots in cartoon) form throughout the area of contact between the glass and the cell. These microclusters are laterally mobile and migrate within the 2D plane of contact between the cell and stimulatory surface. **C –** for imaging assays, the 2D plane of contact between the glass and the cell is observed. SLP-76 MC form throughout the area of contact and accumulate in the center of this region.

4.6 Signaling Events within SLP-76 MC Control T cell Activation

4.6.1 The TCR Complex

Combining imaging and traditional biochemical approaches has given us a more complete understanding of the events leading to T cell activation. These signaling events are initiated at the TCR. The TCR is expressed as a heterodimer of αβ or γδ, with TCRαβ being more common and well-studied. However, the TCR possesses only a short cytoplasmic segment that is incapable of transmitting extracellular signals to the inside of the cell; the CD3 complex accomplishes this function. The TCR interacts non-covalently with the CD3 complex, composed of εδ and εγ heterodimers, and a ζζ homodimer. This association is required for the TCR to be expressed on the surface of the cell. Signal transmission is accomplished by Immunoreceptor Tyrosine-based Activation Motifs (ITAMs) present in the intracellular portion of CD3. Upon TCR ligation, the Src family kinases Lck and Fyn phosphorylate the ITAMs of CD3, which then serve as docking sites for other signaling proteins. In the context of the TCR:CD3 complex, the TCR provides antigen specificity, while CD3 provides signaling capability.

Following phosphorylation of ITAMs by Src family kinases, ZAP-70 is recruited to CD3 zeta through its tandem SH2 domains, which bind phosphorylated tyrosine residues. Following recruitment to CD3, ZAP-70 becomes phosphorylated by Src family kinases. This phosphorylation activates ZAP-70 and potentiates its own kinase activity. Together, the TCR and ZAP-70 form the TCR microcluster, which is assembled adjacent to and separate from SLP-76 containing microclusters [Nguyen, Sylvain et al. 2008].

4.6.2 Signaling events from the TCR to transcription factor activation

Following its activation, ZAP-70 phosphorylates the adapter LAT on several residues, creating docking sites for several adapters and effectors, such as Grb2 and Gads [Zhang, Trible et al. 2000]. The critical adapter SLP-76 is also recruited to LAT through its constitutive association with Gads. Imaging studies have confirmed that these proteins are indeed recruited into microcluster structures [Bunnell, Singer et al. 2006; Houtman, Yamaguchi et al. 2006]. Once SLP-76 is recruited to LAT, the kinase ZAP-70 phosphorylates SLP-76 on tyrosines 112, 128, and 145, creating docking sites for effector proteins that mediate calcium flux and cytoskeletal reorganization: Nck, Vav, and Itk. In addition, the effector molecule PLCγ also binds to SLP-76, placing it in close proximity to its kinase Itk. Phosphorylation of PLCγ is a critical event in TCR signaling as it potentiates the phospholipase activity of this protein and is a critical event in the generation of intracellular calcium flux. Consistent with the role of the SLP-76 MC in generating calcium responses [Bunnell, Hong et al. 2002], these microclusters were also shown to contain PLCγ [Braiman, Barda-Saad et al. 2006].

Once activated by Itk, PLCγ cleaves PIP2 (Phosphatidyl Inositol 4,5 bis-Phosphate) in the membrane, forming IP3 (Inositol trisphosphate) and DAG (diacyl glycerol). IP3 and DAG will initiate separate signaling cascades that culminate in the activation of transcription factors and gene expression. IP3 binds to the IP3 receptor (IP3R) present in the ER and induces the release of stored calcium. Calcium binds to calmodulin, which in turn activates calcineurin. Calcineurin then dephosphorylates NFAT family transcription factors in the cytoplasm, allowing it to translocate to the nucleus and mediate gene

transcription [Macian 2005]. The second product of PLCγ activity, DAG leads to Ras activation through RasGRP. Son of Sevenless (SOS), which is the major activator of Ras, is also recruited to the signaling complex through its association with Grb2 [Houtman, Yamaguchi et al. 2006]. Activated Ras initiates a MAPK cascade that results in the sequential activation of Raf, MEK, and Erk.

DAG production also leads to the translocation of PKCθ to the plasma membrane and its activation by PDK1, which results in activation of the transcription factor NF-κB. In resting cells, NF-κB dimers are inactivated by association with IκB (Inhibitor of NF-κB). Following PKC-θ activation downstream of ZAP-70, the IκB Kinase (IKK) complex is activated through CARMA1 (CARD (caspase-recruitment domain)-MAGUK (membrane-associated guanylate kinase) protein 1), BCL-10 (B-cell lymphoma 10), and MALT1 (mucosa-associated lymphoid-tissue lymphoma translocation gene 1). The activated IKK complex will then phosphorylate IκB, leading to its degradation and the release of NF-κB. Once free, NF-κB dimers translocate to the nucleus where they bind their cognate DNA-binding sites and induce gene transcription [Siebenlist, Brown et al. 2005].

In addition to PLCγ1, several Guanine nucleotide exchange factors (GEFs) bind to SLP-76 and other microcluster components. One such GEF, Vav1, activates Rac and Cdc42 [Crespo, Schuebel et al. 1997]. Activation of these GTPases leads to the activation of the MAPK cascades culminating in the activation of p38 and JNK. Phosphorylated Jun, together with Fos, forms the transcription factor AP-1. Activated transcription factors

will then induce transcription of genes required for T cell activation. In addition, activation of GTPases such as Rac and Cdc42 is required for the activity of the proteins WAVE2 and WASP, respectively. These proteins then modulate cytoskeletal reorganization that is required for T cell activation [Billadeau, Nolz et al. 2007]. A summary of these signaling events is depicted in Figure 4.

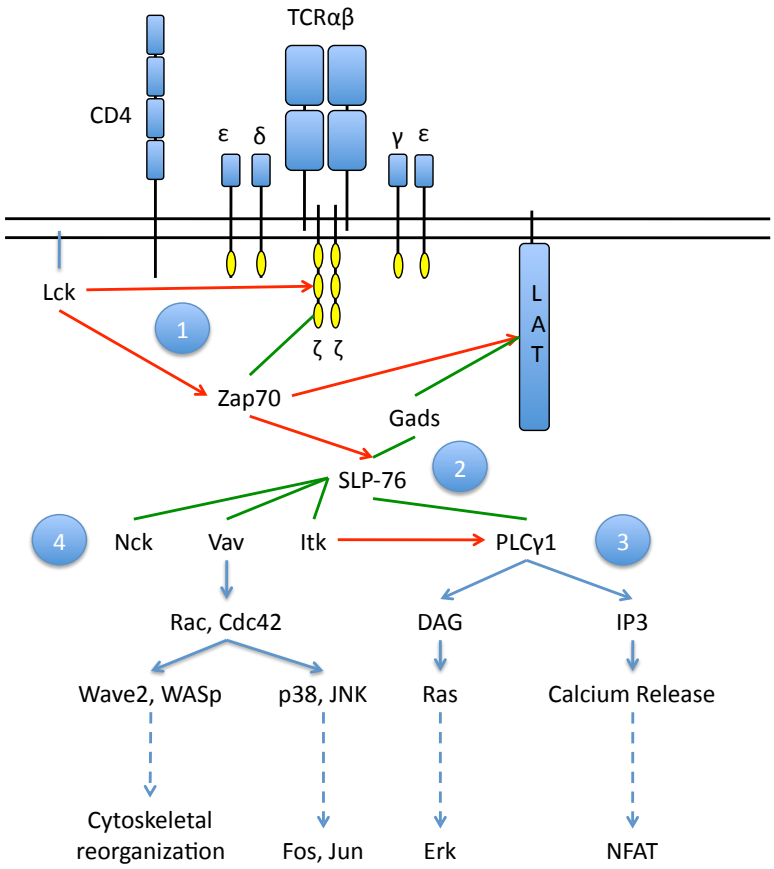

Figure 4: The TCR complex and proximal signaling events

TCR signaling begins with ligation of the αβ TCR with its cognate peptide-MHC. **1)** This results in the activation of Src family kinases such as Lck, which phosphorylate ITAMs present on CD3 zeta chains (phosphorylation is shown by red arrows). ZAP-70 is then recruited to CD3 through its tandem SH2 domains (protein-protein interactions are shown by green lines), where it phosphorylates several critical tyrosine residues on LAT. **2)** The adapters Gads and SLP-76 are recruited to phosphorylated LAT, where they become phosphorylated by ZAP-70. This creates docking sites for additional adapters and effectors. **3)** PLCγ1 is recruited to SLP-76 where it is phosphorylated by Itk, which also binds SLP-76. Phosphorylated PLCγ1 then cleaves PIP2 present in the cell membrane to form IP3 and DAG, which go on to mediate MAPK signaling and transcription factor activation. **4)** The Rho family GEF Vav1 is also recruited to SLP-76. Vav1 activates GTPases that mediate cytoskeletal reorganization as well as transcription factor activation.

4.6.3 SLP-76 MC as platforms for the recruitment of signaling molecules

The exact composition of SLP-76 MC remains unknown. However, in addition to LAT, Gads and SLP-76, they are known to include SOS1, Vav1, Nck, WASP, and PLCγ1 [Barda-Saad, Braiman et al. 2005; Braiman, Barda-Saad et al. 2006; Bunnell, Singer et al. 2006; Douglass and Vale 2005; Houtman, Yamaguchi et al. 2006]. This list of molecules encompasses both adapter proteins and effectors whose activity is critical for T cell activation. Adapters such as SLP-76, Gads, and Grb2 provide protein-protein interactions that maintain the structural integrity of the microcluster. In the absence of these interactions, persistent, long-lived SLP-76 MC do not form. In the absence of persistent microcluster formation, T cell activation is likewise inhibited [Bunnell, Singer et al. 2006; Houtman, Yamaguchi et al. 2006]. These data suggest that the formation of stable, persistent microclusters is a prerequisite for downstream TCR-mediated signaling.

The adapter proteins recruited into SLP-76 MC provide docking sites for effectors such as PLCγ1, Itk, and Vav1 [Beach, Gonen et al. 2007; Dombroski, Houghtling et al. 2005]. These effectors are involved in activation of GTPases required for cytoskeletal reorganization and generation of second messengers. Itk phosphorylates and activates PLCγ1; however, mutations that reduce microcluster persistence also reduce this phosphorylation [Bunnell, Singer et al. 2006; Gonen, Beach et al. 2005]. Given these data, I propose the SLP-76 microcluster can serve as platforms for the recruitment of downstream signaling proteins. Moreover, the recruitment of these proteins to one location facilitates their activation and increases accessibility to their target proteins. In

essence, the microcluster acts as a 'hub' for the recruitment and efficient activation and activity of effector proteins.

4.6.4 Persistence and movement of SLP-76 MC requires association with cytoskeleton

Though protein-protein interactions are critical for the structural integrity of the SLP-76 MC, interactions with the cytoskeleton also play a crucial role in the formation, persistence, and movement of these structures. In addition, the cytoskeleton provides the framework for mediating cellular adhesion, migration, and architecture. New microclusters are formed within the lamellipodium, a region at the leading edge of the cell that is enriched in branched actin networks [Bunnell, Hong et al. 2002; Varma, Campi et al. 2006]. Dynamic rearrangement of the cytoskeleton is not only required for the formation of SLP-76 MC, but also for their movement. In the absence of retrograde actin flow, the inward movement of TCR microclusters is prevented. This movement requires actin polymerization as well as the activity of the motor protein myosin IIa [Ilani, Vasiliver-Shamis et al. 2009; Varma, Campi et al. 2006]. Myosin II organizes actin filaments into bundles in the lamellum, the region immediately behind the lamellipodium. Contraction of myosin along these filaments could contribute to retrograde actin flow, which could in turn contribute to the movement of SLP-76 MC [Vicente-Manzanares, Ma et al. 2009]. In addition, the centripetal movement of SLP-76 MC requires the integrity of both the actin and microtubule cytoskeleton [Bunnell, Hong et al. 2002; Nguyen, Sylvain et al. 2008]. The TCR and SLP-76 microclusters also bind to the actin cytoskeleton [Billadeau, Nolz et al. 2007], although the association of the TCR with the actin cytoskeleton is less tightly coupled, since anti-TCR antibodies on

immobilized surfaces do not slow retrograde actin flow [Nguyen, Sylvain et al. 2008]. Though association with the cytoskeleton seems to drive the inward movement of SLP-76 MC, dynamic actin rearrangement is also required for the formation of SLP-76 MC [Varma, Campi et al. 2006]. These data highlight the importance of the cytoskeleton in microcluster-mediated signaling. The mechanical segregation model described by Seminario *et al.* proposes that actin polymerization generates the forces necessary to bring the T cell into tight contact with an APC and create a permissive microenvironment for signaling to occur [Seminario and Bunnell 2008].

4.7 Models for T cell activation

4.7.1 Generating discrete functional outcomes from analogue signals

Ligation of the TCR does not immediately lead to the production of second messengers and the activation of the T cell. As discussed in the previous section, several phosphorylation events must occur and SH2 domain-containing proteins must be recruited. A time delay exists between ligation of the TCR and the functional output. According to the kinetic proofreading model proposed by McKeithan, this time delay allows the cell to discriminate between TCR ligands of varying affinities [McKeithan 1995]. In this model of T cell activation, ligation of the TCR promotes phosphorylation events, the recruitment of SH2-domain containing proteins, and the formation of a signaling 'complex' that is competent to transduce signals that result in discrete functional outcomes. Formation of this 'complex' is a stepwise process that involves tyrosine phosphorylation and requires the association of the TCR with its pMHC ligand (Figure 5). In the absence of TCR ligation, the complex is dissociated and the constituent proteins revert to their basal state through the action of phosphatases. This dissociation must occur sufficiently rapidly so that nonspecific interactions are unable to form a stable complex and cause T cell activation. This model explains how the half-life of the interaction between a pMHC complex with the TCR determines the fate of the T cell [Davis, Boniface et al. 1998]. Ligands with higher affinity for the TCR will have higher 'dwell time' and will consequently be able to generate more signal before dissociating. Imaging studies have revealed that ZAP-70 is recruited and activated in a time frame that is compatible with the kinetic proofreading model [Bunnell, Hong et al. 2002; Huse,

Klein et al. 2007], indicating that signaling microclusters may be the 'complexes' predicted by this model.

However, more recent studies suggest that the simple kinetic proofreading model proposed above is insufficient to explain T cell activation. Weakly-interacting TCR ligands induce binding of the inhibitory tyrosine phosphatase SHP-1 to TCR complexes [Dittel, Stefanova et al. 1999]. In this negative feedback loop, activated Lck phosphorylates SHP-1, which then binds to Lck and dephosphorylates it, terminating TCR signaling. In contrast, agonist ligands induce Erk activation, which modifies Lck such that it is no longer accessible to SHP-1 [Stefanova, Hemmer et al. 2003]. Mathematical modeling confirmed that competition based on digital positive feedback mediated by Erk and analogue negative feedback mediated by SHP-1 were required for sharp ligand discrimination displayed by the TCR [Altan-Bonnet and Germain 2005]. Therefore, in addition to the simple kinetic segregation model, competing feedback loops also contribute to TCR signaling and contribute to the high sensitivity and selective power of the TCR.

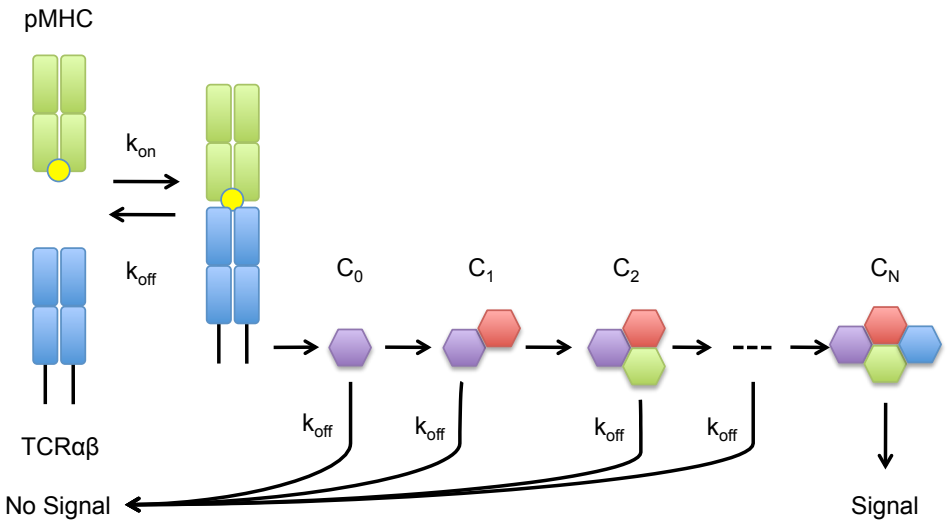

Figure 5: Kinetic Proofreading

The kinetic proofreading model postulates that binding of the TCR to peptide-MHC (pMHC) creates a complex (with association rate constant of K_{on}) that initiates signaling events. This signaling proceeds through a series of intermediate complexes (C_0, C_1, etc.) to generate the final signaling complex (C_N) which is competent to transduce signals to the cell. If this complex is formed before dissociation of the TCR-pMHC complex (designated by rate constant K_{off}), then signaling will proceed. Therefore, for productive signaling to occur, the affinity of the TCR-pMHC must be sufficiently high to allow for generation of the C_N complex. Cartoon adapted from [George, Stark et al. 2005].

4.7.2 The kinetic segregation model of TCR triggering

The kinetic proofreading model described above explains how ligand affinity leads to phosphorylation of the TCR by tyrosine kinases and initiation of the intracellular signaling cascade. However, this model does not explain the mechanism by which receptor ligation 'triggers' the activation of Src family kinases such as Lck. A recent study has shown that a large fraction of Lck is active in a resting cell [Nika, Soldani et al. 2010], suggesting that the triggering mechanism relies less on the 'activation' of Lck and may involve accessibility of the ITAMs or their protection from phosphatases. One model of TCR triggering, termed the kinetic segregation model, proposes that close adhesion of a T cell and an APC excludes inhibitory phosphatases that have large extracellular domains, such as CD45, while allowing the interactions of the relatively short TCR and MHC molecules within the zone of close contact [Davis and van der Merwe 2006]. The kinetic segregation model proposes that, in a resting cell, surface molecules randomly associate due to diffusion in the membrane. As a result of these random interactions, Lck randomly phosphorylates ITAMs present on CD3 and the phosphatase CD45 randomly dephosphorylates these ITAMs in a resting cell. Due to these opposing activities, there is no net increase in phosphorylation. Contact between a T cell and APC will create a zone of tight contact, mediated by adhesion molecules. Such a contact would exclude the CD45 phosphatase, which has a large extracellular domain [Davis and van der Merwe 2006]. The exclusion of phosphatases would therefore favor the phosphorylation of TCR present in this zone of tight contact. In agreement with the kinetic segregation model, SLP-76 MC were found to exclude CD45 [Bunnell, Hong et al. 2002; Varma, Campi et al. 2006]. Subsequent studies have

confirmed the size-dependent exclusion of tyrosine phosphatases from zones of tight contact contributes to the establishment of a permissive signaling environment [Irles, Symons et al. 2003; Lin and Weiss 2003]. Conversely, lengthening the TCR-pMHC complex with chimeric receptors inhibited T cell activation [Milstein, Tseng et al. 2008]. Moreover, the observed size of SLP-76 microclusters corresponds to the predicted size for the minimal area of contact by the kinetic segregation model (~500 nm) [Burroughs, Lazic et al. 2006].

4.7.3 The Mechanical Segregation Model

Although these models recapitulate many aspects of TCR triggering and signal transduction, they do not account for important features of physiological immune synapses. First, these models do not account for the uniformly small, tight contacts characteristic of TCR microclusters nor do they explain the sustained generation of these tight contacts in the periphery of the synapse [Bunnell, Hong et al. 2002; Bunnell, Kapoor et al. 2001; Varma, Campi et al. 2006]. Second, these models do not account for the contribution of the actin cytoskeleton, although this system has a well-established role in supporting TCR signaling [Billadeau, Nolz et al. 2007; Valitutti, Dessing et al. 1995; Varma, Campi et al. 2006]. The mechanical segregation model integrates multisubunit scaffolds that influence microcluster formation as well as the forces applied by the actin cytoskeleton [Seminario and Bunnell 2008]. In this model, the T cell scans APCs using filopodia and lamellipodia. The actin polymerization generated within these protrusions provides the force to bring the surfaces of the T cell and APC into close contact and to shear the contacts between the TCR and large glycoproteins [Chen, Chen et al. 2007]. As a result, large glycoproteins such as CD43 and CD45 are excluded from the tight contact,

consistent with the kinetic segregation model. Once activated within this zone of tight contact, TCR and ZAP-70 containing complexes associate with the cytoskeleton in an Lck-dependent manner [Rozdzial, Pleiman et al. 1998]. This interaction maintains the TCR within the zone of tight contact and allows serial triggering of the TCR. Multisubunit, SLP-76 containing signaling microclusters then form adjacent to microclusters containing the TCR. The formation and persistence of these structures is a critical event in TCR signaling and may facilitate Erk activation and SHP-1 inactivation. Furthermore, enzymes which activate Rho family GTPases are recruited into the microcluster [Braiman, Barda-Saad et al. 2006]. These GTPases contribute to the formation of filopodia and lamellipodia, which can drive expansion of the immune synapse. Finally, the actin-dependent movement of microclusters to the center of the contact contributes to their down-regulation within the cSMAC structure [Seminario and Bunnell 2008].

4.8 The role of Vav1 in T cell signaling

4.8.1 Imaging Data Suggest that Vav1 is a Critical Component of SLP-76 MC

Using live cell imaging assays, Bunnell et al. examined the contribution of various regions of SLP-76 to microcluster formation and function. They found that the three N-terminal tyrosines of SLP-76 were critical for normal microcluster behavior. In Jurkat T cells expressing the SLP-76 Y3F mutation, microclusters formed but quickly dissipated near their sites of formation [Bunnell, Singer et al. 2006]. This result suggested that the binding partners of this region are critical for SLP-76 MC persistence and movement. Biochemical studies have shown that these tyrosines bind to the Rho-family GEF Vav1, the adapter Nck, and the tyrosine kinase Itk [Jordan, Sadler et al. 2006; Tuosto, Michel et al. 1996]. However, the loss of interaction between Vav1 and SLP-76 is likely to be significant for several reasons. First, Vav1 and SLP-76 act synergistically to enhance T cell activation following TCR stimulation [Fang and Koretzky 1999; Raab, da Silva et al. 1997; Wu, Motto et al. 1996]. In addition, the phenotype of Vav1 deficient mice parallels that seen in the SLP-76 Y3F mutant [Clements, Yang et al. 1998; Fujikawa, Miletic et al. 2003; Jordan, Smith et al. 2008; Kumar, Pivniouk et al. 2002; Pivniouk, Tsitsikov et al. 1998]. These data establish that Vav1 and SLP-76 act synergistically to augment T cell activation. Therefore, the loss of Vav1 from the SLP-76 Y3F mutant could be responsible for the defect observed in SLP-76 MC persistence and T cell activation.

Vav1 was first identified as a proto-oncogene in cells of hematopoietic origin [Katzav, Martin-Zanca et al. 1989]. Two other Vav family member proteins, Vav2 and Vav3,

have also been identified [Tybulewicz 2005]. While Vav1 is mainly expressed in cells of hematopoietic lineage, Vav2 and Vav3 are expressed more broadly [Bustelo 2001]. Studies involving Vav-family knockout mice have shown that the other Vav isoforms have overlapping functions in development and activation. In particular, Vav3 is able to partially compensate for the loss of Vav1 in both development, proliferation, and activation, as measured by calcium flux [Fujikawa, Miletic et al. 2003]. In Vav1 deficient cells, Vav3 is able to rescue defects in IL-2 production, whereas Vav2 is not [Cao, Janssen et al. 2002]. This work focuses on the role of Vav1 in T cell signaling and activation since the loss of Vav1 accounts for the majority of the defect observed in Vav deficient mice and Vav1 is mainly expressed in cells of hematopoietic lineage [Bustelo 2001; Fujikawa, Miletic et al. 2003].

Vav1 contains both adapter and effector domains and binds to several proteins that are required for optimal T cell signaling and cytoskeleton reorganization, as shown in Figure 6. It possesses an SH2 domain flanked by SH3 domains, which mediate protein-protein interactions with other proteins involved in T cell signaling. In addition, Vav1 is a guanine nucleotide exchange factor (GEF) for Rho family GTPases [Tybulewicz 2005]. A simplified cartoon diagram of the Vav1 domains and their known binding partners is shown in Figure 6. Vav1 is involved in many facets of T cell activation and development, such as actin cytoskeletal reorganization, MTOC polarization, mitogen activated protein kinase (MAPK) pathways, IL-2 production, and calcium flux [Costello, Walters et al. 1999; Fischer, Kong et al. 1998; Reynolds, de Bettignies et al. 2004;

Reynolds, Smyth et al. 2002], as shown in Figure 7. However, the mechanisms by which Vav performs these many functions remain unresolved.

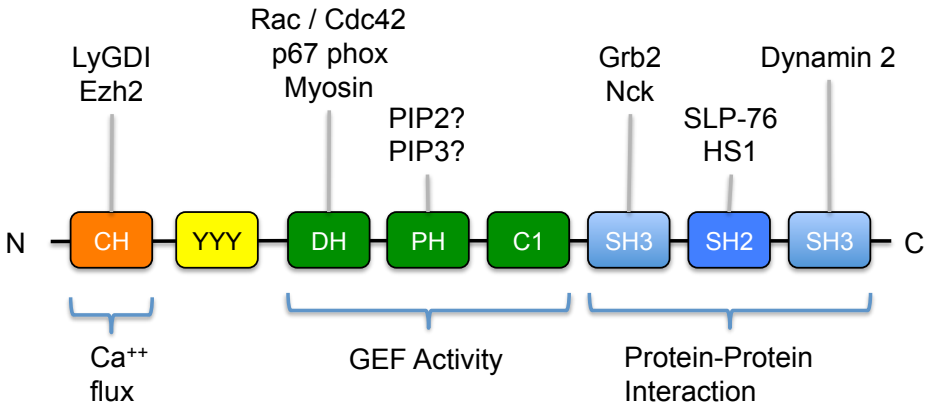

Figure 6: Vav domains and binding partners

Simplified cartoon showing the domain organization of Vav1. Known Vav1 binding partners are shown above the protein, while Vav1-dependent functions are shown below. The Calponin homology domain (CH – orange) is required for Vav1-mediated calcium flux. The N-terminal acidic region (yellow) contains three critical tyrosines which become phosphorylated upon TCR stimulation. The Dbl homology (DH), Pleckstrin homology (PH) and C1 domain form the GEF cassette (green) and are required for the enzymatic activity of Vav1. The C-terminal Src-homology (SH – blue) mediate protein-protein interactions.

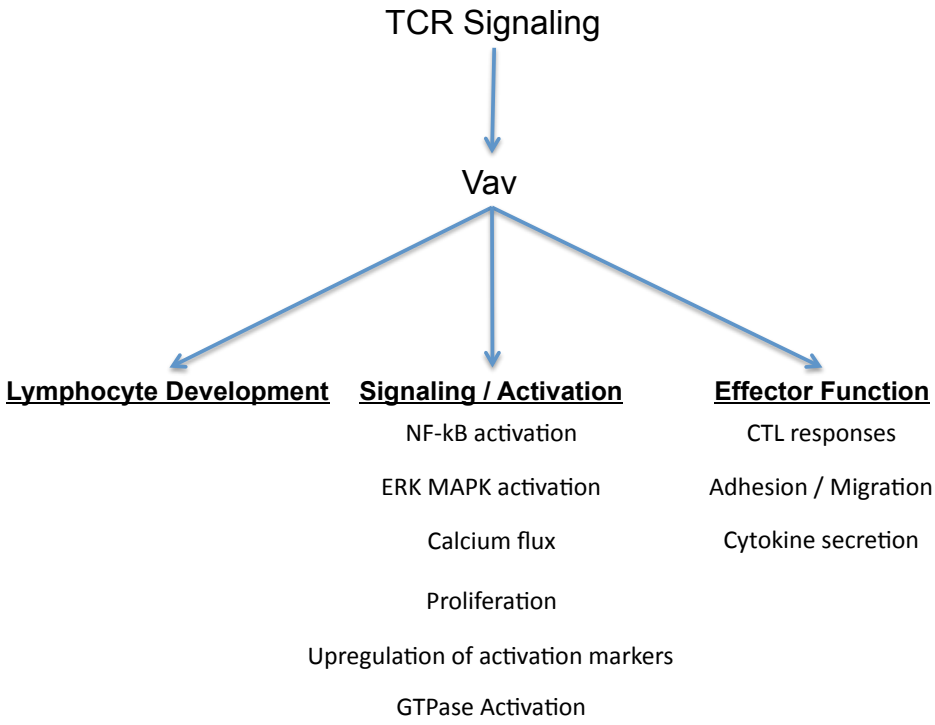

Figure 7: Vav1-dependent T cell functions

Downstream of TCR signaling, Vav1 becomes phosphorylated and activated. Vav1 participates in a number of critical events required for T cell function. These events are subdivided into lymphocyte formation, signaling, and function. In this thesis, I focus on the T cell signaling functions of Vav1, but also address its role in cytoskeletal reorganization. This figure was based on data presented in [Tybulewicz 2005].

4.8.2 Enzymatic Activity of Vav1

The Dbl homology (DH) domain of Vav1 mediates the Guanine-nucleotide Exchange Factor (GEF) activity (Figure 6). GEFs act on a class of molecules known as GTPases. These molecules are commonly thought of as 'molecular switches' which cycle between an active, GTP-bound form and an inactive, GDP bound form. When in the active form, GTPases interact with other signaling molecules to activate them and transmit signals downstream. To mediate this exchange activity, GEFs interact with the switch regions of Rho GTPases. This induces a remodeling of the switch regions which in turn alters the shape of the nucleotide-binding pocket of the GTPase and causes the release of GDP. GTP will then preferentially bind the GTPase since it is more abundant in the cell than GDP [Rossman, Der et al. 2005]. In this manner, GEFs activate GTPases and allow them to perform their biologic function. Vav1 performs nucleotide exchange for Rac, RhoA, and Cdc42 [Han, Das et al. 1997]. Activation of Rac by Vav1 leads to the phosphorylation and activation of JNK via a MAPK cascade [Crespo, Schuebel et al. 1997]. In this manner, the Vav1 GEF activity is likely to be required for optimal T cell signaling and for transcription factor activation.

In contrast to its biologic activity, GTPases also possess an enzymatic, GTP-cleaving activity. After binding GTP, a GTPase will function for a certain amount of time before cleaving GTP to GDP and inactivating itself. Proteins known as GTPase Activating Proteins (GAPs) enhance the enzymatic activity of the GTPase, which in turn inactivates its biologic function. A class of molecule known as Guanine-nucleotide Dissociation Inhibitors (GDIs) stabilizes GTPases in the inactive, GDP-bound state, thereby

preventing their biologic activity [Rossman, Der et al. 2005]. Though it is appreciated that the actions of activating GEFs and inactivating GDIs and GAPs must be precisely regulated to achieve optimal T cell signaling, the exact interactions of these molecules remains unknown.

Consistent with Dbl family GEFs, the DH domain is followed by a Pleckstrin homology (PH) that is required for its enzymatic activity [Palmby, Abe et al. 2002; Zugaza, Lopez-Lago et al. 2002]. PH domains are traditionally thought to mediate binding to lipids, which may be true of other Dbl family GEFs. In the Dbl family GEFs Dbs and Lfc, the PH domain is required for the transforming activity of the protein, though loss of the PH domain is partially compensated by adding the membrane-targeting sequence of Ras [Whitehead, Lambert et al. 1999]. The importance of lipid binding in the Vav1 PH domain has not been addressed in a live cell. *In vitro*, the Vav1 enzymatic activity is increased in the presence of PIP3, but not PIP2, indicating that the PH domain may be capable of lipid binding and that this may help to regulate the GEF activity [Han, Luby-Phelps et al. 1998]. However, the Vav1 PH domain is insufficient to localize the protein to the plasma membrane [Palmby, Abe et al. 2002]. Moreover, crystal structure data show that the PH domain packs against a helix of the DH domain and could contribute to its structural stability [Rapley, Tybulewicz et al. 2008]. Currently, it is unclear whether the Vav1 PH domain is capable of lipid binding, as is normally ascribed to these domains, or whether it primarily plays a structural role in the stabilization of the GEF cassette. Though the mechanism remains unknown, it is clear that the Vav1 PH domain is required for optimal enzymatic activity [Zugaza, Lopez-Lago et al. 2002].

Adjacent to the PH domain is a cysteine-rich C1 domain, which also packs against the DH domain and could be another structural component of the GEF cassette, as suggested by Rapley et al [Rapley, Tybulewicz et al. 2008]. This domain is also required for the enzymatic activity of Vav1 [Zugaza, Lopez-Lago et al. 2002]. C1 domains are DAG-binding domains, though it is unknown whether the Vav1 C1 domain performs this function. Whether this domain is capable of binding other ligands or mainly serves to stabilize the GEF cassette has not been addressed.

Conflicting reports in the literature differ on the exact role of the Vav1 GEF activity in TCR-mediated signaling [Kuhne, Ku et al. 2000; Miletic, Graham et al. 2009; Saveliev, Vanes et al. 2009]. However, it is clear that Vav1 possesses both GEF-dependent and GEF-independent functions. The GEF activity is dispensable for the role of Vav1 in polarization, Erk activation, and intracellular calcium flux following TCR stimulation [Kuhne, Ku et al. 2000; Miletic, Graham et al. 2009; Saveliev, Vanes et al. 2009]. These GEF-independent scaffolding functions of Vav1 are required for the efficient activation of PLCγ [Braiman, Barda-Saad et al. 2006], which produces IP3 and DAG. IP3 leads directly to the release of calcium stores, while DAG activates RasGRP to generate active Ras. Once activated, Ras activates the GEF Sos, leading to further production of active Ras. Ras initiates MAPK cascades that result in Erk and c-fos activation. In contrast, the Vav1 GEF activity is required for many of its roles in T cell activation such as JNK, AP-1 and AKT activation, the formation of T-B cell conjugates, and IL-2 production downstream of the TCR [Kaminuma, Deckert et al. 2001; Saveliev, Vanes et al. 2009].

The Vav1 enzymatic activity acts through Rac1, leading to MAPK cascades that result in JNK phosphorylation and AP-1 activation. These data indicate that Vav1 possesses both effector and scaffolding functions. Transcription factor activation is also required for the transforming activity of Vav1. However, the GEF function by itself is insufficient for transforming activity; Vav1 must also be localized to the plasma membrane to potentiate transformation [Zugaza, Lopez-Lago et al. 2002]. One explanation for this result is that Vav1 must be localized to the appropriate microenvironment to become activated.

4.8.3 Vav1 Adapter Domains

Though Vav1 is involved in many aspects of TCR signaling, the enzymatic activity is only required for a subset of these effects. This indicates that Vav1 is also involved in important scaffolding interactions that facilitate T cell activation. The Vav1 C-terminus contains an SH2 domain flanked by SH3 domains that mediate protein-protein interactions. The N-terminal SH3 domain (N-SH3) is an atypical domain in which the normal binding pocket for proline-rich regions is occupied by a helix of Vav1. Instead, this domain contains a proline-rich sequence on the opposite side of the domain and therefore acts as a target for other SH3 domains [Ogura, Nagata et al. 2002]. This domain binds the adapter Grb2 [Ramos-Morales, Romero et al. 1995; Ye and Baltimore 1994], which in turn is capable of binding LAT. The Vav1 N-SH3 domain is also capable of binding to the adapter Nck [Barda-Saad, Shirasu et al. 2010], and this interaction is required for actin polymerization. The SH2 domain binds to phosphorylated SLP-76 on tyrosines 112 and 128 [Raab, da Silva et al. 1997]. This domain is required for the synergy between Vav1and SLP-76 and is also required for its transforming activity. The C-terminal SH3 (C-SH3) domain is a typical SH3 domain that

binds proline rich regions. This domain of Vav1 binds to the GTPase DynaminII, which is involved in membrane internalization and regulation of actin polymerization [Gomez, Hamann et al. 2005]. This interaction specifically involves the C-terminal SH3 domain of Vav1 with the proline rich domain of DynaminII and is required for JNK phosphorylation and IL-2 production. When the Vav1 C-terminal SH3-SH2-SH3 domains are expressed in isolation, they act as a potent inhibitor of antigen-dependent signals [Arudchandran, Brown et al. 2000; Wu, Motto et al. 1996]. Therefore, while these domains are important for full Vav1 function, they are insufficient to mediate full T cell signaling. The adapter functions of Vav1 also serve to enhance the co-localization and co-immunoprecipitation of SLP-76 and PLCγ1, indicating that Vav1 is involved in the structural stabilization of signaling complexes containing SLP-76 [Braiman, Barda-Saad et al. 2006; Reynolds, de Bettignies et al. 2004; Reynolds, Smyth et al. 2002].

4.8.4 Regulation of the Vav1 GEF by N-terminal Domains

Deletion of the N-terminus of Vav1 potentiates its enzymatic activity, indicating that this region of the protein is involved in auto-regulation of the GEF [Zugaza, Lopez-Lago et al. 2002]. This N-terminal region consists of a Calponin homology (CH) domain as well as three tyrosines (residues 142, 160, and 174) that have been highly conserved through evolution. In the inactive state, these tyrosines bind to the CH domain and to a cleft in the DH domain adjacent to the GTPase-binding site. These interactions maintain the protein in an auto-inhibited, ‘closed’ conformation [Amarasinghe and Rosen 2005; Yu, Martins et al. 2010]. Upon TCR signaling, Lck phosphorylates Vav1, activating its GEF activity [Han, Das et al. 1997]. Crystal structure data have shown that phosphorylation on Y174 induces a conformational change and causes the protein to adopt an ‘open’

conformation which is accessible to GTPases [Yu, Martins et al. 2010]. In addition, these tyrosines can bind to signaling proteins such as Lck, PLCγ1, and PI3K p85 in pulldown assays [Miletic, Sakata-Sogawa et al. 2006], though whether this binding occurs *in vivo* and what its significance may be remains unknown. The CH domain also binds to the PH domain to increase the stability of the Vav1 auto-inhibitory fold, further inhibiting the accessibility of the DH domain [Yu, Martins et al. 2010].

In addition to its role in regulating the enzymatic activity, the CH domain is required for Vav1-mediated increases in intracellular calcium [Billadeau 2000; Cao, Janssen et al. 2002]. While the mechanism of Vav1-mediated calcium flux remains unknown, Cao *et al.* have shown that the CH domain binds to calmodulin and have suggested that this interaction is required for Vav1 to play a role in calcium flux [Cao 2007]. Since calmodulin binding to the IP3 receptor is required for optimal calcium entry [Kasri, Torok et al. 2006], the association of the Vav1 CH domain with calmodulin could be required for calmodulin delivery to the IP3 receptor. In addition, the Vav1 CH domain also interacts with Ly-GDI, a Rac inactivator [Groysman, Russek et al. 2000]. Normally, Ly-GDI inhibits calcium-dependent NFAT activation, however, then Vav1 and Ly-GDI are expressed together, NFAT activity is increased [Groysman, Hornstein et al. 2002]. Association with Ly-GDI may prevent this protein from inactivating Rho family GTPases, either by preventing its access to its targets, or by inactivating the protein through its association with Vav1.

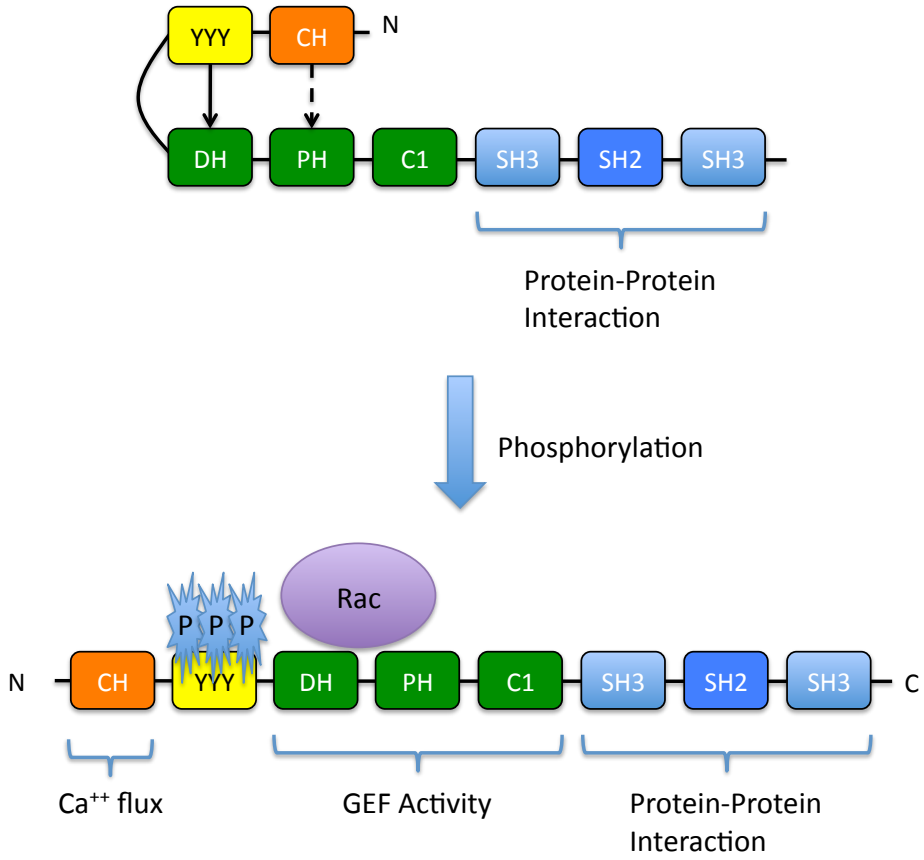

Figure 8: Autoinhibitory interactions within the N-terminus regulate the Vav1 GEF activity

In a resting cell, the CH domain and acidic region participate in an autoinhibitory fold to prevent the Vav1 GEF activity. Crystal structure data have shown that the tyrosines within the acidic region (yellow) bind to the CH as well as the DH domain (solid arrow) and that the CH domain interacts with the PH domain (dashed arrow). In this conformation, the DH domain is inaccessible to GTPases such as Rac. Upon tyrosine phosphorylation, the protein shifts to an open conformation, potentiating the GEF activity [Yu, Martins et al. 2010].

5 Summary / Hypothesis

Microclusters containing the adapter SLP-76 are critical structures for T cell activation. These SLP-76 MC form in the periphery of the contact between a T cell and a stimulatory surface and persist for several minutes as they migrate toward the center of the contact. Dynamic actin rearrangements are necessary for the formation of these structures within the periphery of the contact. Though the exact mechanism by which actin rearrangements participate in microcluster formation remains unknown, the mechanical segregation model proposes that actin polymerization generates the forces required to form tight junctions between T cells and stimulatory surfaces [Seminario and Bunnell 2008].

In mutational studies, SLP-76 MC persistence and movement are observed together and both of these phenomena are predictive of effective signaling. However, physical barriers to microcluster movement and costimulatory signals which immobilize SLP-76 MC do not inhibit signaling, indicating that immobile microclusters are competent to transduce signals. Therefore, microcluster movement is not required for T cell activation, but is correlated with events that are important for activation. Since dynamic rearrangement of the actin cytoskeleton is required for microcluster movement [Nguyen, Sylvain et al. 2008; Varma, Campi et al. 2006], I propose that the movement of SLP-76 MC may reflect efficient coupling of microcluster components to actin meshworks. Mutational data also show a link between SLP-76 MC persistence and T cell function.

While this could also be a correlation, optimal T cell activation has not been observed under conditions that produce non-persistent microclusters.

Mutations affecting the N-terminal tyrosines of SLP-76 inhibit both microcluster movement and persistence. Since this mutation so drastically perturbs the microcluster, it is not a useful tool for addressing how SLP-76 MC are assembled, stabilized, and transported. In order to address these issues, I examined individual binding partners of the SLP-76 N-terminal tyrosines. I chose to examine Vav1 because Vav1 and SLP-76 act synergistically to enhance T cell activation following TCR stimulation [Fang and Koretzky 1999; Raab, da Silva et al. 1997; Wu, Motto et al. 1996]. In addition, the phenotype of Vav1 deficient mice parallels that seen in the SLP-76 Y3F mutant [Clements, Yang et al. 1998; Fujikawa, Miletic et al. 2003; Jordan, Smith et al. 2008; Kumar, Pivniouk et al. 2002; Pivniouk, Tsitsikov et al. 1998].

The goal of this thesis was to perturb the individual functions of Vav1 and observe the effect on the SLP-76 MC. I wanted to address whether specific aspects of microcluster behavior (movement and persistence) track with specific molecular features of Vav1. By performing these experiments I have moved to a more refined understanding of how SLP-76 MC are assembled and regulated during immune responses.

6 Materials and Methods

6.1 Reagents

6.1.1 Antibodies

For cell stimulations, anti-CD3 antibodies used were OKT3 (mouse IgG2a, Bio-Express), UCHT1 (mouse IgG1, BD Bioscience), or C305 ascites (provided by Gary Koretzky).

Primary antibodies used for Western Blot and immunofluorescent assays were: CD3 zeta (mouse monoclonal, Santa Cruz Biotechnology), Dynamin (rabbit polyclonal, Santa Cruz Biotechnology), Dynein (mouse monoclonal, Sigma), Ezh2 (mouse IgG1, BD Transduction Laboratories), Gads (rabbit polyclonal IgG, Upstate Biotech), Grb2 (mouse IgG1, BD Biosciences), LAT (rabbit polyclonal, Cell Signaling Technology), Myosin IIa (MyH9, rabbit polyclonal, Covance), Nucleolin (mouse IgG2b, Zymed Laboratories), PLCγ1 (rabbit polyclonal Cell Signaling Technology), Phosphotyrosine - PY-100 (mouse IgG1, Cell Signaling), Phosphotyrosine – 4G10 (mouse IgG2b, Millipore), Pyk2 (mouse IgG1, BD Transduction Laboratories), SLP-76 (mouse IgG2a, Antibody Solutions), γTubulin (rabbit polyclonal, Sigma), Ubiquitin (mouse IgG1, Covance), Vav1 (rabbit polyclonal IgG, Upstate Biotech), Rac1/2/3 (rabbit polyclonal, Cell Signaling Technology), RhoG (mouse IgG2a, Santa Cruz Biotechnology), phospho-ZAP-70 (rabbit polyclonal, Cell Signaling Technology), GFP for Western blot: JL-8 (mouse IgG2a, Clontech), GFP for IP: ab290 (rabbit polyclonal, Abcam).

Fluorescent-conjugated primary antibodies were: Phycoerythrin (PE)-coated anti-CD3 (mouse IgG1, BD Biosciences), phospho-JNK Alexa 647 conjugate (mouse IgG1, Cell Signaling Technology), Cy-Chrome-conjugated anti-CD69 (mouse IgG1, BD Biosciences)

Secondary antibodies for Western blot were: Goat anti-Mouse or Goat anti-Rabbit (Jackson ImmunoResearch Laboratories) diluted 1:5000. Fluorescent-conjugated secondary antibodies were Alexa 647-conjugated goat anti mouse IgG (Molecular Probes). For immunofluorescent staining, all primary antibodies were diluted 1:200 and all secondary antibodies were diluted 1:1000

6.1.2 Recombinant Proteins

Human recombinant VCAM-1-Fc was from R&D Systems.

6.1.3 Pharmacological agents and inhibitors

The calcium chelator EGTA was from Fisher Scientific. Reversible cross-linkers DSP and DTME were from Thermo Scientific.

6.2 Generation of Vav1 Mutant Panel

All Vav1 chimeras were tagged with fluorescent protein at the C-terminus by subcloning into a variant form of pEYFP-n1 (Clontech) containing the monomerizing A206K mutation. Primers used in the generation of mutant Vav1 constructs and promoters are listed in section 6.2.4.

6.2.1 Expression Vector and Promoter Cloning

The commonly used CMV promoter fails to drive protein expression in J.Vav cells (Figure 9B + C). In addition, expression of proteins under the CMV promoter increases greatly following treatment with PMA (Figure 9A-C). Stimulation with PMA was used as a positive control for CD69 upregulation assays, necessitating the use of a promoter that is insensitive to PMA. To resolve these issues, the EF1α promoter was amplified by PCR with primers SCB279 and SCB280. The EF1α promoter was then subcloned into the pEYFP-n1 vector (Clontech) using the restriction enzymes AseI and NheI. The EF1α promoter was able to drive robust expression of mYFP in the J.Vav cell line and was unaffected by the addition of PMA (Figure 9). Since the region of the EF1α promoter flanked by SacII sites is not required for its activity [Wakabayashi-Ito and Nagata 1994], I removed this region by cutting with SacII and religating the vector. This was done to make the promoter more amenable to future cloning; I then confirmed that this deletion did not affect protein expression (Figure 9A – compare first 3 lanes to middle 3 lanes). To facilitate further cloning, I removed XmaI, ApaI, SacI, and XhoI sites within the promoter, as these restriction sites were also present in the multi-cloning site of the pEYFP-n1 vector. This was accomplished by individually cleaving these sites, treating with Mung Bean Endonuclease, and religating. The EF1α promoter was still able to drive robust expression of Vav1 following these modifications (termed EF1α.v2 - Figure 9C).

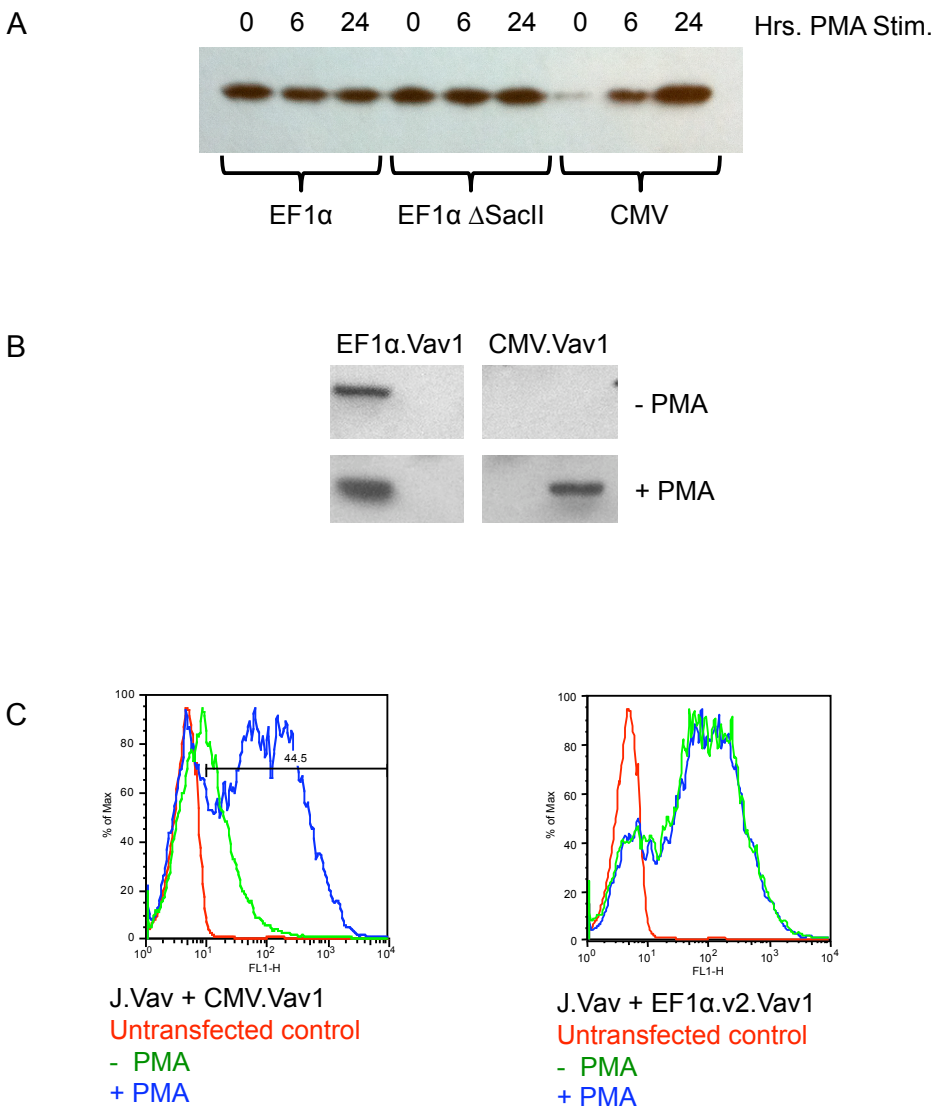

Figure 9: The EF1α promoter drives protein expression in Jurkat cells

A - Jurkat E6 cells were transfected with mYFP expression constructs under the control of the CMV, EF1α, or EF1α promoter in which the DNA flanked by SacII sites was deleted (EF1α ΔSacII). YFP expression was monitored by Western blot following stimulation with PMA for the indicated times. **B –** J.Vav cells were transfected with plasmids encoding mYFP-tagged wild-type Vav1 under either the EF1α or CMV promoter. Protein expression was monitored after 24 hours in the presence or absence of PMA. **C –** J.Vav cells were transfected with Vav1.mYFP constructs (CMV or EF1α.v2 promoter) and treated with PMA as in Panel B. Protein expression was monitored by FACS.

6.2.2 Vav1 mutant generation

The Vav1 atypical N-terminal SH3 (P657A), C-terminal SH3 (WW820/821YY), and SH2 domain (R696A) inactivating point mutations were obtained from Dan Billadeau, tagged at the C-terminus with mYFP, and subcloned into pEYFP-n1 (Clontech). All additional Vav1 mutants were generated by PCR and were subcloned into the parental EF1a:Vav1.mYFP vector using NheI and AgeI, unless otherwise indicated. Truncations mutants were generated as follows: ΔCH, removing residues M1-I120, using oligos SCB243 and SCB244 with BamHI and XmaI; Δ323, removing residues F600-C845, using oligos NS763 and NS766; SH323, residues E591-C845 remaining, using oligos NS767 and SCB045. Point mutations and internal deletions were generated by overlap extension PCR as follows: Y174F, using oligos NS763-NS765, and SCB045; Y3F, incorporating Y142F and Y160F into a Y174F backbone, using oligos NS763, NS773, NS774 and SCB045; ΔDH-PH, removing residues C198-N505, using oligos NS763, NS770, NS771 and SCB045. The DH domain mutation L278Q described by Swat [Miletic, Graham et al. 2009] was generated by overlap extension PCR using primer pairs of NS763 with NS831 and NS830 with NS724 using WT Vav1 as a template (3018). The L334A / K335A (termed LK-AA) described by Tybulewicz [Saveliev, Vanes et al. 2009] was generated by overlap extension PCR using primer pairs of NS763 with NS833 and NS832 with NS724 using WT Vav1 as a template (3018). A fusion protein consisting of the Vav1 CH domain fused to the SH3-SH2-SH3 motif (termed CH-323) was generated by overlap extension PCR using the primers NS827, NS829, SCB045, and NS763 using WT Vav1 as a template. Deletion of the DH, PH, and C1 domains (ΔGEF

mutation) was performed by PCR using the primers NS836 and NS837 using WT Vav1 as a template.

Vectors encoding mRFP and mStrawberry fluorescent proteins were gifts from Roger Tsien [Shaner, Campbell et al. 2004]; red fluorescent proteins were amplified by PCR and subcloned into the parental EF1a:Vav1.mYFP vector using AgeI and NotI. All Vav1 truncations and point mutants were confirmed by sequencing.

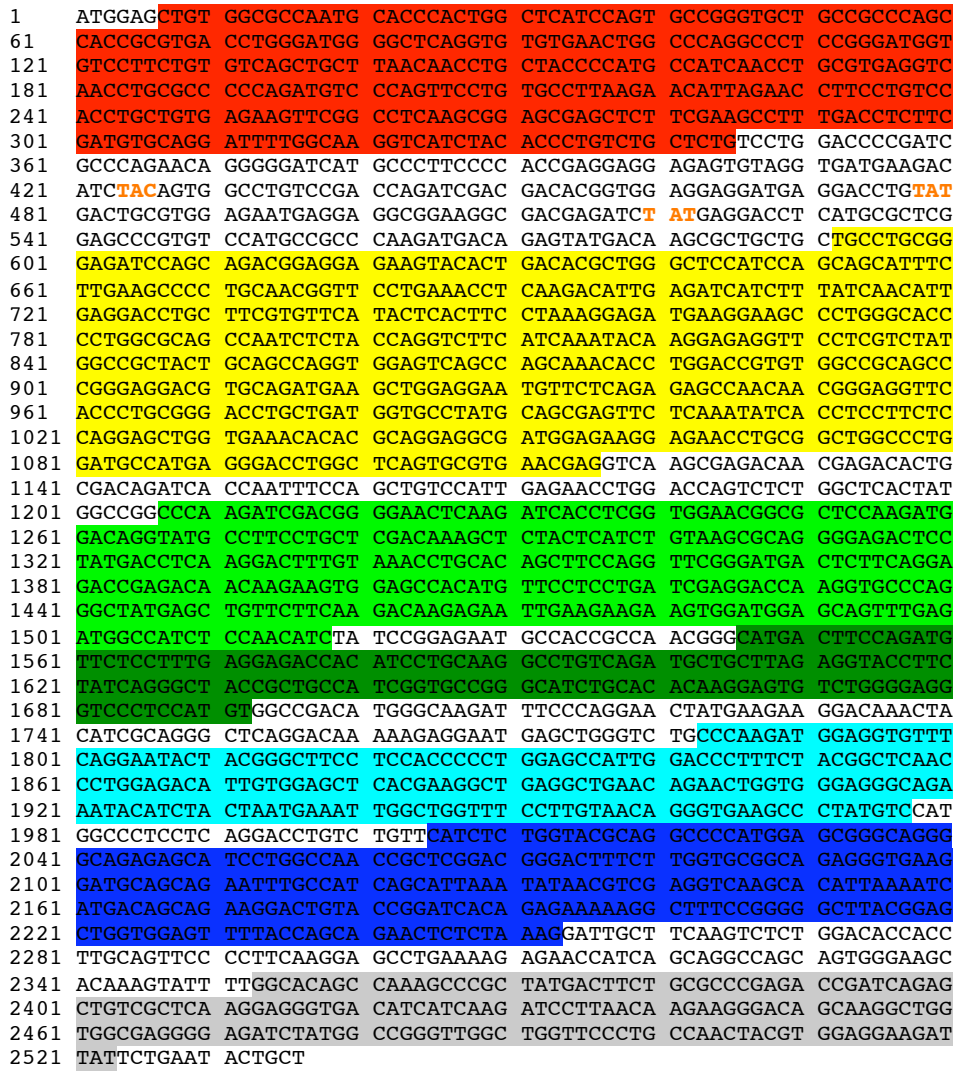

Figure 10: Vav1 cDNA sequence

Accession number NM_005428. The various domains of Vav1 are indicated by the following colors: CH domain - red. Tyrosines 142, 160, and 174 are highlighted in orange. DH - yellow. PH – light green. C1 – dark green. N-terminal SH3 domain – light blue. SH2 domain – dark blue. C-terminal SH3 domain – grey.

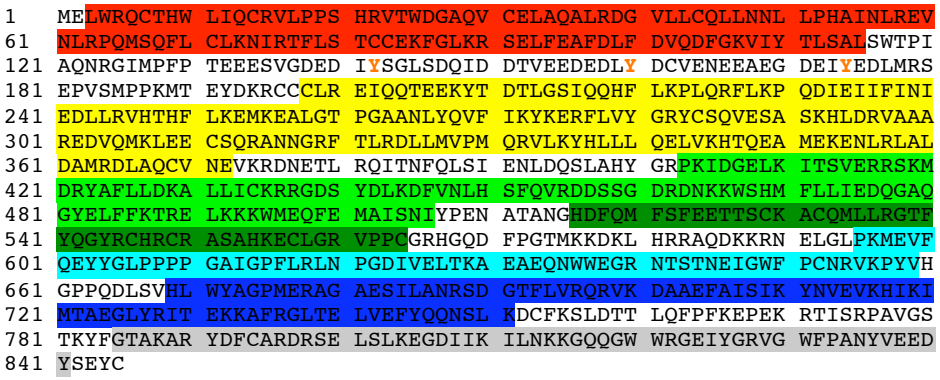

Figure 11: Vav1 amino acid sequence

The Vav1 amino acid sequence is color coded as in Figure 10.

6.2.3 Generation of Vav1 RNAi hairpin

To generate Vav1-specific RNAi hairpins, target sequences were identified using the siDESIGN Center (www.Dharmacon.com). The most effective hairpin tested targets the sequence GAAGGACTGTACCGGATCA and was created by annealing NS705-708 and subcloning the resulting fragment into the suppression vector pFRT-H1p/Hygro, provided by Dan Billadeau. Vav1 was rendered immune to this hairpin by site-directed mutagenesis using NS723 and NS724 (Stratagene Quick Change protocol).

6.2.4 Oligonucleotides used in Vav1 mutant generation

The primers used to generate the various Vav1mutations are as follows:

SCB045	5’ CTC GCC CTC GCC GGA CAC
SCB243	5’ GCC GGG ATC CGC CCA GAA CAG GGG GAT C
SCB244	5’ CAT GGC ATC CAG GGC CAG CCG CAG
NS705	5’ GA TCC GAA GGA CTG TAC CGG ATC A
NS706	5’ TTG AAT GAT CCG GTA CAG TCC TTC G
NS707	5’ TT CAA GAG ATG ATC CGG TAC AGT CCT TCT TTT TGG A
NS708	5’ AG CTT CCA AAA AGA AGG ACT GTA CCG GAT CAT CTC
NS723	5’ CAT GAC AGC AGA AGG CCT CTA TCG GAT CAC AGA G
NS724	5’ CTC TGT GAT CCG ATA GAG GCC TTC TGC TGT CAT G
NS763	5’ GA GTG GGT GGA GAC TGA AGT TAG GCC AGC
NS764	5’ GCG CAT GAG GTC CTC AAA AAT TTC GTC GCC TTC CG
NS765	5’ GCG GAA GGC GAC GAA ATT TTT GAG GAC CTC ATG CG
NS766	5’ CCGAC CGG TAC CTC CAT CTT GGG CAG ACC CAG

NS767	5’ GCC GCT AGC GCC ACC ATG GAA CTG GGT CTG CCC AAG ATG GAG
NS770	5’ CGG ATA GAT GCA GCA GCG CTT GTC ATA CTC TGT C
NS771	5’ CGC TGC TGC ATC TAT CCG GAG AAT GCC ACC GCC
NS773	5’ CGT GTC GTC GAT CTG GTC GGA CAG GCC TCT GAA GAT GTC TTC ATC ACC
NS774	5’ CAG ATC GAC GAC ACG GTG GAG GAG GAT GAA GAC CTG TTT GAC TGC GTG GAG
NS775	5’ CTC CAC GCA GTC AAA CAG GTC TTC ATC CTC CTC CAC
NS827	5’ GCC GGA TCC CTG GGT CTG CCC AAG ATG GAG
NS828	5’ CGC GCG TGA TCA GCA GCA GCG CTT GTC ATA CTC
NS829	5’ CGC GCG AGA TCT CAG AGC AGA CAG GGT GTA GAT GAC
NS830	5’ C AAA TAC AAG GAG CGC TTC CAG GTC TAT GGC CGC
NS831	5’ GCG GCC ATA GAC CTG GAA GCG CTC CTT GTA TTT G
NS832	5' G ATG GTA CCT ATG CAA CGC GTG GCG GCC TAT CAC CTC CTT CTC CAG
NS833	5' CTG GAG AAG GAG GTG ATA GGC CGC CAC GCG TTG CAT AGG TAC CAT C
NS836	5’ GAC AAG CGC TGC TGC GGC CGA CAT GGG CAA GAT TTC CCA GG
NS837	5’ G CCC ATG TCG GCC GCA GCA GCG CTT GTC ATA CTC

6.3 Cell Lines and Culturing

6.3.1 Cell Lines

The parental Jurkat cell line used throughout this thesis is the E6.1 subclone. A SLP-76 deficient Jurkat cell line (J14) reconstituted with EGFP-tagged SLP-76 or SLP-76 in which tyrosines 112, 128, and 145 were mutated to phenylalanine (Y3F) has been described previously [Bunnell, Singer et al. 2006]. J14 cells reconstituted with YFP-tagged SLP-76 and E6.1 cells expressing GFP-tagged actin have been described previously [Bunnell, Singer et al. 2006]. Vav1 deficient Jurkat T cells (J.Vav) were the gift of Robert T. Abraham [Cao, Janssen et al. 2002]. The J.Vav1 cell line stably expressing SLP-76 tagged with mCFP (JV.SC) was generated by transfecting a linearized DNA encoding WT Vav1 construct and a hygromycin resistance gene. The cells were grown for three weeks in media containing 200µg/ml hygromycin and sorted for mCFP expression by FACS. Expression of SLP-76.mCFP was then confirmed by Western blot.

6.3.2 Cell Culturing

Jurkat T cells were maintained in RPMI 1640 (BioWhittaker) supplemented with 10% fetal bovine serum, 10mM glutamine, and 10µg/ml ciprofloxacin. Cells were kept at 37^{o}C with 5% CO_2 and were split frequently to maintain a density of 3-12x10^5 cells per mL.

6.3.3 Transfections

Prior to transfection, cells were resuspended at a concentration of 4x10^7 cells per mL. The maximum total DNA used was 30µg per transfection, which accounted for less than 10% of the total volume. Transfections were performed in 4mm gap cuvettes using a

BTX ECM 830 square wave electroporator with a single pulse at 300V for 10ms. After 5 minutes, cells were transferred to prewarmed complete medium and allowed to recover 12-16 hours prior to analysis.

6.4 Imaging Analysis

6.4.1 Equipment Setup

For all imaging experiments described in this report, a Perkin-Elmer Ultraview spinning disk confocal system was used. This system was equipped with 5 laser lines at 442, 488, 514, 568, and 647 nm. Either a CFP/YFP (442/514) or RGB (488/568/647) dichroic was used in conjunction with appropriate emission filters. Images were acquired using a ORCA-ER CCD camera (Hamamatsu).

6.4.2 Plate Preparation

Stimulatory surfaces were prepared by coating 96-well glass bottom plates (Whatman) 1% poly-L-lysine (PLL -) for 15 minutes at room temperature. PLL was then aspirated off and plates were dried for 30 minutes at 37^{o}C. Prior to imaging analysis, plates were coated with 100µl of 3µg/ml OKT3 for 1 hr at 37^{o}C, unless otherwise indicated. The plates were then blocked with 100µl of 1% BSA in PBS for 1 hr at 37^{o}C. Following each step, wells were rinsed 3x 100µl of PBS. Following the final washing, plates were stored with 100µl PBS at 4^{o}C until use.

6.4.3 Live Cell Imaging

Prior to imaging assays, the imaging plate and microscope were heated using 40^{o}C air and 35^{o}C objective heater to maintain a temperature of 37^{o}C within the imaging well. Each well was filled with 100µl of cell culturing media (Section 6.3.2) supplemented

with 25mM HEPES pH 7.4 to maintain a constant pH. Cells were pipetted into the bottom of the well and allowed to settle. The cells were then imaged immediately after contacting the coverglass. Unless otherwise indicated, cells were imaged for 5 minutes.

6.4.4 Fixed Cell Imaging

Imaging plates were prepared as in Section 6.4.2. Prior to stimulation, 100µl of culturing media (Section 6.3.2) was added to each well and the plate was allowed to equilibrate to 37^{o}C for 15 minutes. 2x10^{5} cells were added per well and stimulated for 5 minutes to capture the early stages of microcluster formation, which corresponded to our live cell imaging assays. After this time the culture media was removed and the cells were fixed in 1% paraformaldehyde (PFA) in PBS for 30 minutes at room temperature. Cells were then imaged at room temperature.

For immunofluorescent staining cells were stimulated and fixed as described above. Following fixation, cells were permeabilized and blocked using 'PFN Block' buffer (PBS + 8% fetal calf serum + 0.02% sodium azide + 0.1% Saponin, supplemented with 2% sera from the same species as the secondary antibody) for 30 minutes at room temperature. Cells were blocked with donkey or goat serum (Jackson Laboratories) to block all non-specific binding sites for the secondary antibodies. Following this step, cells were washed with 'PFN Wash' buffer (PBS + 8% fetal calf serum + 0.02% sodium azide + 0.1% Saponin). Primary antibodies were used at 1:100 dilution and secondary antibodies were used at 1:1000 (antibodies used are listed in Section 6.1.1). Cells were washed 3 times with 'PFN Wash' in between staining steps. Images were collected using confocal microscopy at room temperature.

6.5 Image Processing

6.5.1 Software

All images were processed using iVision software for Mac version 4.0.14 (BioVision Technologies). Where appropriate, script commands provided by iVision were used to automate imaging analysis.

6.5.2 Kymograph Generation

To generate kymographs from representative cells, a region of interest (ROI) (320x20 pixels) was designated that passed through the center of the contact and extended in either the X or Y dimension. This ROI was collected for all frames in the imaging run and compiled into kymographs showing SLP-76 microcluster movement over time. Kymographs were scaled such that 1 pixel in the x-axis corresponds to 164nm of distance and 1 pixel in the y-axis corresponds to 1 second in time.

6.5.3 Quantitation of MC dynamics

For each cell, 2 kymographs were generated and individual SLP-76 MC paths were manually traced for each kymograph. By measuring displacement along the X- and Y-axes, iVision software was then used to extract SLP-76 microcluster movement and persistence from the individual traces. For each cell the average duration, distance travelled and maximum speed were calculated from these cluster traces. The fraction of SLP-76 intensity in microclusters and number of microclusters were measured directly from each kymograph. Finally, a composite kymograph representing the weighted average of all SLP-76 MC paths was calculated for each cell. For each condition, 10 or more cells were analyzed. Parameter average were derived from the per cell values, and

composite kymographs were averaged to obtain a plot of SLP-76 MC movement over time, with the brightness of the line corresponding to the fraction of SLP-76 MC remaining. These processes were automated using scripting commands from iVision software.

SLP-76 MC originating later than 2.5 minutes into the imaging run were ignored, as these would generate artificially short traces. Similarly, SLP-76 MC originating 15 pixels (2.46 μm) from the center of the contact were also excluded, as these would generate artificially immobile SLP-76 MC. Unless otherwise indicated, 10 individual cells were analyzed across three experiments.

6.6 Biochemical Assays

6.6.1 Western Blotting

Jurkat T cells were stimulated with the anti CD3ε antibody OKT3 (Bio-Express). Western blotting was performed using antibodies for GFP (JL-8 - Clontech), Vav, or phosphotyrosine (4G10 - Millipore). For immunoprecipitations, Jurkat E6.1 cells were transfected with Vav1mutant chimeras tagged with mYFP. Two days post transfection, the bulk population of cells was stimulated with 1:500 soluble C305 for 5 minutes at 37˚C. Stimulation was stopped by a quick rinse in ice-cold PBS with 10 mM NaF and 1 mM Na_3VO_4. Cells were then lysed immediately in buffer containing 20 mM Tris-HCl pH 8.0, 100 mM NaCl, 1 mM EDTA, 1% Triton X-100, 10 mM NaF, 1 mM Na_3VO_4, and Complete Protease Inhibitor Cocktail (Roche).

6.6.2 Co-Immunoprecipitation

Jurkat E6.1 cells were transiently transfected with Vav1 constructs fused with mYFP. One day post-transfection $5x10^6$ cells per condition were stimulated with 1:500 C305 for 5 minutes at 37^oC. Ice-cold PBS with 10mM NaF and 1mM Na_3VO_4 was added to stop the stimulations. Vav1 constructs were immunoprecipitated using anti-GFP antibody (ab290 - Abcam) bound to Protein A beads (Pierce) for 16 hours at 4˚C.

6.7 Functional Assays

6.7.1 NF-AT Activation

NFAT activation was carried out as described previously [Nguyen, Sylvain et al. 2008]. Cells were cotransfected with a construct in which Renilla was expressed under a constitutively active promoter and a construct for Luciferase under the control of an NFAT AP-1 element of the IL-2 promoter. In addition, cells were transfected with either Vav1 shRNA or an empty hairpin control and either a fluorescent protein marker or a Vav1 chimera that had been rendered immune to the shRNA through point mutation. To measure NFAT activity, cells were stimulated on anti-TCR coated glass coverslips and luminescence was read on a Trilux plate reader. NFAT-Luciferase responses were normalized to an internal Renilla luciferase control and reported as a percentage of maximum stimulation with PMA and ionomycin.

6.7.2 CD69 Upregulation

Both CD69 upregulation and calcium flux analyses were performed by FACS, using a BD LSRII. In all cases, cells were transfected with vectors encoding either mYFP or

Vav1.mYFP fusion proteins, and CD69 upregulation was measured in gated on populations of cells expressing equal amounts mYFP. For CD69 assays, $2x10^5$ Jurkat T cells were stimulated with 10 ng/ml OKT3 or 50 ng/ml PMA for 16 hours at 37°C. Cells were stained with anti-CD69 antibodies conjugated with phycoerythrin (PE)-Cy5 (BD Pharmingen) for 30 minutes on ice. CD69 upregulation was determined by FACS and normalized to Vav1 deficient cells reconstituted with wild-type Vav1. To ensure comparisons between cell populations expressing comparable amounts of exogenous protein, cells were gated based on Vav1.mYFP expression.

6.7.3 Calcium Flux

Calcium flux assays were performed by FACS, using a BD LSRII. $1x10^6$ cells were stained with 10 uM Indo-1 for 1 hour at 37°C in HBSS supplemented with 1.25 mM $CaCl_2$, 0.9 mM $MgCl_2$ and 0.05% BSA. Basal calcium was read for 2 minutes at which point OKT3 was added to a final concentration of 30 ng/ml and calcium flux was measured over 10 minutes. After this time, ionomycin was added to a final concentration of 10 μM and peak calcium was read for 3 minutes. Null, moderate, and high subpopulations of cells were gated on the basis of the amount of mYFP in the cells in each group. Calcium responses were calculated as the ratio of calcium-bound to unbound indo-1 fluorescence (420nm/460nm). Comparisons between subpopulations and across samples were made by determining the percentage change in the area under the curve relative to the internal null population. Calcium flux data was analyzed using FlowJo (Version 8.5.3) and Microsoft Excel software.

6.8 Statistical Analysis

Unless otherwise indicated, error bars are presented as Standard Error of the Mean (SEM). To determine statistical significance, data were analyzed using Student's two-tailed t-test for unpaired samples with equal variance. P values less than or equal to 0.05 were considered statistically significant.

For CD69 upregulation and calcium flux assays, statistically significant differences are denoted by colored boxes. When $P < 0.05$ for the indicated conditions, a black box is used. For dominant-negative effects (below mYFP), a red box was used; green boxes were used to indicate responses that were enhanced compared to WT Vav1. Trends ($0.05 < P < 0.10$) are denoted by gray, orange, and yellow boxes. White boxes indicate no significant differences.

7 Results

7.1 Result I: Vav1 is recruited into SLP-76 MC and increases their persistence and function

7.1.1 Rationale I

In the absence of the three N-terminal tyrosines of SLP-76 (112, 128, 145 – termed SLP-76 Y3F), SLP-76 MC form but do not persist and are not competent to transduce signals leading to T cell activation [Bunnell, Singer et al. 2006]. These tyrosines become phosphorylated following TCR stimulation and serve as docking sites for other adapter and effector proteins. Therefore, the proteins recruited to the N-terminal tyrosines could be required for the persistence and function of SLP-76 MC. One of the proteins that bind to the phosphorylated tyrosines of SLP-76 is the Rho-family GEF Vav1 [Jordan, Sadler et al. 2006]. Defects in Vav1 deficient mice mirror those seen in SLP-76 deficient mice [Fujikawa, Miletic et al. 2003; Pivniouk, Tsitsikov et al. 1998]. In addition, Vav1 and SLP-76 synergize to enhance T cell activation [Wu, Motto et al. 1996], suggesting that these two proteins function in the same pathway. I hypothesized that Vav1 is recruited to the tyrosines of SLP-76 following TCR stimulation, where it enhances SLP-76 MC persistence and function. To test this hypothesis, I performed imaging experiments to determine whether Vav1 is recruited to SLP-76 MC following TCR stimulation and whether the absence of Vav1 could replicate the defect observed in the SLP-76 Y3F mutant.

7.1.2 Vav1 enters SLP-76 MC following TCR stimulation

To determine whether Vav1 is present in SLP-76 microclusters following TCR stimulation, I performed live cell imaging using Jurkat T cells responding to anti-TCR coated glass coverslips. Prior to imaging, Jurkat E6 cells were transfected with plasmids encoding SLP-76 tagged with CFP (SLP-76.CFP) and either wild-type Vav1 tagged with YFP (Vav.YFP) or YFP alone. Upon contacting the stimulatory surface, SLP-76 entered signaling microclusters. In contrast, in the absence of a fusion partner, YFP remained uniformly distributed in the cytoplasm (Figure 12, top row). When wild-type Vav1 was expressed as a fusion protein tagged with YFP, Vav1 entered signaling microclusters that colocalized with SLP-76 microclusters (Figure 12, bottom row). In the merged image, all microclusters observed were yellow, indicating a high degree of colocalization between Vav1 and SLP-76. Single Vav1 (green) or SLP-76 (red) microclusters were not observed, indicating that these proteins are recruited into the same complex. In addition, Vav1 seemed to enhance the recruitment of SLP-76 into microclusters, as the background fluorescence of SLP-76 (representing the fraction of protein that was not recruited into microclusters) was reduced in the presence of exogenous Vav1 (Figure 12 – top middle vs. bottom middle panels). These results confirm that Vav1 is recruited into SLP-76 containing signaling microclusters following TCR stimulation.

The phosphorylation of the N-terminal tyrosines of SLP-76 is required for many aspects of SLP-76 mediated T cell activation [Jordan, Sadler et al. 2006]. Immunoprecipitation experiments have shown that these critical tyrosines bind to Vav1 through SH2-dependent interactions [Tuosto, Michel et al. 1996]. This interaction could provide a

direct mechanism for Vav1 to enter SLP-76 MC. However, Vav1 also binds the adapters Grb2 and Nck through its N-terminal SH3 domain [Barda-Saad, Shirasu et al. 2010; Ogura, Nagata et al. 2002; Ramos-Morales, Romero et al. 1995]. Either of these proteins provides another potential route for Vav1 to enter SLP-76 MC: Grb2 also binds phosphorylated LAT and Nck binds to phosphorylated SLP-76. To determine whether the N-terminal tyrosines of SLP-76 are required for Vav1 to enter SLP-76 microclusters, I imaged SLP-76 MC formation in SLP-76 deficient (J14) Jurkat T cells that had been stably reconstituted with either WT SLP-76 or with the SLP-76 Y3F mutant. Prior to imaging, these cells were transiently transfected with Vav1 tagged with mRFP (Vav1.mRFP) or the mRFP fluorescent protein alone as a control. I found that WT Vav1 was able to enter SLP-76 MC in the presence of WT SLP-76, but not in the presence of SLP-76 Y3F (Figure 13, compare middle and bottom rows). These results show that the N-terminal tyrosines of SLP-76 are required for Vav1 to enter SLP-76 MC and are the primary route through which Vav1 enters SLP-76 MC.

Although ZAP-70 is the direct upstream kinase of SLP-76, these two proteins are found in separate, but adjacent, microclusters [Nguyen, Sylvain et al. 2008]. The TCR and ZAP-70 form the TCR microcluster, while downstream proteins such as LAT and SLP-76 form the SLP-76 microcluster. Although, Vav1 binds to the phosphorylated N-terminal tyrosines of SLP-76 (Figure 13 and [Raab, da Silva et al. 1997]), it has also been reported to bind directly to ZAP-70 [Katzav, Sutherland et al. 1994]. Since Vav1 can become phosphorylated in the absence of the Vav1-binding tyrosines of SLP-76 [Bezman, Lian et al. 2008], the interaction with ZAP-70 could provide a mechanism for

Vav1 to become activated in the absence of SLP-76. To determine whether Vav1 is primarily recruited to SLP-76 microclusters or TCR microclusters, I performed 3 color imaging of fixed cells to concurrently observe the positions of Vav1, SLP-76, and ZAP-70 (Figure 14). I imaged Vav1.mCFP (blue) and SLP-76.YFP (red) with respect to phosphorylated ZAP-70 (pY 319 – green). As observed previously by our lab [Nguyen, Sylvain et al. 2008], I found that SLP-76 and ZAP-70 entered distinct microclusters. I observed that Vav1 predominantly enters SLP-76 MC (purple overlay) and does not colocalize with ZAP-70 (green). Therefore, SLP-76 and Vav1 enter microclusters that are distinct from ZAP-70-containing microclusters.

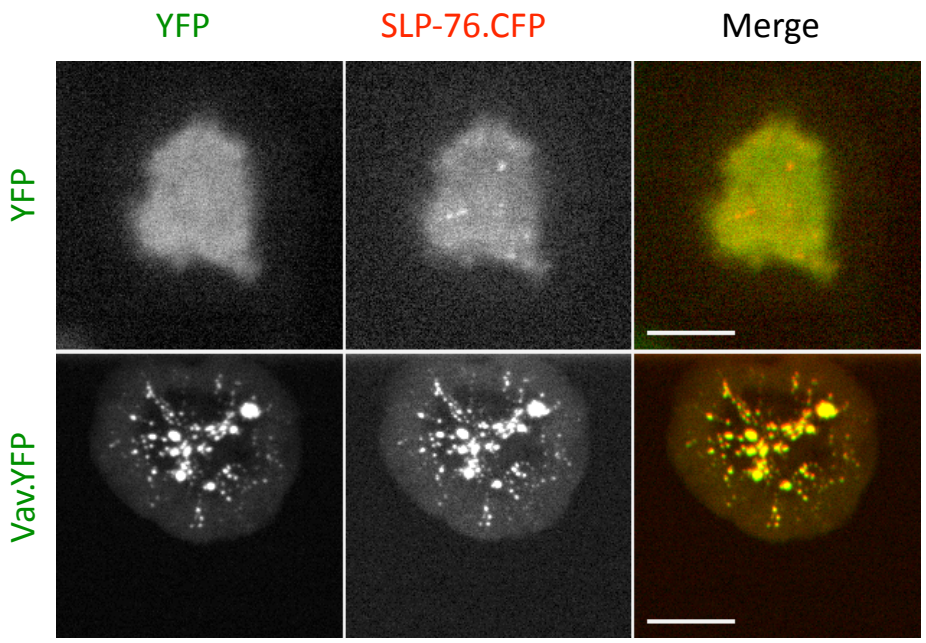

Figure 12: Vav1 and SLP-76 colocalize in microclusters

Jurkat E6 cells transiently expressing Vav1 tagged with YFP (Vav1.YFP – shown in green) and SLP-76 tagged with CFP (SLP-76.CFP – shown in red) were imaged on glass coverslips coated with 10 µg/ml OKT3. Still images were collected from cells responding to the stimulatory coverslips. Representative images from three experiments are shown. Scale bars represent 10 µm.

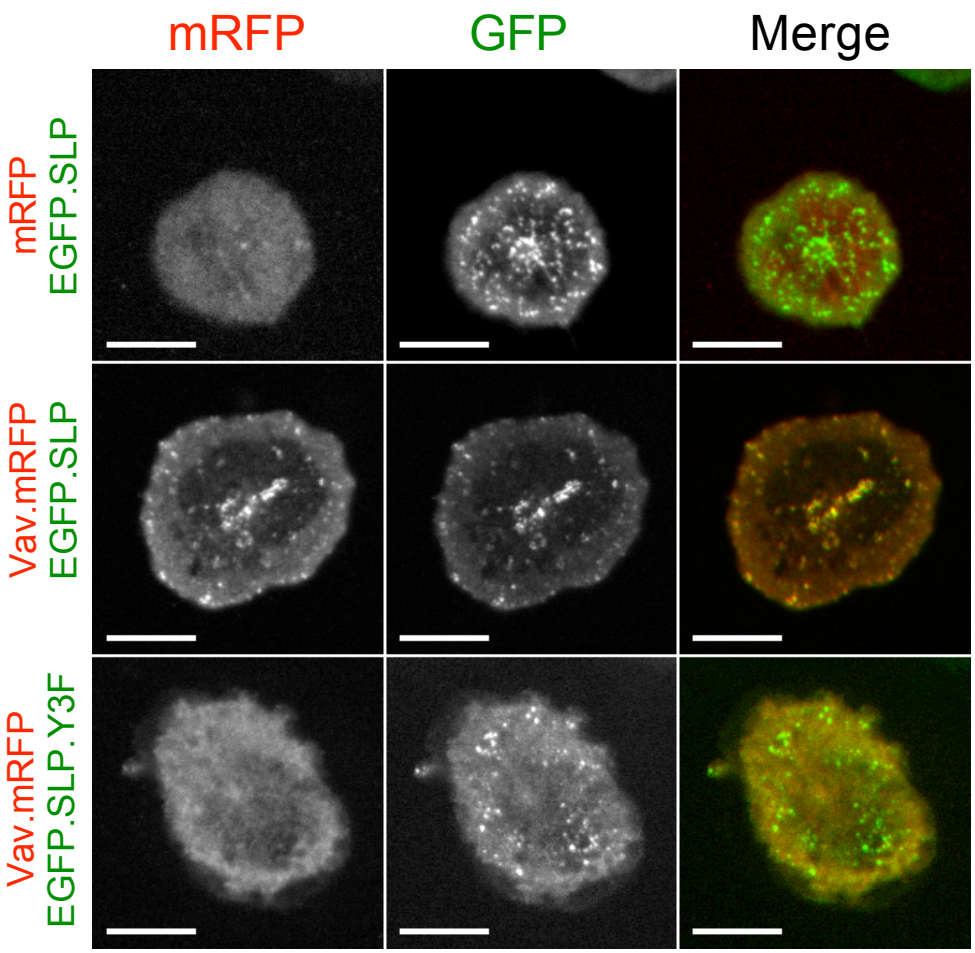

Figure 13: Vav1 binds to N-terminal tyrosines of SLP-76

SLP-76 deficient J14 cells stably expressing EGFP.SLP or EGFP.SLP.Y3F (green) were transiently transfected with plasmids encoding either mRFP or Vav.mRFP (red). These cells were then stimulated on glass coverslips coated with 3 µg/ml OKT3. After 5 minutes, the cells were fixed with 1% PFA and imaged by confocal microscopy. Images are representative of 3 experiments. Scale bars represent 10 µm.

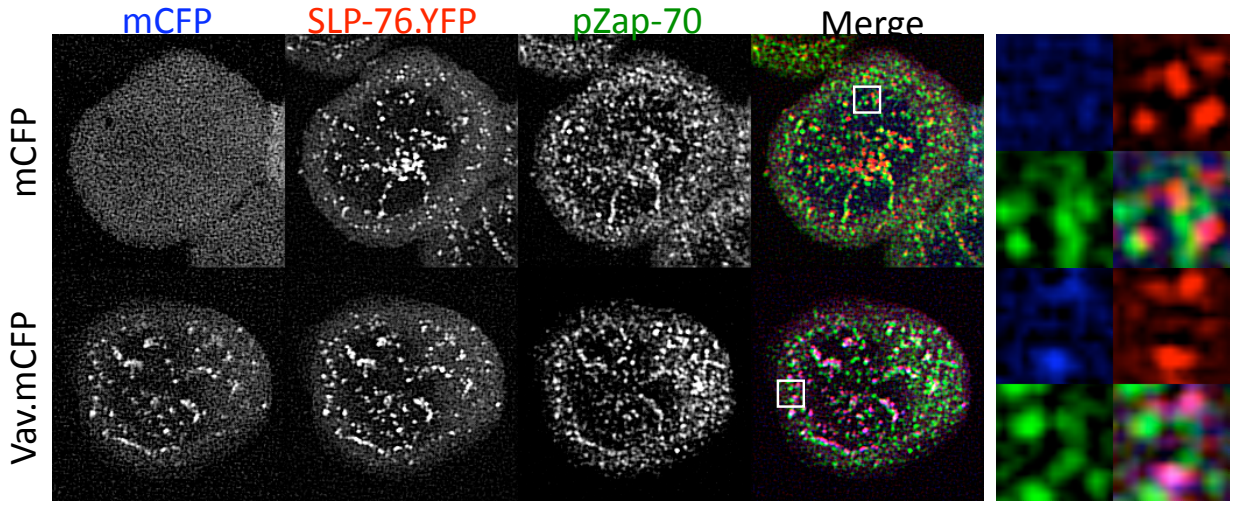

Figure 14: SLP-76 and Vav1 form distinct microclusters from ZAP-70

J14 cells stably expressing SLP-76 tagged with YFP (SLP-76.YFP - red) were transiently transfected with plasmids encoding either mCFP or Vav.mCFP (blue) and stimulated as described in Figure 13. The cells were fixed and stained with an antibody against ZAP-70 phosphorylated at tyrosine 319 (pZAP-70 - green). Close-up images of the area highlighted in the merged image are shown in the right hand panels. Post-acquisition, images were sharpened with a linear filter to more clearly define microcluster boundaries. Images are representative of 3 experiments.

7.1.3 Vav1 knockdown reduces MC persistence and movement

In the absence of the Vav1-binding tyrosines of SLP-76, microclusters form in response to TCR ligation, but they are short-lived and unable to mediate T cell activation [Bunnell, Singer et al. 2006]. These data suggest that Vav1 is required to form persistent SLP-76 MC that are competent to transduce TCR signals. To test this hypothesis, I observed SLP-76 MC in the absence of endogenous Vav1. I reduced Vav1 expression using a Vav1-specific short hairpin RNA (shRNA) expression vector. The Vav1 target sequence was chosen using the Dharmacon website (www.Dharmacon.com). This vector was cotransfected into J14.SY cells with a fluorescent protein marker to identify those cells receiving the knockdown hairpin. In addition, I created a Vav1 construct bearing a point mutation in the shRNA-targeting sequence to render the construct immune to the shRNA-mediated knockdown. Using these constructs together, I was able to reduce endogenous Vav1 levels and express exogenous, fluorescently-tagged Vav1 construct (Figure 15).

To determine the effect of Vav1 knockdown on SLP-76 MC formation and persistence, transfected cells were stimulated on a dose curve of anti-TCR antibody bound to glass coverslips and images were collected by confocal microscopy. Microcluster formation and persistence was assayed by eye. To quantify SLP-76 MC behavior, a numerical score from 1 to 3 was given to each cell representing the quality of the movement and persistence of the resultant microclusters. A score of 1 indicates short-lived microclusters that dissipate near their points of origin, while a score of 3 indicates persistent, mobile microclusters. The average scores from multiple cells per condition were averaged (Figure 16). I found that Vav1 sufficient cells begin to spread and form

microclusters on doses of 100 ng/ml OKT3. Generally, SLP-76 MC persistence and movement increase with higher doses of TCR stimulation. However, Vav1 deficient cells do not adhere or spread on lower TCR doses (not shown) and therefore did not form microclusters until they were stimulated with 1000 ng/ml OKT3. Approximately 10-fold higher concentrations of OKT3 were needed for Vav1 deficient cells to achieve the same score as Vav1 sufficient cells. These data indicate that Vav1 plays a role in cell spreading and adhesion to stimulatory surfaces, especially under weakly stimulating conditions. In addition, when SLP-76 MC do form in Vav1 deficient cells, they are less mobile and persistent than those formed in Vav1 sufficient cells. The greatest difference between Vav1 sufficient and –deficient cells was observed at OKT3 doses of 3000 ng/ml. Since this condition produced the largest dynamic range, all subsequent imaging experiments were performed using 3000 ng/ml OKT3.

In the presence of Vav1, SLP-76 MC form in the periphery and migrate toward the center of the cell:glass contact. To show this movement in a still image, I produced maximum-over-time (MOT) projections from movies by populating each pixel with the maximum value observed at that point over time. The resulting MOT image depicts persistent, mobile SLP-76 MC as radial spokes (Figure 17A). Using Vav1 shRNA, I found that Vav1 knockdown produces SLP-76 MC that do not persist and do not move from their points of origin, as seen by the static spots observed in MOT images. The defect in SLP-76 MC persistence and movement is corrected by the addition of exogenous Vav1. To obtain quantitative data regarding the movement and persistence of SLP-76 MC, kymographs were generated from diametric regions of interest for 10 cells from each

condition. To generate kymographs, a region of interest (ROI) was defined for each cell and an image was compiled from this ROI at all timepoints in the imaging run. In empty hairpin control cells, SLP-76 MC form in the periphery of the cell and migrate toward the center of the cell:glass contact. In the kymographs, this movement is represented by the diagonal lines that originate in the left and right edges of the kymoghraph and migrate toward the center, where they accumulate. In Vav1-knockdown cells, the microcluster traces appear vertical, indicating that no movement over time is occurring. In addition, the vertical length of the traces is reduced compared to Vav sufficient cells, indicating that microcluster persistence is also reduced. These defects are corrected by the addition of exogenous Vav1, which restores the inward movement (movement of lines in horizontal plane) and persistence (length of vertical traces) of SLP-76 MC (Figure 17B).

To obtain quantitative data regarding the behavior of SLP-76 MC in Vav1 sufficient and deficient cells, I manually traced individual SLP-76 MC paths from kymographs generated as above. For each trace, the distance travelled on the horizontal axis was directly proportional to the total movement of each microcluster and the vertical height was proportional to its duration. These values were extracted using the image processing software iVision. I also generated composite microcluster traces for each cell by taking the weighted position over time. To visualize the movement and persistence of SLP-76 MC obtained from multiple Vav1 sufficient and –deficient cells, the weighted average position was taken from 10 cells per condition (Figure 17C). Data derived from Vav1 mock knockdown microclusters are shown in red. These MC move an average distance of 2.5 ± 0.5 μm and persist for 180.8 ± 12.4 seconds. Vav1 knockdown (blue line)

reduces MC movement (0.8 ± 0.1 μm, $p < 0.05$) and persistence (108.1 ± 13.2 seconds, $p < 0.005$). Adding back exogenous Vav1 (green line) restores MC movement (2.0 ± 0.5 μm) and persistence (202.5 ± 11.3 seconds) such that the difference from mock knockdown cells are not statistically significant (Figure 17D). These data indicate that Vav1 is a critical factor required for the stability and mobility of SLP-76 MC.

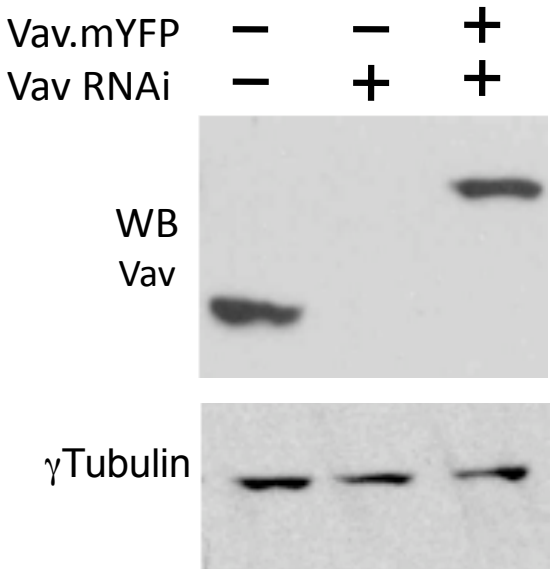

Figure 15: Vav1 shRNA reduces endogenous Vav1 expression

Jurkat T cells were cotransfected with plasmids encoding either an empty hairpin control or Vav1 shRNA and either a plasmid encoding either mYFP or Vav1.mYFP that had been rendered immune to the hairpin through silent point mutation. Four days post transfection, bulk whole cell lysates were analyzed for Vav1 expression by Western blot. γTubulin was used as a loading control.

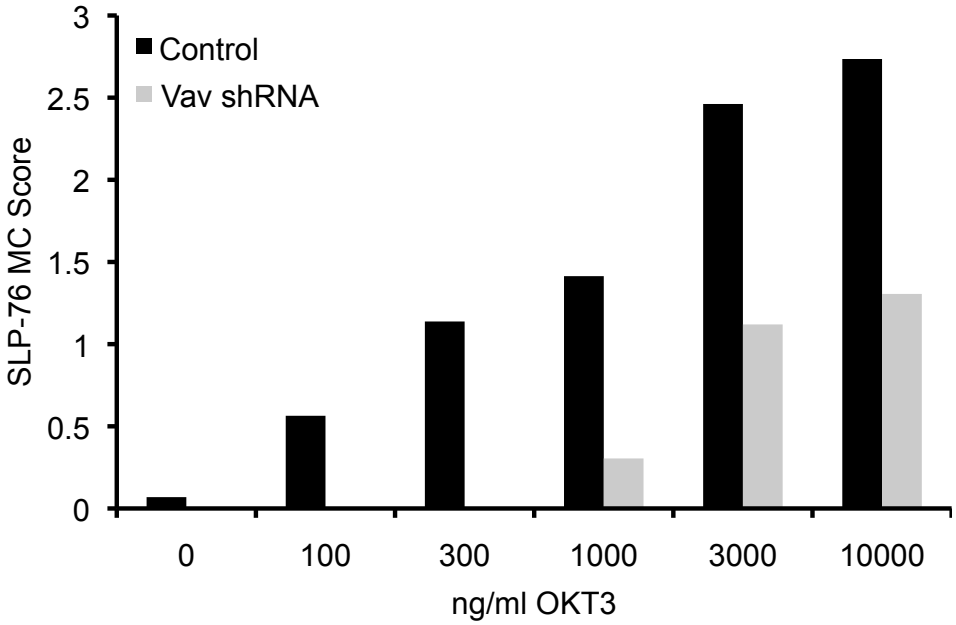

Figure 16: Vav1 affects T cell response across varying degrees of stimulation

J14.SY cells were cotransfected with plasmids encoding an mCFP marker and either Vav1 shRNA or an empty hairpin control. Four days post-transfection, cells were stimulated on varying doses of OKT3 and SLP-76 MC were observed by confocal microscopy. The persistence and movement of microclusters in mCFP-expressing cells was observed and assigned a numerical value (0-3) based on the persistence and movement of SLP-76 MC observed. The average score is presented from greater than 20 individual cells per condition across two experiments.

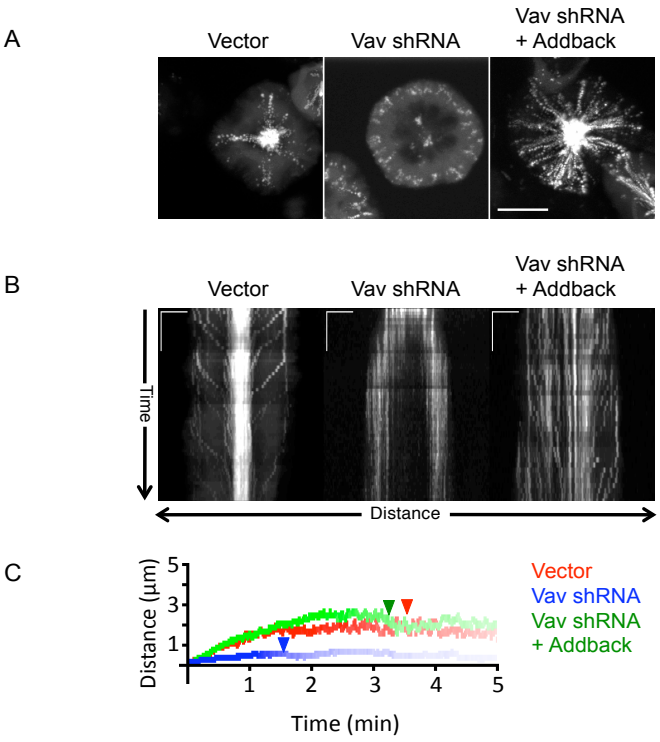

D

	Vector	Vav shRNA	Vav shRNA + Addback
Persistence (sec)	202.51 ± 11.29	108.05 ± 13.25 **	180.76 ± 12.41
Movement (µm)	2.00 ± 0.49	0.83 ± 0.13 *	2.47 ± 0.46
Speed (nm/sec)	163.30 ± 24.58	136.80 ± 11.63	170.10 ± 21.94
% SLP in Clusters	56.40 ± 2.76	31.20 ± 4.81 **	66.60 ± 4.57
Clusters per cell	19.00 ± 1.19	21.90 ± 2.06	21.40 ± 1.64

Figure 17: Vav1 knockdown reduces SLP-76 MC persistence and movement

J14.SY cells were transiently transfected with plasmids encoding an empty hairpin control and an mCFP marker (Vector), Vav1 shRNA and an mCFP marker (Vav shRNA), or Vav1 shRNA and Vav1.mCFP rendered immune to knockdown through silent point mutation (Vav shRNA + Addback). **A –** Representative MOT images of Vav1 sufficient and –deficient cells from three experiments. Scale bars represent 10 µm. **B -** Representative kymographs depicting the inward movement of SLP-76 MC (x-axis) over time (y-axis) are shown. Kymographs were generated from 10 representative cells per condition across 3 experiments. Scale bars (top left) represent 5 µm and 60 s. **C -** Individual SLP-76 MC paths were manually traced from kymographs generated in B. Mean microcluster traces for each cell were averaged to yield composite kymographs depicting fractional persistence (line intensity) over time (x-axis) and microcluster movement (y-axis). Arrowheads represent the half-life of SLP-76 MC for each condition. **D -** Mean values for the duration and movement of SLP-76 MC were extracted from individual traces. These mean values are shown ± SEM. Single and double asterisks indicate statistical significance relative to cells transfected with vector control ($P < 0.05$ and $P < 0.005$, respectively). For B, C, and D, 10 cells per condition were analyzed across 3 experiments; each individual cell was weighted equally.

7.1.4 Vav1 knockdown reduces T cell activation

To determine the functional significance of the reduced microcluster persistence observed in the absence of Vav1, I stimulated Vav1 sufficient and deficient cells with anti-TCR antibody and measured NF-AT activity and upregulation of surface CD69. Vav1 is involved in each of these outcomes following TCR stimulation [Cao, Janssen et al. 2002; Kaminuma, Deckert et al. 2001]. Vav1 activated a composite NFAT-AP-1 element derived from the Il2 promoter in a GEF-independent manner [Kuhne, Ku et al. 2000], suggesting that calcium flux and NFAT activity are mediated by scaffolding functions of Vav1. Conversely, upregulation of CD69 is thought to be dependent upon the Vav1 GEF activity, which functions through the activation of JNK and AP-1 [Cao, Janssen et al. 2002; Castellanos, Munoz et al. 1997; Zugaza, Lopez-Lago et al. 2002].

NF-AT activity was measured across a dose curve of plate-bound anti-TCR antibody. Vav1-knockdown cells consistently showed reduced NF-AT responses at all doses of OKT3 tested (Figure 18), comparable to the reduced SLP-76 MC persistence observed in our imaging assays. I also found that reconstitution with exogenous WT Vav1 restored NF-AT activity to cells receiving the Vav1 shRNA. In addition, Vav1 knockdown reduced surface expression of CD69 following TCR stimulation (Figure 19), in agreement with previous studies [Cao, Janssen et al. 2002]. These data indicate that Vav1 is required for optimal T cell activation following stimulation through the TCR. However, Vav1 knockdown cells are still able to moderately increase CD69 expression, which could be due to compensation by endogenous Vav2 and Vav3. In addition, the results presented in this section and in section 7.1.3 are consistent with the hypothesis

that the formation and persistence of SLP-76 MC are required for T cell activation. In particular, the scaffolding interactions mediated by Vav1 contribute to generation of calcium flux to drive NFAT activity, while the GEF activity drives AP-1 activation through JNK. However, these experiments do not discriminate between structural and enzymatic functions of Vav1 with respect to SLP-76 microcluster persistence.

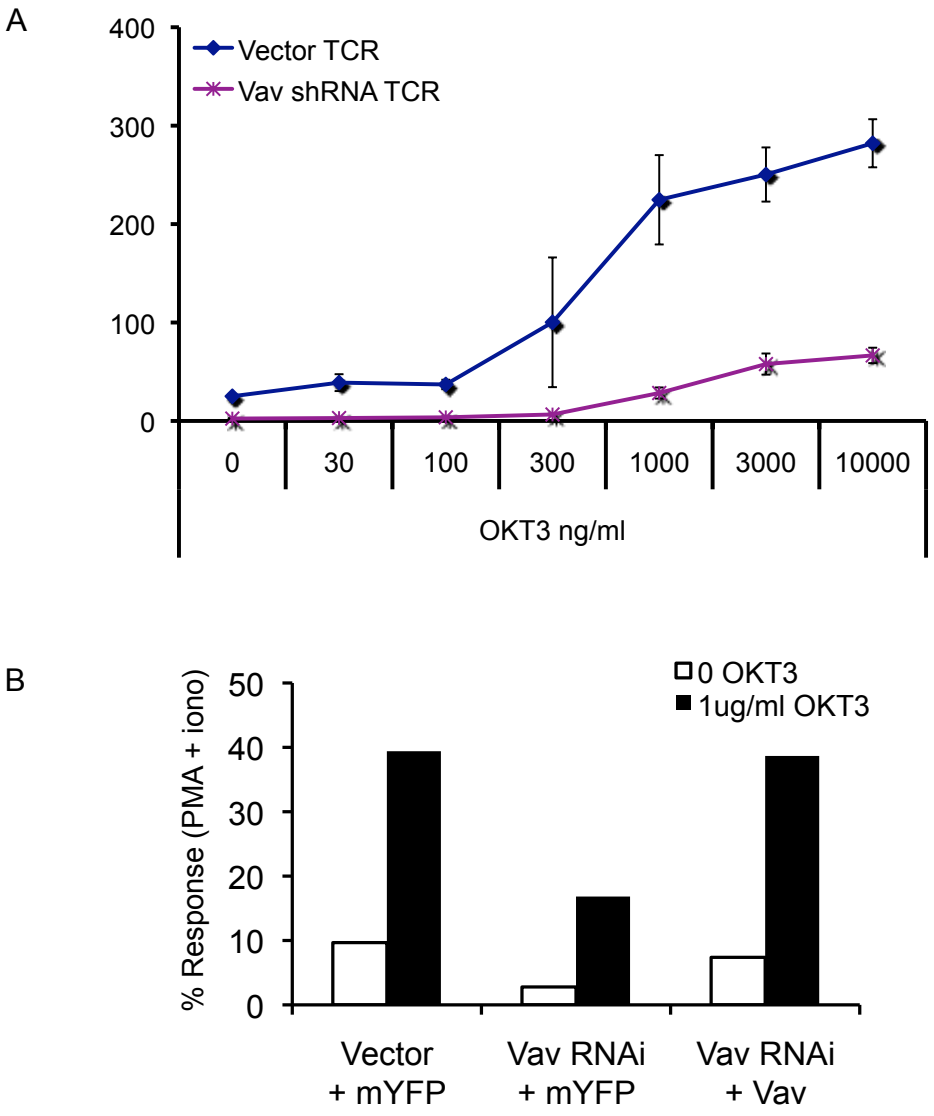

Figure 18: Vav1 knockdown reduces NFAT activity

NFAT activity was assayed in J14.SY cells expressing empty hairpin control, Vav1 shRNA, or Vav1 shRNA with exogenous Vav1.mCFP added back. **A -** Cells were stimulated on a dose curve of plate-bound OKT3 antibody. NFAT activity was measured by the production of luciferase from a composite NFAT-AP-1 element derived from the IL-2 promoter and normalized to renilla expression under the control of a constitutively active promoter. Data are presented as the average of 3 experimental per condition ± standard deviation. **B -** NFAT activity was measured in cells stimulated on plates coated with 1 μg/ml OKT3. One representative experiment of 4 is shown.

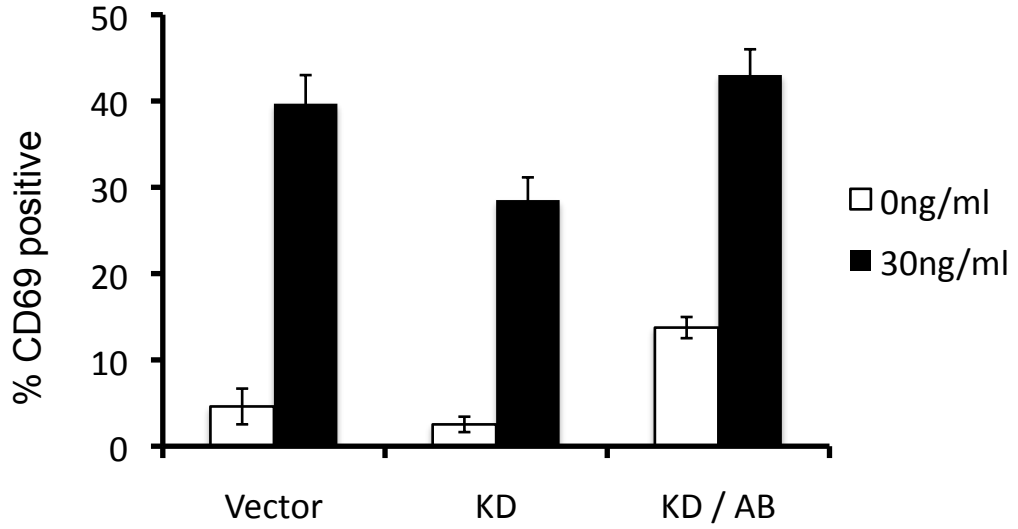

Figure 19: Vav1 knockdown reduces CD69 upregulation

Surface expression of CD69 was measured in J14.SY cells expressing empty hairpin control and mCFP marker (Vector), Vav1 shRNA and mCFP marker (KD), or Vav1 shRNA with exogenous Vav1.mCFP added back (KD / AB). Cells were stimulated for 16 hours with 30 ng/ml of soluble OKT3. The surface expression of CD69 was then measured by FACS in a population of cells tightly gated for moderate levels of mCFP. The average of 3 experiments ± SEM is shown.

7.1.5 Vav1 C-terminal domains are required for localization to SLP-76 MC

Since the Vav1 is not recruited into SLP-76 MC in the absence of the N-terminal tyrosines of SLP-76 (Figure 13) and the Vav1 SH2 domain binds to SLP-76 [Tuosto, Michel et al. 1996], I hypothesized that this domain of Vav1 was critical to its entry into SLP-76 MC. However, the Vav1 SH3 domains mediate protein-protein interactions with other SLP-76 MC components. These scaffolding interactions may be required to stabilize the SLP-76 MC. Therefore, I also wanted to determine how these domains contribute to SLP-76 MC persistence and movement. A diagram of the Vav1 mutants used in this section is presented in Figure 20.

To evaluate SLP-76 MC in the presence of various Vav1 mutants, I used a model system in which Vav1 mutant chimeras could be added to a Vav1-null background. For this purpose I used the Vav1 deficient Jurkat cell line J.Vav [Cao, Janssen et al. 2002]. To make this cell line amenable to our imaging assay, I stably transfected J.Vav cells with an mCFP-tagged SLP-76 chimera (SLP-76.mCFP) to produce the J.Vav SLP-76.mCFP cell line (JV.SC). When transfected with vectors expressing mYFP alone, JV.SC cells produce immobile SLP-76 MC that remain near their points of origin (Figure 21A), as seen by spots in MOT images. In contrast, when JV.SC cells are reconstituted with WT Vav1, mobile, persistent SLP-76 MC are formed, as seen in the radial 'spokes' in MOT images. In addition, Vav1 and SLP-76 colocalize in JV.SC cells, as indicated by the yellow overlay, in agreement with experiments performed in the J14.SY cell line. I also confirmed that expressing wild-type Vav1.mYFP fusion proteins in the parental J.Vav cell line could restore Vav1 function. Using a FACS-based assay, I compared

populations of cells expressing equal amounts of either mYFP or Vav1.mYFP fusion protein. I found that Vav1 deficient cells showed defective calcium flux following TCR stimulation, in agreement with previous studies [Cao, Janssen et al. 2002]. However, J.Vav cells were able to weakly increase calcium levels following TCR stimulation due to compensation by other Vav-family members (most likely Vav3) present in this cell line [Fujikawa, Miletic et al. 2003]. Calcium elevations were increased in cells expressing a wild-type Vav1.mYFP fusion protein compared to untransfected cells from within the same population (Figure 21B). These data confirm that the J.Vav cell line is an appropriate model system to use for both imaging and functional reconstitution studies.

To determine how the C-terminal Src homology domains influence the behavior and function of SLP-76 MC, I transiently expressed Vav1 mutant chimeras in JV.SC cells. Individual Src homology domains were rendered non-functional by point mutation on key residues. Because Vav1 binds to the phosphorylated tyrosines of SLP-76 [Jordan, Sadler et al. 2006] and these tyrosines are required for Vav1 to enter SLP-76 MC (Figure 13), I hypothesized that the SH2 domain of Vav1 is critical for colocalization with SLP-76. As anticipated, inactivation of the Vav1 SH2 domain (R696A, SH2*) prevents Vav1 from entering microclusters (Figure 22). The Vav1 SH2 mutant appears cytoplasmic in imaging assays, similar to control Vav1 deficient cells expressing mYFP alone. Moreover, the SH2* mutant fails to increase SLP-76 MC movement or persistence, as seen by spots in MOT images, and short, vertical traces in kymographs. These imaging data show that the SH2 domain of Vav1 plays a critical role in the recruitment of Vav1 to

SLP-76 MC and the stabilization of SLP-76 MC. These data also suggest that Vav1 is unable to increase SLP-76 MC persistence because it does not enter the microcluster.

To quantify the movement and persistence of SLP-76 MC formed in the presence of the Vav1 SH2* mutant, I generated kymographs and manually traced microcluster paths as described in section 7.1.3. Individual SLP-76 MC traces show that cells expressing Vav1 SH2* produced SLP-76 MC that were immobile and dissipated shortly after formation (Figure 23). To identify mobile, persistent SLP-76 MC, I set an arbitrary threshold to show individual SLP-76 MC persisting for more than 90 seconds or moving more than 2 μm. Of 204 SLP-76 microclusters analyzed, only 64 (30.4%) were above the threshold (Figure 23A – left panel). I generated composite kymographs showing SLP-76 MC movement and persistence from all microclusters traced from JV.SC cells expressing mYFP, Vav1.mYFP, or Vav1 SH2*.mYFP (Figure 23A – right panel). These composite kymographs show that SLP-76 MC movement and persistence in the presence of the Vav1 SH2* mutant closely resemble that observed in Vav1 deficient cells. To quantify these defects, SLP-76 MC movement, persistence, and speed were extracted from individual microcluster traces. I found that persistence, distance traveled, and speed were not significantly different than SLP-76 MC formed in the absence of Vav1 and were significantly reduced compared to SLP-76 MC formed in the presence of WT Vav1 (Figure 23B). Moreover, Vav1 SH2* was unable to increase the fraction of SLP-76 recruited into microclusters. This measurement reflects the stability of the microcluster and could indicate that the multivalent interactions that retain proteins within the microcluster are not present when Vav1 is absent from the microcluster. In addition, the

total number of SLP-76 MC observed per cell was reduced, which indicates defects in the mechanism of microcluster formation. These imaging data show that the SH2 domain of Vav1 is critical for its entry into SLP-76 MC and for increasing SLP-76 MC persistence and movement. These data suggest that Vav1 must enter SLP-76 MC to stabilize these structures.

Each of the Vav1 SH3 domains binds to proteins that could contribute to the recruitment of Vav1 into the microcluster. The N-terminal SH3 domain binds to the adapters Nck and Grb2, which bind SLP-76 and LAT, respectively [Barda-Saad, Shirasu et al. 2010; Ye and Baltimore 1994]. The C-terminal SH3 domain binds the GTPase Dynamin2, which also binds Grb2 and presents a potential mechanism to recruit Vav1 to SLP-76 MC [Yoon, Koh et al. 1997]. However, neither the atypical binding surface of the N-terminal SH3 domain (P657A, N-SH3*) nor classical binding surface of the C-terminal SH3 domain (WW820/821YY, C-SH3*) were required for Vav1 to enter SLP-76 MC (Figure 24 – left panels). In addition, each of these mutants increased SLP-76 MC persistence and movement, though the N-SH3* mutant performed less well than the C-SH3* mutant (Figure 24 – right panels). To quantify SLP-76 MC behavior, I generated kymographs and manually traced SLP-76 MC paths as above. Both mutants significantly increased the stoichiometry of SLP-76 recruitment into microclusters and the persistence and movement of SLP-76 MC relative to JV.SC cells expressing mYFP alone (Figure 25A and B). Composite traces revealed that 84.5% of N-SH3* microclusters and 90.6% of C-SH3* microclusters crossed our arbitrary persistence and movement thresholds. By all measures, the N-SH3* mutant performs slightly less well than the C-SH3* mutant,

though neither were significantly different than WT Vav1. In contrast to the SH2 domain, the individual SH3 domains of Vav1 are not necessary for recruitment to and stabilization of SLP-76 MC.

Though the mutation of the individual SH3 domains did not significantly reduce SLP-76 MC persistence and movement, multivalent interactions can contribute to the overall avidity of signaling complexes [Braiman, Barda-Saad et al. 2006; Bunnell, Singer et al. 2006; Houtman, Yamaguchi et al. 2006]. The Vav1 SH3 domains each mediate protein-protein interactions that could contribute to multivalent interactions, increasing microcluster avidity; the N-terminal SH3 domain binds to Grb2 and Nck, which bind LAT and SLP-76, respectively [Barda-Saad, Shirasu et al. 2010; Hobert, Jallal et al. 1994; Lazer, Pe'er et al. 2007; Ye and Baltimore 1994]. In addition, the C-terminal SH3 domain binds Dynamin2, which interacts with Grb2 [Gomez, Hamann et al. 2005; Yoon, Koh et al. 1997]. To test whether the Vav1 SH3 domains possess redundant functions, I observed the behavior of a Vav1 construct in which both SH3 domains were point mutated (N3*C3*). This mutant was recruited into SLP-76 MC that were initially mobile (Figure 24). However, the N3*C3* mutant significantly exacerbates the persistence defects seen in the individual SH3 mutants. SLP-76 MC dissociated after moving 1.91 ± 0.34 μm and did not accumulate in the center of the cell:glass contact (Figure 24, right panels). While the SH3 domains were not required for the recruitment of Vav1 into SLP-76 MC or for the movement of SLP-76 MC, this mutant displayed the unique phenotype of movement despite the reduced persistence. This indicates that the SH3 domains of Vav1 are involved in the persistence of SLP-76 MC, rather than their movement. In

addition, it shows that the defect in SLP-76 MC movement observed in Vav1-null cells and the Vav1 SH2* mutant are not secondary defects caused by reduced SLP-76 MC persistence. Quantification of individual SLP-76 MC revealed an intermediate phenotype for SLP-76 MC persistence, movement, speed, and in the stoichiometry of SLP-76 recruitment into microclusters (Figure 25). Also, composite traces reveal that SLP-76 MC containing the N3*C3* mutant begin to slow down at approximately 90 - 120 seconds, which is closely related to the mean persistence of these microclusters (98.38 seconds). This indicates that the instability of the SLP-76 MC containing the Vav1 N3*C3* mutant resulted in the premature dissociation of movement-promoting factors. These data indicate that the Vav1 SH3 domains play redundant functions in the stability of SLP-76 MC, but are largely dispensable for their movement.

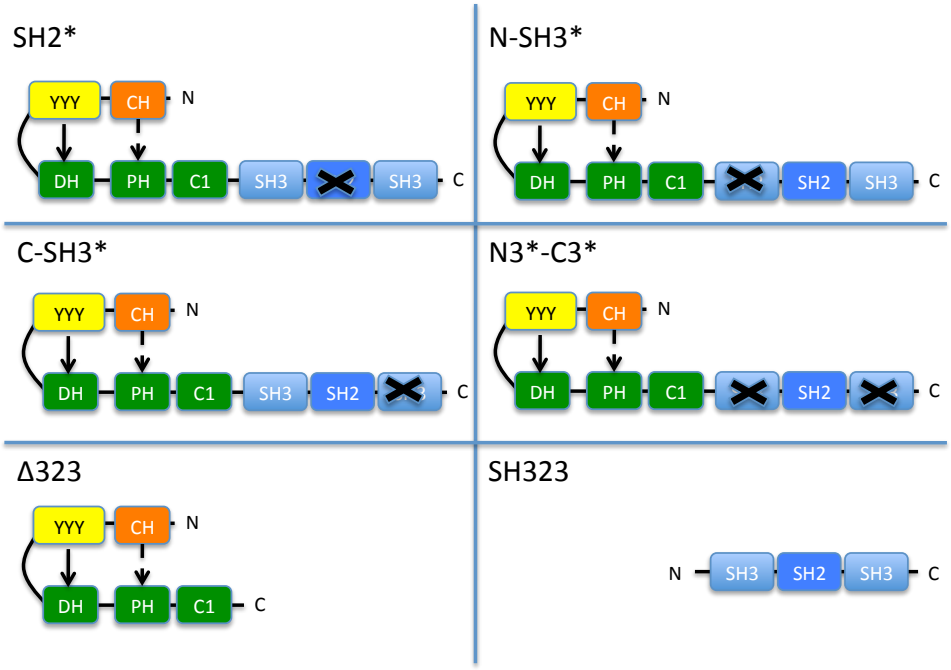

Figure 20: Diagram of Vav1 mutants used in this section

Simplified cartoon diagram of Vav1 mutants used in this section. For each mutant, the predicted effect of each mutation with regards to the open vs. closed conformation of Vav1 is shown. Solid and dashed arrows represent inhibitory folding mediated by the CH domain and N-terminal tyrosines.

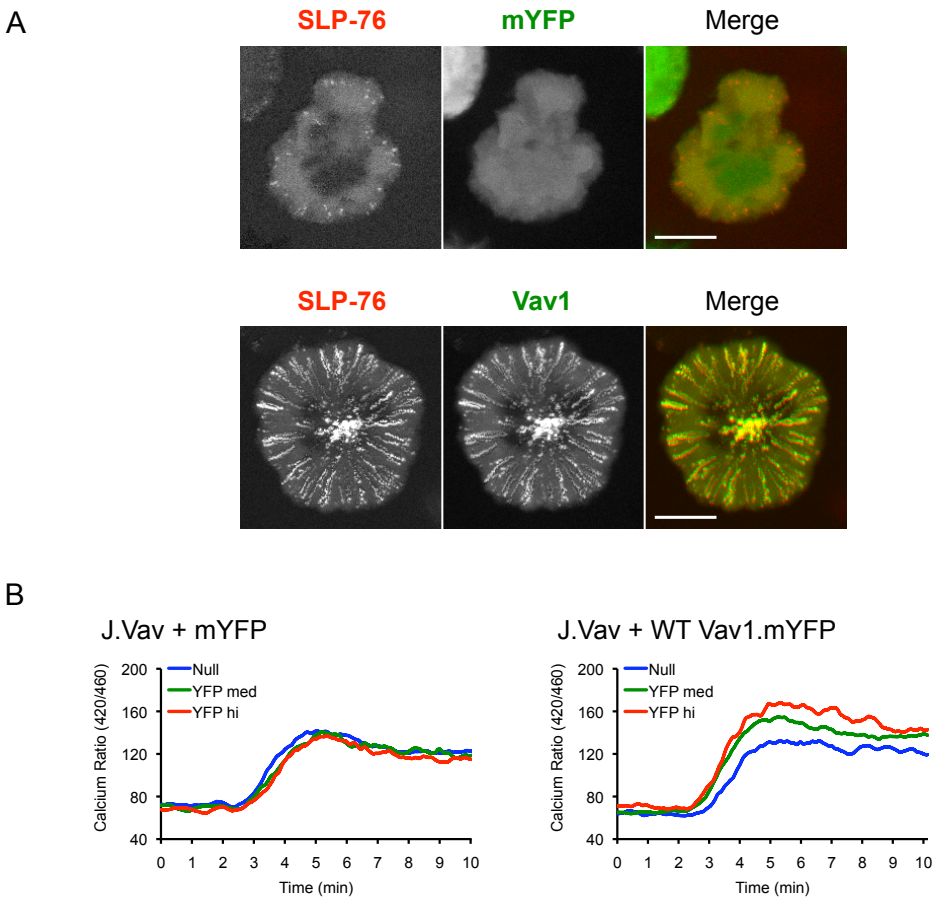

Figure 21 JV.SC cell line as a model for Vav1 reconstitution

A - JV.SC cells were transiently transfected with plasmids encoding mYFP or Vav1.mYFP. One day post-transfection, cells were stimulated on glass coverslips coated with 3 µg/ml OKT3 and imaged for 5 minutes by confocal microscopy. Representative MOT projections are shown. Vav1.mYFP and mYFP are shown in green and SLP-76 is shown in red. Scale bars correspond to 10 µm. **B** – J.Vav cells were transiently transfected with plasmids encoding mYFP or wild-type Vav1.mYFP. One day post transfection, cells were stained with the ratiometric calcium-sensitive dye Indo-1 and calcium flux was monitored by FACS on tightly gated populations of cells lacking mYFP expression (null) and cells expressing medium and high amounts of fluorescent protein.

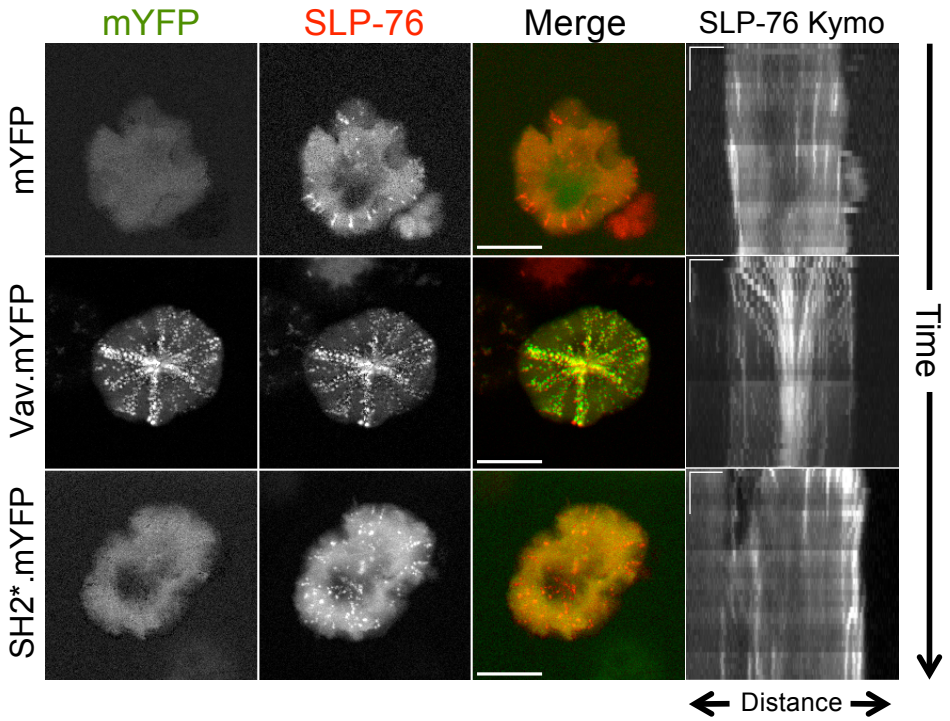

Figure 22: Vav1SH2 domain is required for localization to MC

JV.SC cells were transiently transfected with plasmids encoding either mYFP or the indicated Vav1 construct as an mYFP fusion protein. One day post transfection, cells were imaged on glass coverslips coated with 3 µg/ml OKT3 for 5 minutes. SLP-76.mCFP is shown in red and mYFP constructs are shown in green. In the left panels, one representative MOT image from 3 experiments is shown. Scale bars correspond to 10 µm. In the right panels, kymographs were generated from these cells showing the inward movement (x-axis) over time (y-axis) of individual SLP-76 MC. Scale bars correspond to 5 µm and 60 s.

A

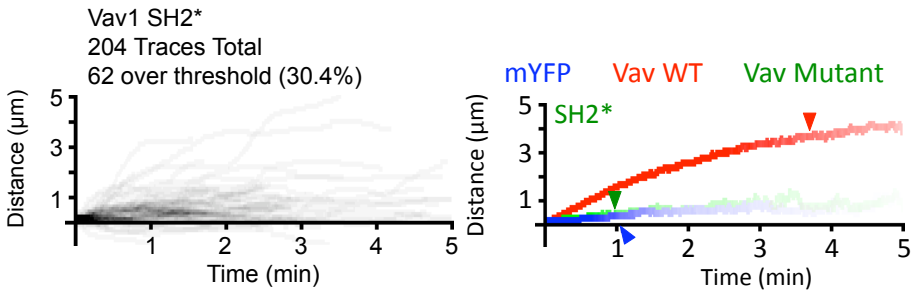

B

	Persistence (sec)	Movement (µm)	Speed (nm/sec)	% SLP in Clusters	Clusters per cell
mYFP	68.57 ± 3.93 ††	0.65 ± 0.03 ††	56.62 ± 2.12 ††	5.90 ± 0.67 ††	10.80 ± 0.84 ††
WT	180.51 ± 6.95 **	3.34 ± 0.19 **	102.96 ± 3.26 **	43.59 ± 2.83 **	19.15 ± 0.81 **
SH2*	74.23 ± 8.51 **	0.69 ± 0.05 ††	52.78 ± 4.35 ††	7.43 ± 1.34 ††	13.67 ± 1.82 ††

Figure 23: The SH2 domain is required for Vav1-dependent increases in SLP-76 MC persistence and movement

A – Left: Individual SLP-76 MC paths were traced from cells expressing the Vav1 SH2* mutant. Kymographs from 10 cells across 3 experiments were traced. Of the total SLP-76 MC traced, the graph displays all traces persisting for more than 90 s or moving more then 2 µm. The fraction of microclusters passing these criteria are shown compared to the total number of microclusters traced. **Right**: All microcluster traces acquired from each cell were averaged to yield composite kymographs depicting fractional persistence (line intensity) over time (x-axis) and microcluster movement (y-axis). Arrowheads represent the half-life of SLP-76 MC for each condition. **B –** To obtain mean values for the duration and movement of SLP-76 MC were extracted from individual traces. These mean values are shown ± SEM. Single and double asterisks indicate statistical significance relative to cells expressing mYFP alone, single and double daggers indicate statistical significance relative to cells expressing wild-type Vav1.mYFP ($P < 0.05$ and $P < 0.005$, respectively).

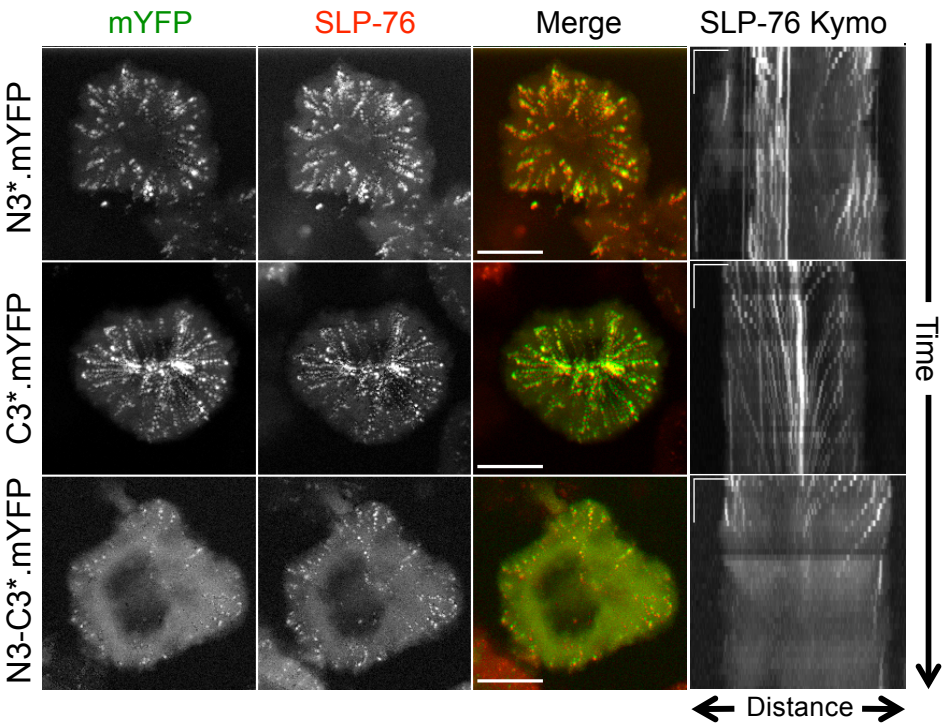

Figure 24: Vav1 SH3 domains function in tandem to increase SLP-76 MC persistence

JV.SC cells were transiently transfected with plasmids encoding the indicated Vav1 construct as an mYFP fusion protein. One day post transfection, cells were imaged on glass coverslips coated with 3 µg/ml OKT3 for 5 minutes. SLP-76.mCFP is shown in red and mYFP constructs are shown in green. In the left panels, one representative MOT image from 3 experiments is shown. Scale bars correspond to 10 µm. In the right panels, kymographs were generated from these cells showing the inward movement (x-axis) over time (y-axis) of individual SLP-76 MC. Scale bars correspond to 5 µm and 60 s.

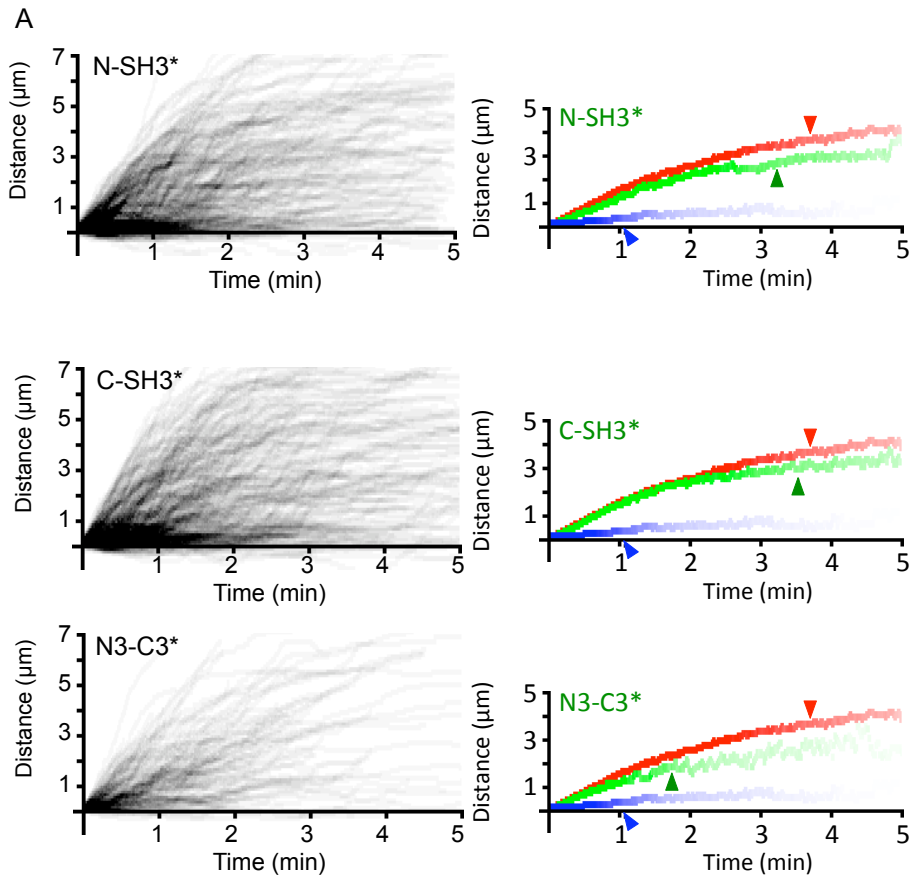

B

	Persistence (sec)	Movement (µm)	Speed (nm/sec)	% SLP in Clusters	Clusters per cell
mYFP	68.57 ± 3.93 ††	0.65 ± 0.03 ††	56.62 ± 2.12 ††	5.90 ± 0.67 ††	10.80 ± 0.84 ††
WT	180.51 ± 6.95 **	3.34 ± 0.19 **	102.96 ± 3.26 **	43.59 ± 2.83 **	19.15 ± 0.81 **
N-SH3*	164.98 ± 11.60 **	2.65 ± 0.26 **	99.67 ± 4.79 **	33.92 ±3.69 **	20.67 ± 1.51 **
C-SH3	181.69 ± 10.94 **	3.12 ± 0.28 **	104.80 ± 4.54 **	40.87 ± 4.45 **	22.67 ± 1.18 **,†
N3*C3*	98.38 ± 11.83 **,††	1.91 ± 0.34 **,††	85.40 ± 8.04 **,†	24.59 ± 5.99 **,†	16.00 ± 1.87 *

Figure 25: SH3 domain mutant analysis

A – Left: Individual SLP-76 MC paths were traced from cells expressing the indicated Vav1 mutant. Kymographs from 10 cells across 3 experiments were traced. Of the total SLP-76 MC traced, the graph displays all traces persisting for more than 90 s or moving more then 2 µm. The fraction of microclusters passing these criteria are shown compared to the total number of microclusters traced. **Right**: All microcluster traces acquired from each cell were averaged to yield composite kymographs depicting fractional persistence (line intensity) over time (x-axis) and microcluster movement (y-axis). Arrowheads represent the half-life of SLP-76 MC for each condition. **B –** To obtain mean values for the duration and movement of SLP-76 MC were extracted from individual traces. These mean values are shown ± SEM. Single and double asterisks indicate statistical significance relative to cells expressing mYFP alone, single and double daggers indicate statistical significance relative to cells expressing wild-type Vav1.mYFP ($P < 0.05$ and $P < 0.005$, respectively).

7.1.6 Contributions of Vav1 C-terminal domains to T cell activation

I propose that SLP-76 MC are the structures responsible for T cell signaling. One prediction from this hypothesis is that mutations of Vav1 that impair SLP-76 MC persistence will consequently decrease T cell activation. To test this model, I measured upregulation of surface CD69 and intracellular calcium flux as markers of T cell activation. Upregulation of CD69 is thought to require the activation of JNK and AP-1 downstream of the Vav1 GEF activity [Cao, Janssen et al. 2002; Castellanos, Munoz et al. 1997; Zugaza, Lopez-Lago et al. 2002]. In addition, the Vav1 CH domain is required for increases in intracellular calcium flux, though the mechanism behind this function remains unclear [Billadeau 2000; Cao, Janssen et al. 2002]. Using these readouts, I assayed the Src homology domain mutants of Vav1 for their ability to mediate TCR-mediated T cell activation. The SH2* mutant was unable to mediate increases in surface CD69 (Figure 26) or intracellular calcium (Figure 27), which I anticipated since this mutant also failed to support persistent SLP-76 MC. The individual SH3 mutants, which did not significantly reduce SLP-76 MC persistence, did significantly reduce CD69 upregulation by approximately 20% compared to cells expressing WT Vav1 (Figure 26). These mutants also displayed significant defects in their ability to mediate intracellular calcium flux (Figure 27). Despite the intermediate effect of the N3*C3* mutant on SLP-76 MC persistence, this mutant fails to augment CD69 expression or calcium flux. These data indicate that the SH3 domains play limited roles in cluster entry of Vav1 and in SLP-76 MC persistence and movement, but are required for optimal TCR-induced calcium flux and CD69 upregulation.

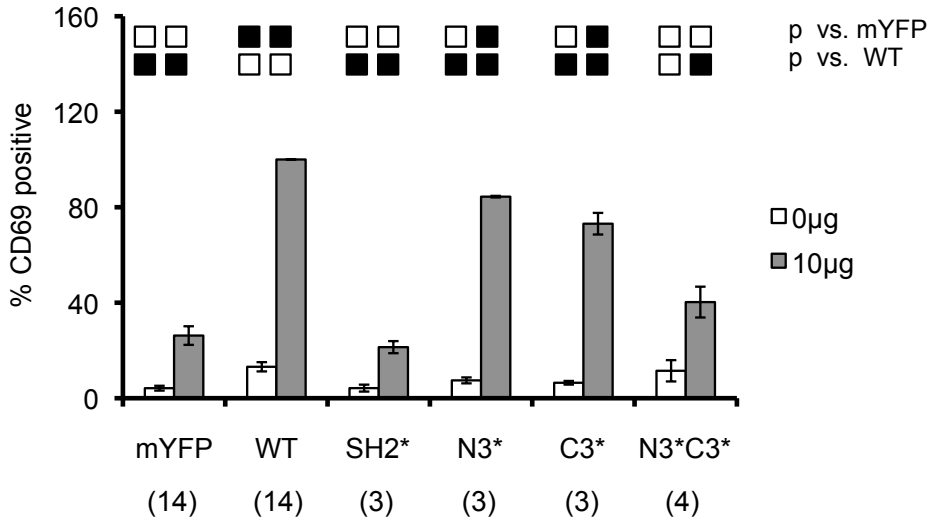

Figure 26: Vav1 SH domains play distinct roles in T cell activation – CD69 upregulation

J.Vav cells were transiently transfected with plasmids encoding the indicated Vav1 constructs fused to mYFP. Cells were stimulated for 16 hours with 10 µg/ml of soluble OKT3. Surface expression of CD69 was then measured by FACS in cell populations expressing tightly gated amounts of mYFP. The fraction of cells expressing CD69 was normalized to the response observed in J.Vav cells reconstituted with WT Vav1.mYFP and is shown as the mean ± SEM. Replicates are listed in parenthesis below each sample. Black boxes indicate significant differences versus the indicated null or WT control, using a cutoff of $p = 0.05$.

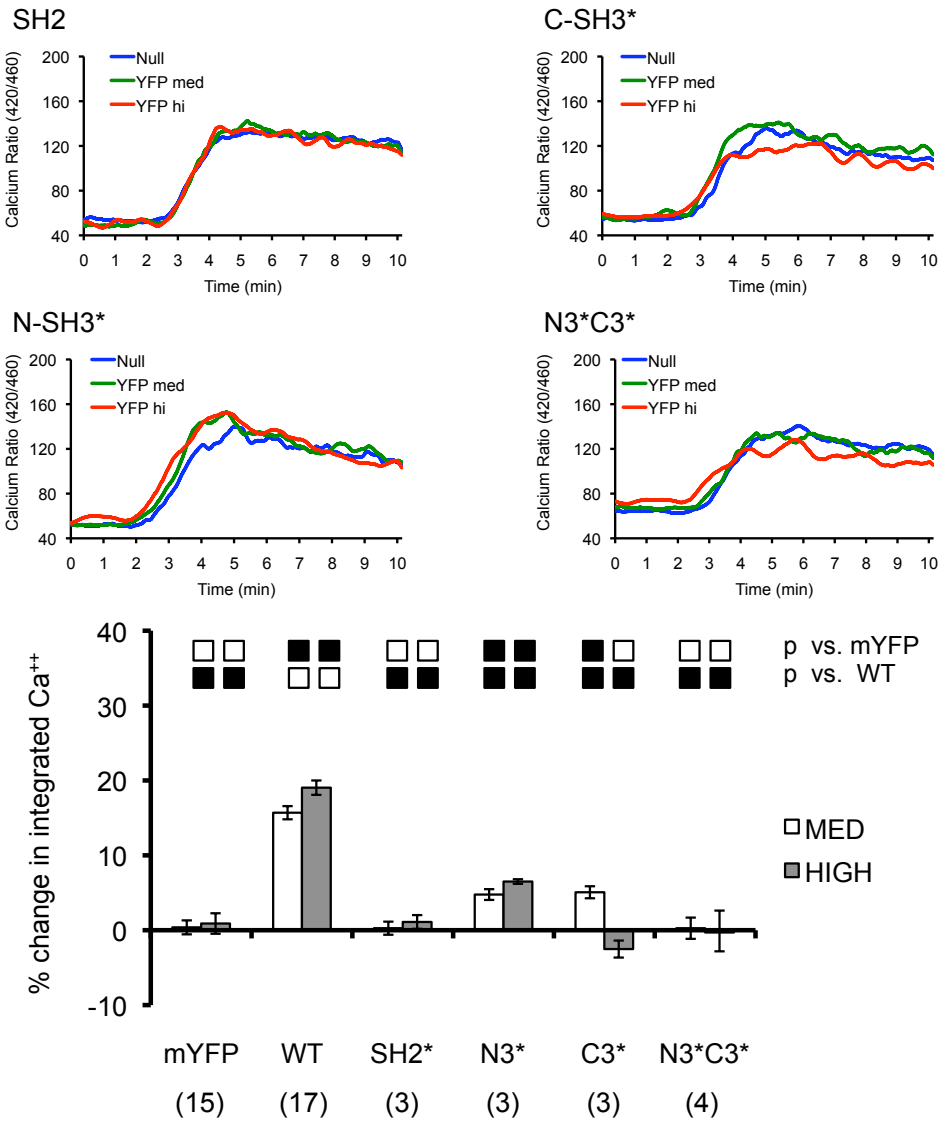

Figure 27: Vav1 SH domains play distinct roles in T cell activation – calcium flux

Intracellular calcium flux was measured in J.Vav1 cells transiently transfected with plasmids encoding the indicated Vav1 mutant protein fused to mYFP. **Top**: Calcium flux was measured in tightly gated populations of cells expressing moderate and high levels of fusion protein compared to untransfected cells (mYFP-null) from the same sample. One representative of three experiments are shown. **Bottom**: The percent change in integrated calcium responses is shown for populations of cells expressing medium and high levels of fusion protein relative to untransfected, mYFP-null cells from the same sample. Error bars indicate ± SEM. Replicates are listed in parenthesis below each sample. Black boxes indicate significant differences versus the indicated null or WT control, using a cutoff of $p = 0.05$.

7.1.7 Vav1 N-terminal domains are required for SLP-76 MC persistence and movement

To determine whether scaffolding interactions mediated by the C-terminus of Vav1 are sufficient to increase SLP-76 MC persistence, I created truncation mutants that separate the C-terminal Src homology domains from the regulatory and catalytic N-terminal domains (termed SH323 and Δ323 mutants, respectively; Figure 20). I found that the Δ323 fragment, in which the SH3-SH2-SH3 domains were deleted, failed to enter SLP-76 MC in JV.SC cells and was uniformly distributed in the cytoplasm (Figure 28). The resultant SLP-76 MC that formed were short-lived and immobile, as seen by the lack of radial 'spokes' in MOT images and the short vertical traces in kymographs. In contrast, the SH323 fragment was recruited into SLP-76 MC, as shown by the yellow microclusters seen in the merged image. However, these SLP-76 MC were similarly immobile and did not persist, as observed from kymographs generated from these cells; they grossly resembled Vav1-null or Δ323 microclusters.

In cells expressing the Δ323 mutant, quantitative analysis revealed that these SLP-76 MC were not significantly different than those formed in JV.SC cells expressing mYFP alone by all parameters measured (Figure 29). This finding supports our previous conclusion that Vav1 must be present within SLP-76 MC to increase microcluster persistence and movement. However, the SH323 fragment mediated small, but significant, increases in SLP-76 MC persistence, speed, and stoichiometry of SLP-76 recruitment. This indicates that scaffolding interactions mediated by the C-terminus of Vav1 do contribute to SLP-76 MC stability, but are insufficient for optimal SLP-76 MC movement and persistence.

Taken together, these data show that the SH3-SH2-SH3 domains of Vav1 are necessary and sufficient for entry into SLP-76 MC, but are unable to optimally stabilize or to promote the movement of SLP-76 MC. I conclude that these functions must be mediated by the N-terminal domains of Vav1, revealing a novel function for these domains.

I also measured the ability of the Vav1 Δ323 and SH323 fragments to mediate CD69 upregulation and intracellular calcium elevations. As mentioned in section 7.1.6, the GEF activity mediated by the DH-PH-C1 domains is thought to be responsible for the activation of AP-1 and JNK, which increase surface expression of CD69. In addition, the CH domain mediates Vav1-dependent calcium flux. To determine how these mutations impacted T cell activation, the SH323 or the Δ323 fragment were tagged with mYFP and expressed in J.Vav cells. The SH323 fragment, which lacks both the calcium and GEF modules, failed to restore surface expression of CD69 (Figure 30) and suppressed TCR-dependent calcium flux in a dose-dependent manner (Figure 31). This dominant-negative effect is consistent with previous studies and suggests that the SH323 fragment displaces endogenous Vav2 and Vav3, which can partially compensate for the lack of Vav1 [Cao, Janssen et al. 2002]. These defects in T cell activation correlate with low microcluster persistence and stoichiometry of SLP-76 recruitment (Figure 29). In contrast, the Δ323 fragment, which possess an intact CH domain and GEF cassette, showed a small positive effect on CD69 upregulation (Figure 30) and a small negative effect on calcium flux (Figure 31). Combined with the imaging data presented in section 7.1.7, these functional data show that the N-terminal domains of Vav1 are not required for Vav1 entry into SLP-76 MC, but are required to increase microcluster persistence and mediate T cell

activation. However, the effector domains present in the N-terminus of Vav1 cannot function unless they are recruited into SLP-76 MC.

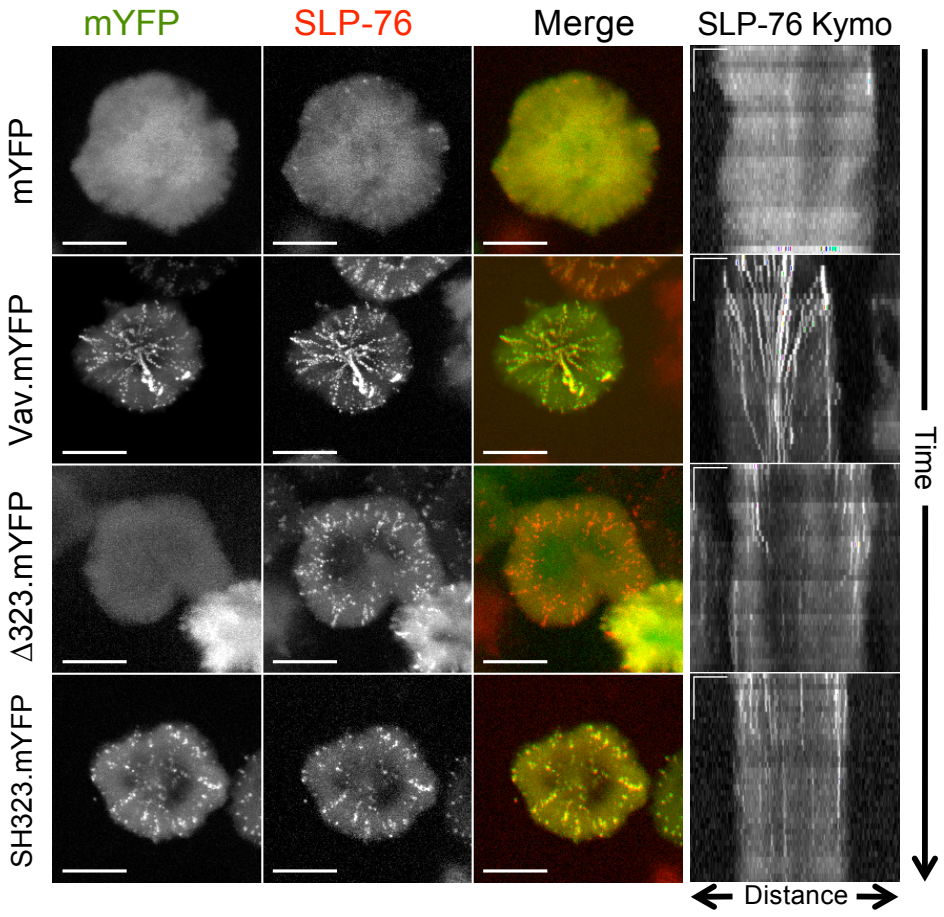

Figure 28: Vav1 SH3-SH2-SH3 domains are necessary and sufficient for MC localization

JV.SC cells were transiently transfected with plasmids encoding either mYFP or the indicated Vav1 construct as an mYFP fusion protein. One day post transfection, cells were imaged on glass coverslips coated with 3 µg/ml OKT3 for 5 minutes. SLP-76.mCFP is shown in red and mYFP constructs are shown in green. In the left panels, one representative MOT image from 3 experiments is shown. Scale bars correspond to 10 µm. In the right panels, kymographs were generated from these cells showing the inward movement (x-axis) over time (y-axis) of individual SLP-76 MC. Scale bars correspond to 5 µm and 60 s.

A

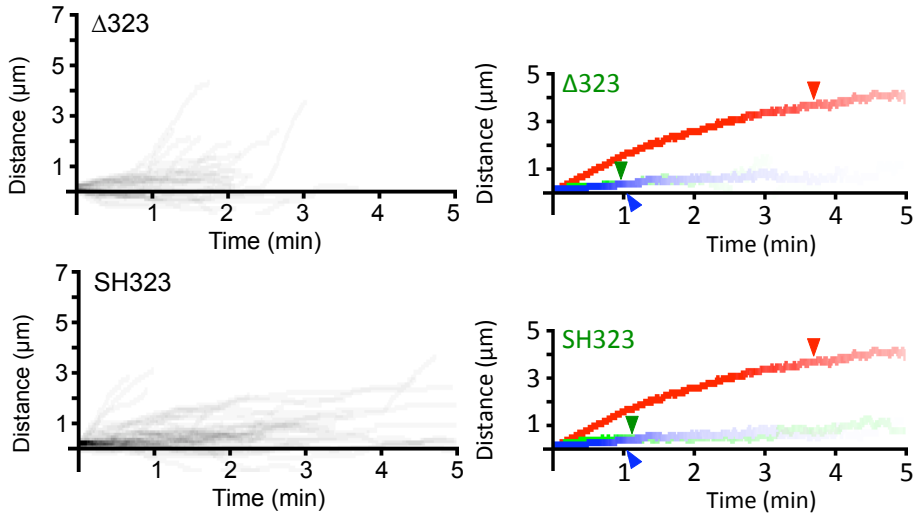

B

	Persistence (sec)	Movement (μm)	Speed (nm/sec)	% SLP in Clusters	Clusters per cell
mYFP	68.57 ± 3.93 ††	0.65 ± 0.03 ††	56.62 ± 2.12 ††	5.90 ± 0.67 ††	10.80 ± 0.84 ††
WT	180.51± 6.95 **	3.34 ± 0.19 **	102.96 ± 3.26 **	43.59 ± 2.83 **	19.15 ± 0.81 **
Δ323	62.15 ± 5.11 ††	0.72 ± 0.08 ††	55.50 ± 5.04 ††	6.55 ± 1.29 ††	12.40 ± 1.98 ††
SH323	91.50 ± 12.92 *,††	0.85 ± 0.10 ††	70.80 ± 8.75 *,††	11.26 ± 3.41 *,††	14.20 ± 1.66 †

Figure 29: Vav1 SH3-SH2-SH3 domains are required for SLP-76 MC persistence and movement

A – Left: Individual SLP-76 MC paths were traced from cells expressing the indicated Vav1 mutant. Kymographs from 10 cells across 3 experiments were traced. Of the total SLP-76 MC traced, the graph displays all traces persisting for more than 90 s or moving more then 2 μm. The fraction of microclusters passing these criteria are shown compared to the total number of microclusters traced. **Right**: All microcluster traces acquired from each cell were averaged to yield composite kymographs depicting fractional persistence (line intensity) over time (x-axis) and microcluster movement (y-axis). Arrowheads represent the half-life of SLP-76 MC for each condition. **B –** To obtain mean values for the duration and movement of SLP-76 MC were extracted from individual traces. These mean values are shown ± SEM. Single and double asterisks indicate statistical significance relative to cells expressing mYFP alone, single and double daggers indicate statistical significance relative to cells expressing wild-type Vav1.mYFP ($P < 0.05$ and $P < 0.005$, respectively).

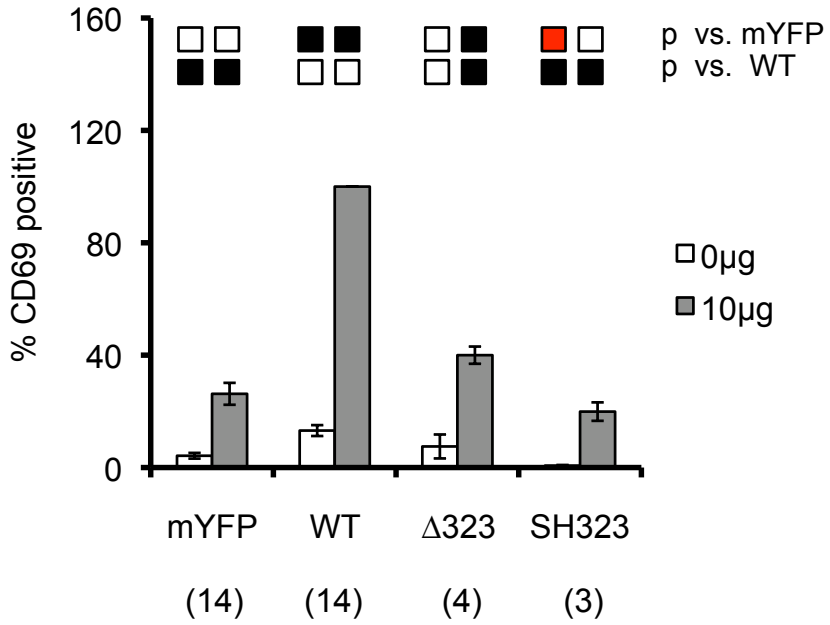

Figure 30: Localization of Vav1 effector domains is required for their function – CD69

J.Vav cells were transiently transfected with plasmids encoding the indicated Vav1 constructs fused to mYFP. Cells were stimulated for 16 hours with 10 µg/ml of soluble OKT3. Surface expression of CD69 was then measured by FACS in cell populations expressing tightly gated amounts of mYFP. The fraction of cells expressing CD69 was normalized to the response observed in J.Vav cells reconstituted with WT Vav1.mYFP and is shown as the mean ± SEM. Replicates are listed in parenthesis below each sample. Black boxes indicate significant differences versus the indicated null or WT control, using a cutoff of $p = 0.05$. A red box also indicates statistical significance, but is used to emphasize dominant-negative effects.

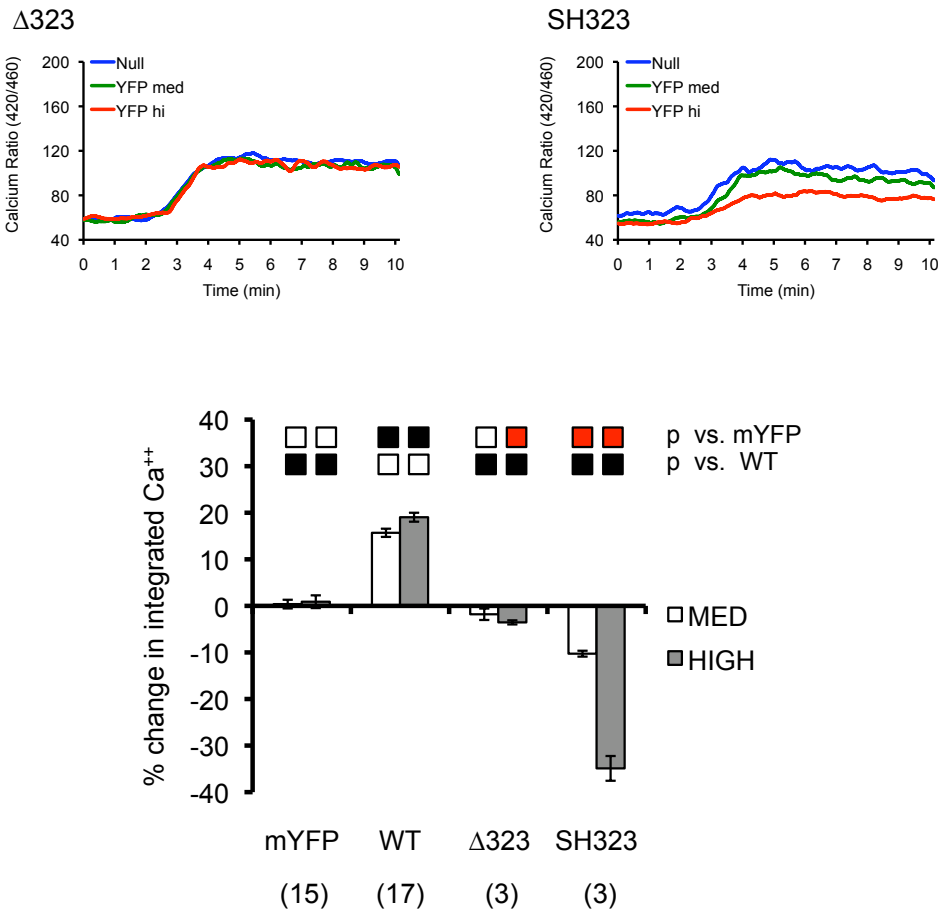

Figure 31: Localization of Vav1 effector domains is required for their function - calcium

Intracellular calcium flux was measured in J.Vav1 cells transiently transfected with plasmids encoding the indicated Vav1 mutant protein fused to mYFP. **Top**: Calcium flux was measured in tightly gated populations of cells expressing moderate and high levels of fusion protein compared to untransfected cells (mYFP-null) from the same sample. One representative of three experiments are shown. **Bottom**: The mean percent change in integrated calcium responses is shown for populations of cells expressing medium and high levels of fusion protein relative to untransfected, mYFP-null cells from the same sample. Error bars indicate ± SEM. Replicates are listed in parenthesis below each sample. Black boxes indicate significant differences versus the indicated null or WT control, using a cutoff of $p = 0.05$. A red box also indicates statistical significance, but is used to emphasize dominant-negative effects.

7.1.8 Summary / Discussion I

SLP-76 MC are multisubunit signaling structures that are required for T cell activation. In imaging assays, SLP-76 MC originate in the periphery of the cell:glass contact and persist for several minutes as they move toward the center of the contact. Although SLP-76 MC formation is a necessary prerequisite for T cell activation, it is not sufficient; the generation of a stable signaling complex is required [Bunnell, Singer et al. 2006; Varma, Campi et al. 2006]. Using shRNA-mediated Vav1 knockdown, I have shown that Vav1 is a critical component of SLP-76 MC that is required for the persistence and movement of these structures. Vav1 is involved in a variety of responses following TCR ligation, though the mechanism of these functions remains unknown. I propose that Vav1 mediates TCR-mediated activation by entering SLP-76 MC and increasing their persistence, thereby allowing optimal TCR signaling. In support of this model, I found that Vav1 enters SLP-76 MC through its SH2-mediated interaction with the phosphorylated N-terminal tyrosines of SLP-76. In addition, Vav1 is unable to contribute to T cell activation in the absence of localization to SLP-76 MC.

Microcluster persistence is determined by the length of time during which the microcluster is visible by eye. Protein-protein interactions, largely mediated by phosphotyrosine-dependent interactions, hold the SLP-76 MC resident proteins together thereby increasing microcluster persistence. However, the composition of SLP-76 MC is not static; proteins continually enter and leave [Bunnell, Hong et al. 2002]. Since microcluster-resident proteins participate in multivalent interactions, any individual

protein-protein interaction may fail without disrupting the overall structure of the microcluster. I refer to this phenomenon as microcluster 'avidity.' Therefore, any protein that increases microcluster persistence could do so by participating directly in protein-protein scaffolding interactions or indirectly by facilitating the interactions of proteins within the microcluster (by regulating the cytoskeleton, for example). Vav1 possesses both scaffolding domains and effector domains that could be involved in mediating SLP-76 MC persistence. In the following results sections, I attempt to clarify which activities of Vav1 are required for optimal SLP-76 MC persistence and function.

In this section, I examined the scaffolding contributions of the C-terminal Src homology domains. These domains bind to several proteins present in SLP-76 MC and could conceivably contribute to scaffolding interactions to increase microcluster persistence. To elucidate the contributions of these domains, I reconstituted Vav1 deficient cells with Vav1 constructs bearing point mutations that abrogate the relevant binding surface. Point mutation of the SH2 domain prevented Vav1 from entering SLP-76 MC and also prevented increases in microcluster persistence, upregulation of surface CD69, and intracellular calcium flux. Therefore, I conclude that Vav1 must be properly localized to SLP-76 MC to exert its functions in T cell signaling. One potential caveat of these point mutations is that they are having unanticipated secondary effects. However, the mechanism of binding through SH2 and SH3 domains is well known and the mutations described in this thesis target well-characterized motifs within these domains. In addition, the atypical binding surface of the Vav1 N-terminal SH3 domain has also been characterized [Nishida, Nagata et al. 2001]. While I think it is unlikely that the mutations

used in this thesis are having secondary effects, circular dichroism could be used to confirm that the secondary structure of these domains remains unaltered by the point mutations used here.

The individual N- and C-terminal SH3 domain mutants showed consistent mild defects in SLP-76 MC persistence, though they were not statistically significant. Of these mutations, the N-SH3* mutant was always slightly worse than the C-SH3* mutant. The N-terminal SH3 domain binds the adapter Grb2, which is also present in SLP-76 MC and binds LAT and SOS [Houtman, Yamaguchi et al. 2006]. Therefore, the inactivation of the Vav1 N-SH3 domain could decrease the avidity of Vav1 binding in the LAT / SLP-76 complex. The N-terminal SH3 domain also binds the adapter Nck independently of SLP-76 [Barda-Saad, Shirasu et al. 2010]. This mutation may result in decreased dwell times of Vav1 and Nck within the microcluster, as they would be unable to stabilize one another.

The C-terminal SH3 domain binds to Dynamin2, a protein involved in actin polymerization and T cell activation [Gomez, Hamann et al. 2005]. Mutation of this domain had a minor impact on the persistence and movement of SLP-76 MC, but significantly reduced calcium flux and CD69 upregulation. These effects could be due to the loss of Dynamin2 from the complex, since phosphorylation of PLCγ1 and JNK are inhibited in the absence of this protein [Gomez, Hamann et al. 2005]. Since Vav1 is also required for JNK phosphorylation, it would be interesting to see whether Dynamin2 is also recruited into signaling microclusters in a Vav1-dependent manner. Also, the

requirements of the various domains of Nck have not been addressed in the context of SLP-76 MC persistence. Both of these Vav1 binding partners play an important role in T cell activation and are likely to be important for the formation of stable signaling structures.

Each individual SH3 domain plays minor roles in SLP-76 MC persistence and recruitment of SLP-76 into microclusters, but plays more significant roles in the activation of signaling pathways that result in calcium flux and upregulation of CD69. Persistent SLP-76 MC form in the presence of either the N-SH3* or C-SH3* mutant but fail to mediate intracellular calcium flux, indicating that SLP-76 MC persistence is necessary but not sufficient to drive signaling downstream of the TCR. Though the mutation of individual SH3 domains produced mild effects on SLP-76 MC persistence and movement, mutation of both SH3 domains produced more severe defects. This result indicates that these domains must have redundant functions. Nevertheless, SLP-76 MC containing the N3*C3* mutant were still markedly different than SLP-76 MC formed in Vav1 deficient cells. The presence of mobile SLP-76 MC indicated that the microcluster is still able to interact with the translocation machinery. Although the persistence of SLP-76 MC is incompletely, but significantly increased compared to Vav1 deficient cells, the N3*C3* mutant is unable to mediate increases in calcium flux or the upregulation of CD69. This indicates that the degree of persistence observed in this mutant is insufficient to mediate T cell activation. This could reflect the loss of effector proteins from the microcluster. Alternatively, SLP-76 MC components may not become optimally activated within short-lived microclusters. Future studies could address the

degree to which T cells become activated, for example, whether Vav1 and PLCγ1 become phosphorylated in the presence of the N3*C3* mutant.

Finally, I found that the SH3-SH2-SH3 module is necessary and sufficient for recruitment into SLP-76 MC and that the isolated SH323 fragment mildly increases microcluster persistence. However, the SH323 fragment is a potent dominant negative and reduces calcium flux compared to Vav1 deficient cells. This dominant negative effect could be caused by the displacement of endogenous Vav3, which is present in J.Vav cells and can partially compensate for the loss of Vav1 [Cao, Janssen et al. 2002; Fujikawa, Miletic et al. 2003]. Within the microcluster, the Src homology domains participate in scaffolding interactions. However, since these domains to not fully restore microcluster persistence, other N-terminal domains must also be involved. The Vav1 N-terminus is required to form persistent, mobile microclusters, potentially through the enzymatic GEF activity or through scaffolding interactions. To test this hypothesis, I assessed SLP-76 MC formation in the presence of GEF-inactive Vav1 (Section 7.2) and also made large-scale deletion mutants within the N-terminus to test for scaffolding interactions within this region (Section 7.3).

7.2 Result II: SLP-76 MC are critical sites of Vav1 recruitment and catalytic activity

7.2.1 Rationale II

I showed in the previous section that the N-terminal domains of Vav1 are unable to promote T cell activation in the absence of localization to SLP-76 MC (Section 7.1.7). Since Vav1 phosphorylation potentiates its enzymatic activity [Aghazadeh, Lowry et al. 2000], I hypothesized that Vav1 becomes phosphorylated and performs its enzymatic activity within SLP-76 MC. In addition to contributing to the function of SLP-76 MC, the GEF activity could also contribute to their structural stabilization through its effects on the cytoskeleton, since dynamic actin reorganization is required for the formation of SLP-76 MC [Varma, Campi et al. 2006]. Vav1-dependent reorganization of the cytoskeleton could be driven by the activation of GTPases such as Rac, which in turn activate actin regulatory proteins such as WAVE2 [Billadeau, Nolz et al. 2007]. Therefore, the Vav1 GEF activity could influence both the function and structure of SLP-76 MC.

7.2.2 Vav1 localization to SLP-76 MC is required for its phosphorylation

In its resting state, the N-terminus of Vav1 adopts an autoinhibitory conformation that prevents its enzymatic activity and is mediated by the CH domain and tyrosines 142, 160, and 174. This autoinhibitory fold opens in response to phosphorylation of the tyrosines, potentiating the Vav1 GEF activity [Aghazadeh, Lowry et al. 2000; Amarasinghe and Rosen 2005; Yu, Martins et al. 2010]. These tyrosines have been evolutionarily conserved, at least since the divergence of humans and fish, highlighting the importance

of this regulatory mechanism (Figure 32). I have shown that the Δ323 fragment, which possesses the GEF cassette, fails to mediate the GEF-dependent upregulation of surface CD69 (Figure 30). This could result if the Δ323 fragment is not being appropriately tyrosine phosphorylated, as phosphorylation activates the catalytic functions of the Vav1 Δ323 fragment. To determine the functional significance of localization to SLP-76 MC, I measured the phosphorylation of Vav1 following TCR stimulation. I expressed either wild-type, SH2*, or Δ323 Vav1 in Jurkat T cells as fusion proteins tagged with mYFP. Following TCR stimulation, Vav1 was immunoprecipitated from stimulated cell lysate and phosphorylation of the various constructs was determined by Western blotting for phospho-tyrosine. I found that those mutations which prevent Vav1 from entering SLP-76 MC (SH2*, Δ323) also prevent Vav1 from becoming phosphorylated, suggesting that the SLP-76 MC is the site of Vav1 phosphorylation (Figure 33). This provides direct biochemical support to show the significance of Vav1 recruitment into SLP-76 MC and suggests that SLP-76 MC are sites of increased enzymatic activity.

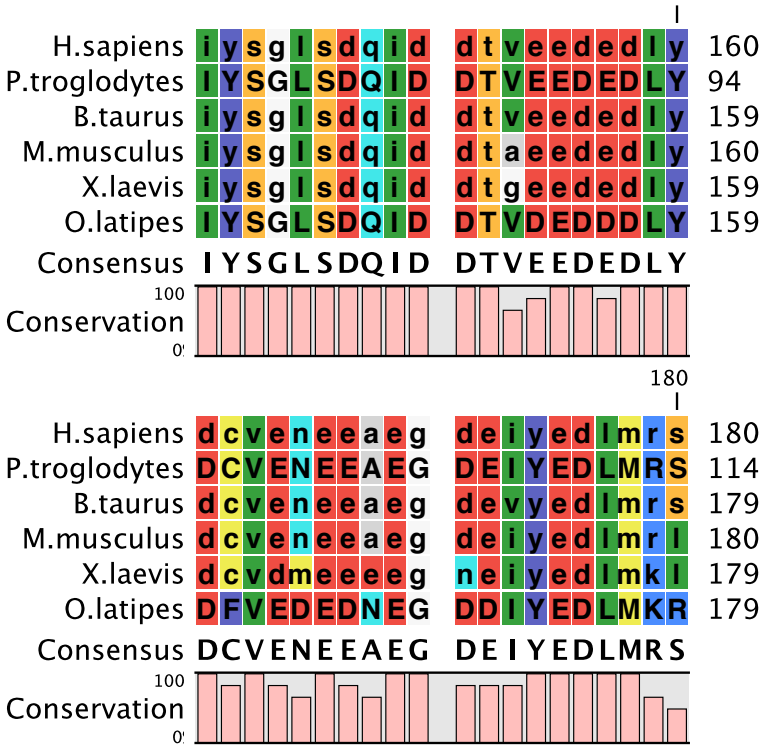

Figure 32: Evolutionary conservation of Vav1 tyrosines

Homo sapiens Vav1 protein sequence was compared to various other species. The histogram at the bottom shows the degree of conservation across all species examined.

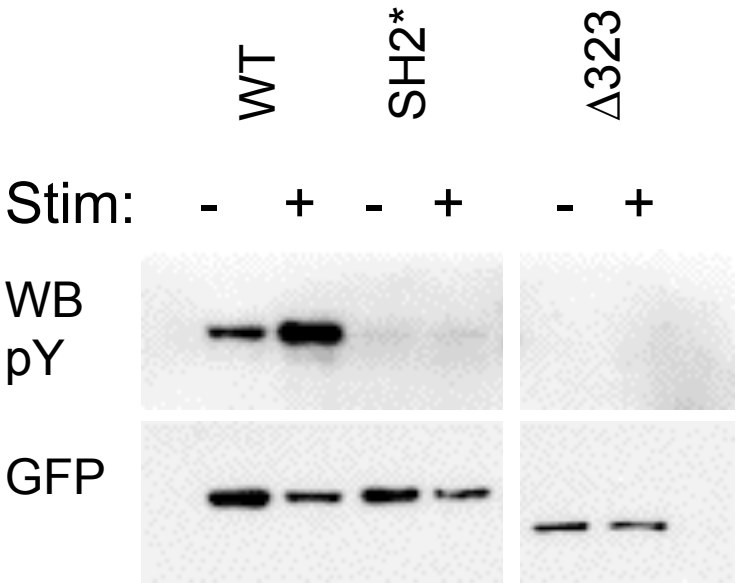

Figure 33: Localization to SLP-76 MC is required for Vav1 phosphorylation

The indicated Vav1 mutants were expressed as mYFP fusion proteins in Jurkat T cells. Following stimulation with C305 anti-TCR antibody, Vav1 fusion proteins were precipitated from stimulated cell lysate using antibodies specific for GFP. Vav1 phosphorylation was determined by Western blotting with antibodies against phosphotyrosine. One representative experiment of three is shown.

7.2.3 Vav1 tyrosines are not required for MC persistence or function

In addition to their role in regulating the Vav1 GEF activity by binding to the CH and DH domains, tyrosines 142, 160, and 174 are also capable of binding signaling proteins such as PLCγ1 and PI3K p85 *in vitro* [Miletic, Sakata-Sogawa et al. 2006]. Tyrosine 174 binds to a pocket adjacent to the GTPase binding site in inactive Vav1; its phosphorylation is a critical event in activation of the Vav1 enzymatic activity [Amarasinghe and Rosen 2005]. To determine whether these tyrosines are capable of mediating protein-protein interactions that contribute to SLP-76 MC persistence, I created point mutations in which tyrosine 174 or all three N-terminal tyrosines were mutated to phenylalanine (Y174F or Y3F respectively). These constructs were transfected into JV.SC cells and SLP-76 MC behavior was observed by confocal microscopy. I were unable to observe any significant difference between SLP-76 MC formed in the presence of wild-type, Y174F, or Y3F Vav1 (Figure 34). Quantitative microcluster analysis showed that these mutants did not significantly differ from WT Vav1 with respect to microcluster persistence, movement distance, and speed (Figure 35). I conclude that the N-terminal tyrosines of Vav1 are not involved in the stabilization or movement of SLP-76 MC.

I further investigated how these N-terminal tyrosines influence T cell signaling. Point mutation or deletion of these domains increases the Vav1 transforming activity and constitutively activates the GEF activity [Lopez-Lago, Lee et al. 2000; Zugaza, Lopez-Lago et al. 2002]. Since the Vav1 GEF activity is linked to activation of AP-1 and upregulation of CD69, I predicted that mutations of the N-terminal tyrosines would

enhance CD69 responses. To test this prediction, Vav1 deficient cells were reconstituted with Y3F Vav1 and stimulated for 16 hours with anti-TCR antibodies. Cells were then stained for surface upregulation of CD69 and measured by FACS. In cells expressing Vav1 Y3F, CD69 upregulation was significantly increased compared to wild-type Vav1 in both stimulated and unstimulated samples (Figure 36). This result is consistent with the constitutive activation of the Vav1 GEF activity by the Y3F mutation.

In addition, I measured the effect of the Y3F mutation on intracellular calcium flux. Vav1 deficient cells were reconstituted with Vav1 Y3F. Cells were then stained with the ratiometric calcium-sensitive dye Indo-1. Calcium flux was then measured by FACS following stimulation with anti-TCR antibodies. Cells were gated based on expression of moderate or high levels of mYFP-tagged Vav1 chimera. Cells expressing high levels of Vav1 Y3F showed calcium levels that were comparable to wild-type Vav1 (Figure 37). Cells expressing moderate levels showed higher calcium levels than cells expressing comparable levels of wild-type Vav1. These data show that the N-terminal tyrosines of Vav1 are not required for Vav1 function and they seem to play an inhibitory role in mediating calcium flux. Since the CH domain has been implicated in Vav1-mediated calcium flux [Billadeau 2000; Cao, Janssen et al. 2002], the increased calcium flux seen in the Y3F mutant could reflect an increased accessibility of the CH domain.

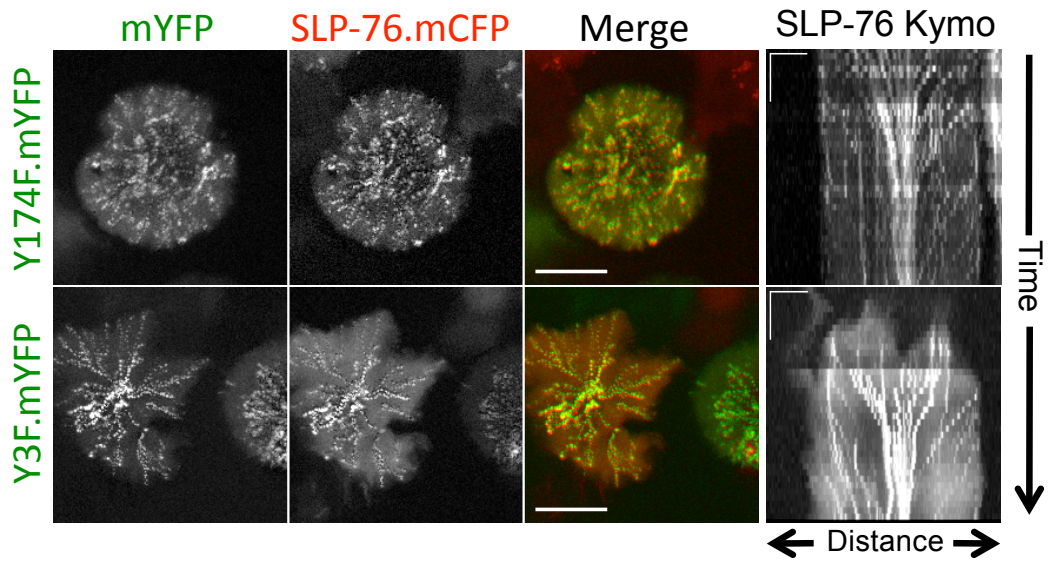

Figure 34: Vav1 N-terminal tyrosines are not required for SLP-76 MC persistence

JV.SC cells were transiently transfected with plasmids encoding the indicated Vav1 construct as an mYFP fusion protein. One day post transfection, cells were imaged on glass coverslips coated with 3 µg/ml OKT3 for 5 minutes. SLP-76.mCFP is shown in red and mYFP constructs are shown in green. In the left panels, one representative MOT image from 3 experiments is shown. Scale bars correspond to 10 µm. In the right panels, kymographs were generated from these cells showing the inward movement (x-axis) over time (y-axis) of individual SLP-76 MC. Scale bars correspond to 5 µm and 60 s.

A

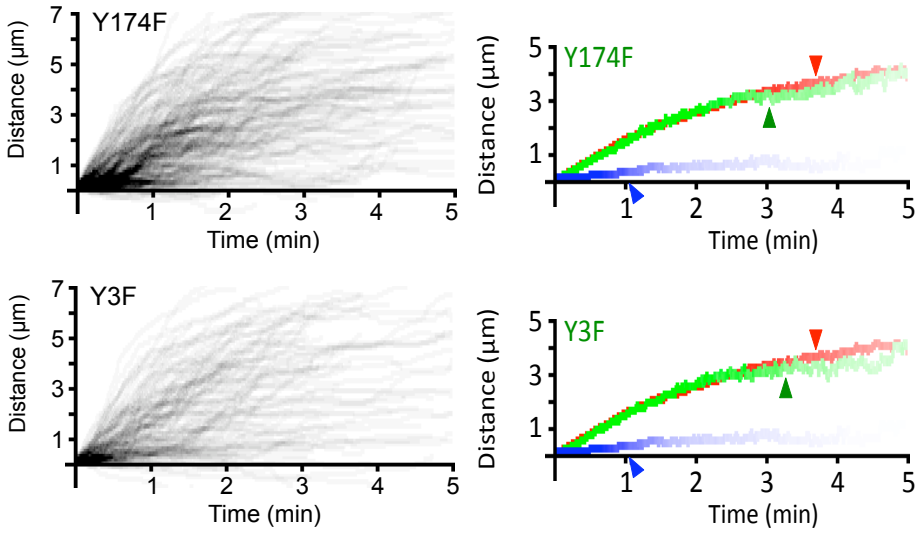

B

	Persistence (sec)	Movement (µm)	Speed (nm/sec)	% SLP in Clusters	Clusters per cell
mYFP	68.57 ± 3.93 ††	0.65 ± 0.03 ††	56.62 ± 2.12 ††	5.90 ± 0.67 ††	10.80 ± 0.84 ††
WT	180.51± 6.95 **	3.34 ± 0.19 **	102.96 ± 3.26 **	43.59 ± 2.83 **	19.15 ± 0.81 **
Y174F	165.64 ± 10.15 **	3.03 ± 0.31 **	98.13 ± 5.08 **	25.68 ± 2.75 **,††	15.73 ± 0.95 **,†
Y3F	158.49 ± 15.11 **	2.97 ± 0.42 **	99.45 ± 8.65 **	22.12 ± 3.35 **,††	13.64 ± 0.98 ††

Figure 35: Vav1 N-terminal tyrosines are dispensable for SLP-76 persistence and movement

A – Left: Individual SLP-76 MC paths were traced from cells expressing the indicated Vav1 mutant. Kymographs from 10 cells across 3 experiments were traced. Of the total SLP-76 MC traced, the graph displays all traces persisting for more than 90 s or moving more then 2 µm. The fraction of microclusters passing these criteria are shown compared to the total number of microclusters traced. **Right**: All microcluster traces acquired from each cell were averaged to yield composite kymographs depicting fractional persistence (line intensity) over time (x-axis) and microcluster movement (y-axis). Arrowheads represent the half-life of SLP-76 MC for each condition. **B –** To obtain mean values for the duration and movement of SLP-76 MC were extracted from individual traces. These mean values are shown ± SEM. Single and double asterisks indicate statistical significance relative to cells expressing mYFP alone, single and double daggers indicate statistical significance relative to cells expressing wild-type Vav1.mYFP ($P < 0.05$ and $P < 0.005$, respectively).

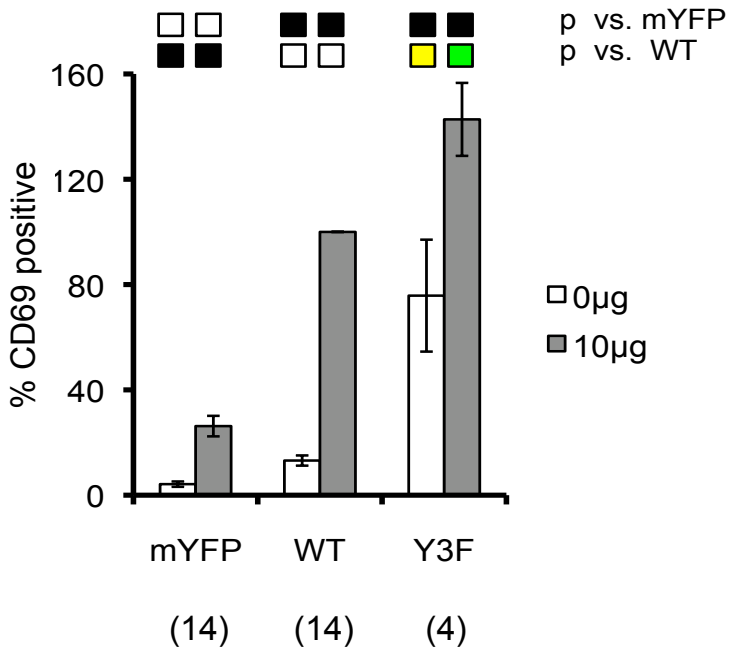

Figure 36: Mutation of the N-terminal tyrosines de-regulates Vav1 – CD69

J.Vav cells were transiently transfected with plasmids encoding the indicated Vav1 constructs fused to mYFP. Cells were stimulated for 16 hours with 10 µg/ml of soluble OKT3. Surface expression of CD69 was then measured by FACS in cell populations expressing tightly gated amounts of mYFP. The fraction of cells expressing CD69 was normalized to the response observed in J.Vav cells reconstituted with WT Vav1.mYFP and is shown as the mean ± SEM. Replicates are listed in parenthesis below each sample. Black boxes indicate significant differences versus the indicated null or WT control, using a cutoff of $p = 0.05$. Yellow and green boxes also indicate statistical significance, but are used to emphasize responses greater than wild-type.

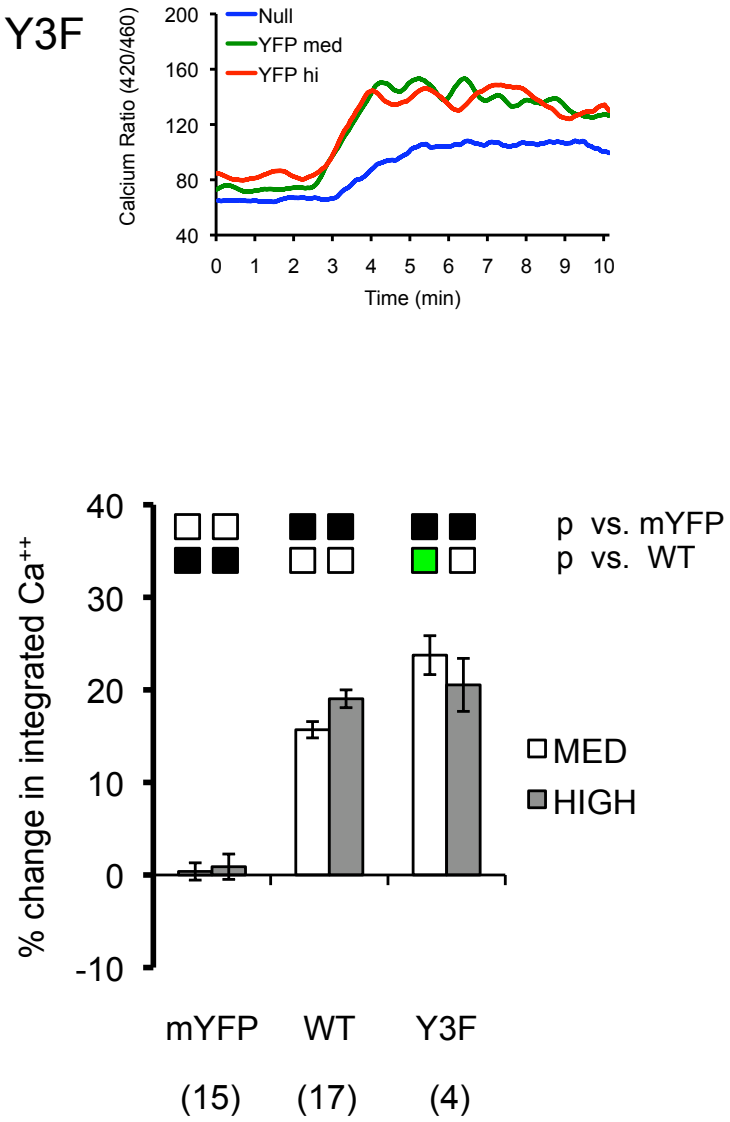

Figure 37: Mutation of the N-terminal tyrosines de-regulates Vav1 - calcium

Intracellular calcium flux was measured in J.Vav1 cells transiently transfected with plasmids encoding the indicated Vav1 mutant protein fused to mYFP. **Top**: Calcium flux was measured in tightly gated populations of cells expressing moderate and high levels of fusion protein compared to untransfected cells (mYFP-null) from the same sample. One representative of three experiments are shown. **Bottom**: The percent change in integrated calcium responses is shown for populations of cells expressing medium and high levels of fusion protein relative to untransfected, mYFP-null cells from the same sample. Error bars indicate ± SEM. Replicates are listed in parenthesis below each sample. Black boxes indicate significant differences versus the indicated null or WT control, using a cutoff of $p = 0.05$. Green boxes also indicate statistical significance, but are used to emphasize responses greater than wild-type.

7.2.4 Role of the Vav1 GEF activity in SLP-76 MC movement and persistence

The Vav1 N-terminus is involved in the structural stabilization of SLP-76 MC (Section 7.1). One of the effects attributed to this region of the protein is the DH-dependent activation of Rho-family GTPases [Zugaza, Lopez-Lago et al. 2002]. The Vav1 DH domain directly binds GTPases and is responsible for the enzymatic GEF activity [Rossman, Der et al. 2005]. Therefore, to determine whether the enzymatic activity of Vav1 is required to increase SLP-76 MC persistence, I examined Vav1 point mutants in which the exchange activity was abolished. Several mutations within the DH domain that abrogate the Vav1 GEF activity have been described, though they have not been directly compared in the same experimental system [Miletic, Graham et al. 2009; Saveliev, Vanes et al. 2009]. Using our imaging system, I compared three Vav1 DH domain mutations that have been described in the literature (mutations used in this section are listed in Figure 38). The first mutant was L213A, which faces the hydrophobic core of the DH domain. The second was L278Q, which is located on the opposite side of the DH domain from the Rac-binding surface and contacts the PH domain. The third mutation, L334A / K335A (termed LK-AA) is located in the Rac-binding surface on residues that face toward the GTPase. The location of these mutations within the DH domain based on crystal structure data is shown in Figure 38. I transfected these constructs into JV.SC cells and observed SLP-76 MC behavior following stimulation on anti-TCR antibody. JV.SC cells reconstituted with either L213A or L278Q formed short-lived microclusters that were very weakly mobile, as indicated by spots in MOT images and short, vertical lines in kymographs (Figure 39). Although these mutants localized to SLP-76 MC, they were unable to increase microcluster persistence and did not support the recruitment of

SLP-76 into microcluster structures (Figure 40). However, the LK-AA mutant localized to SLP-76 MC and increased persistence as well as movement speed and total distance traveled. Visually, the microcluster behavior in the LK-AA mutant closely resembles wild-type Vav1 (Figure 39). These data indicate that the Vav1 GEF activity is not required for the structural stabilization or mobility of SLP-76 MC.

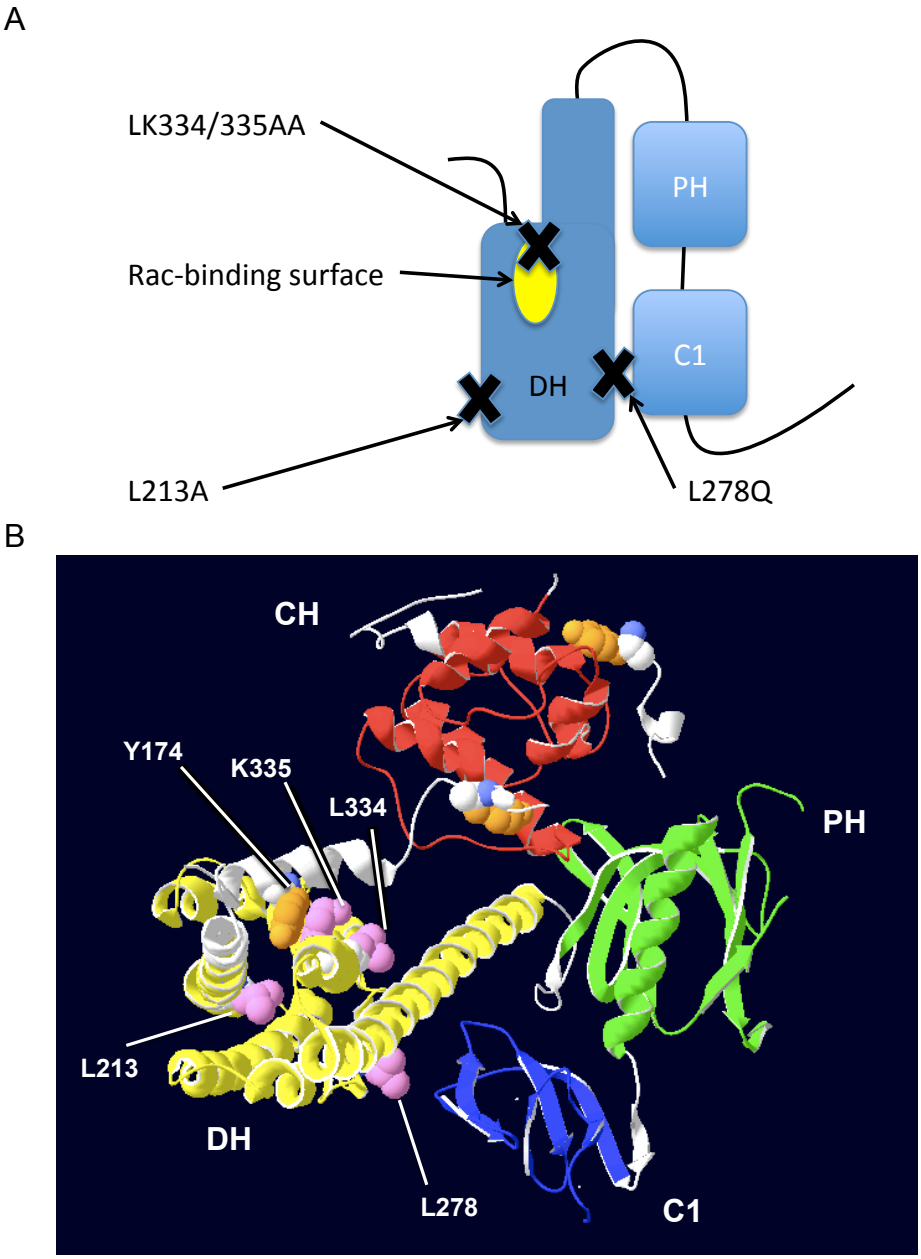

Figure 38: Conformation of the Vav1 N-terminal domains

The location of the various DH domain mutants is shown based on the crystal structure data presented in [Yu, Martins et al. 2010]. **A –** A simplified cartoon diagram showing the various GEF-inactivating point mutations in relation to the GTPase-binding surface of Vav1. **B –** A ribbon diagram of the Vav1 CH, DH, PH, and C1 domains was generated using the program Swiss PDB Viewer. The protein is presented in the autoinhibited state. The domains were colored as follows: CH domain – red, DH – yellow, PH – green, C1 – blue. Tyrosines 142, 160, and 174 were colored orange. The residues targeted in this section, L213, L278, L334, and K335 are shown in pink. In this autoinhibited conformation, the GTPase binding surface is obscured by a helix in the N-terminal acidic region (white).

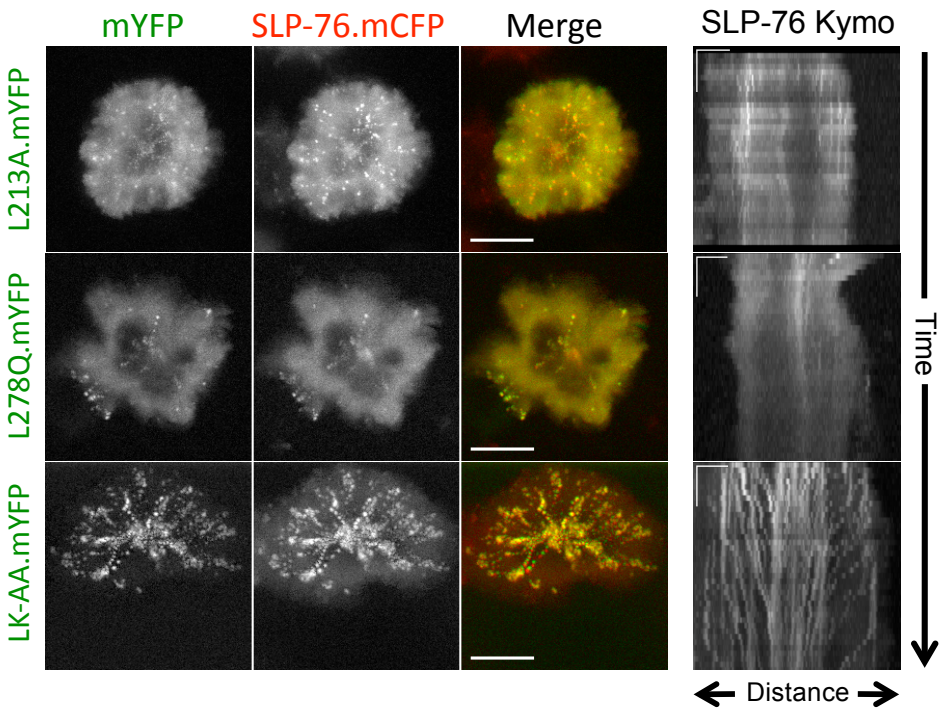

Figure 39: Vav1 GEF activity is not required for SLP-76 MC persistence or movement

JV.SC cells were transiently transfected with plasmids encoding the indicated Vav1 construct as an mYFP fusion protein. One day post transfection, cells were imaged on glass coverslips coated with 3 µg/ml OKT3 for 5 minutes. SLP-76.mCFP is shown in red and mYFP constructs are shown in green. In the left panels, one representative MOT image from 3 experiments is shown. Scale bars correspond to 10 µm. In the right panels, kymographs were generated from these cells showing the inward movement (x-axis) over time (y-axis) of individual SLP-76 MC. Scale bars correspond to 5 µm and 60 s.

A

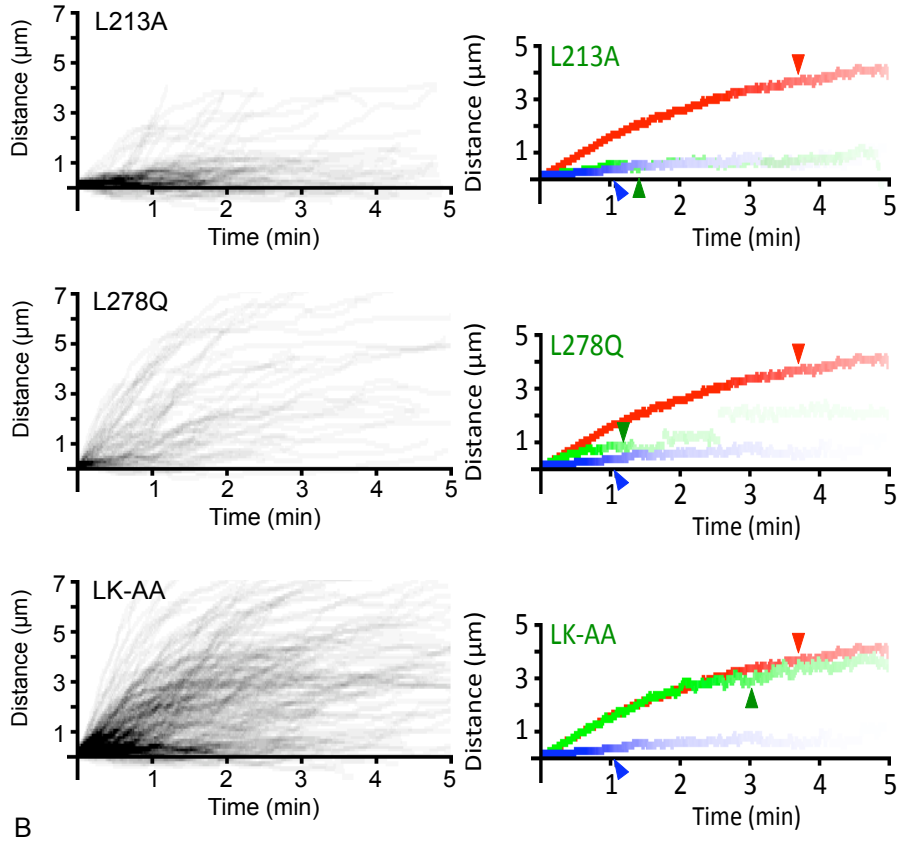

B

	Persistence (sec)	Movement (µm)	Speed (nm/sec)	% SLP in Clusters	Clusters per cell
mYFP	68.57 ± 3.93 ††	0.65 ± 0.03 ††	56.62 ± 2.12 ††	5.90 ± 0.67 ††	10.80 ± 0.84 ††
WT	180.51± 6.95 **	3.34 ± 0.19 **	102.96 ± 3.26 **	43.59 ± 2.83 **	19.15 ± 0.81 **
L213A	101.61 ± 11.99 **,††	0.90 ± 0.10 *,††	66.42 ± 3.65 *,††	12.23 ± 2.31 **,††	15.17 ± 1.84 ††
L278Q	93.97 ± 15.04 *,††	1.45 ± 0.30 **,††	73.33 ± 8.80 *,††	11.65 ± *,††	10.54 ± 1.38 ††
LK-AA	170.85 ± 7.34 **	2.99 ± 0.32 **	101.20 ± 5.14 **	32.22 ± 3.26 **,††	18.80 ± 1.44 **

Figure 40: Vav 1 GEF activity is not required for SLP-76 MC movement or persistence

A – Left: Individual SLP-76 MC paths were traced from cells expressing the indicated Vav1 mutant. Kymographs from 10 cells across 3 experiments were traced. Of the total SLP-76 MC traced, the graph displays all traces persisting for more than 90 s or moving more then 2 µm. The fraction of microclusters passing these criteria are shown compared to the total number of microclusters traced. **Right**: All microcluster traces acquired from each cell were averaged to yield composite kymographs depicting fractional persistence (line intensity) over time (x-axis) and microcluster movement (y-axis). Arrowheads represent the half-life of SLP-76 MC for each condition. **B –** To obtain mean values for the duration and movement of SLP-76 MC were extracted from individual traces. These mean values are shown ± SEM. Single and double asterisks indicate statistical significance relative to cells expressing mYFP alone, single and double daggers indicate statistical significance relative to cells expressing wild-type Vav1.mYFP ($P < 0.05$ and $P < 0.005$, respectively).

7.2.5 Vav1 GEF in T cell signaling

Although the Vav1 GEF activity is not required for the structural stabilization of SLP-76 MC, it is required for a number of Vav1-dependent signaling outcomes. Recently published papers have come to divergent conclusions regarding the role of the Vav1 GEF in T cell development and proliferation. Saveliev *et al.* reported that T cell development, proliferation, and NFAT activity were impaired in the absence of the Vav1 GEF activity, whereas Miletic *et al.* did not observe differences in these readouts between enzymatically active or inactive Vav1. However, both groups reported that the GEF activity was dispensable for calcium flux and T cell polarization [Miletic, Graham et al. 2009; Saveliev, Vanes et al. 2009]. Because of the different developmental models and GEF inactivating mutations used in these studies, the role of the Vav1 GEF in T cell activation remains unresolved. To clarify this issue, I compared the effect of three distinct GEF-inactivating mutations on TCR-mediated activation and microcluster formation. J.Vav1 cells were reconstituted with either the L213A, L278Q, or LK-AA mutants and calcium flux and CD69 upregulation were measured following stimulation with anti-TCR antibodies. Vav1 deficient cells reconstituted with high levels of the LK-AA mutant showed calcium flux comparable to wild-type Vav1 (Figure 41). In cell populations expressing moderate levels of protein, calcium flux in LK-AA exceeded that of wild-type. These data show that the Vav1 GEF activity is not required for mediating calcium flux following TCR stimulation. However, the L213A and L278Q mutants failed to flux calcium. This result is similar to the imaging data presented in Section 7.2.3 in that the LK-AA mutant resembled the wild-type protein, whereas the L213A and L278Q mutants were non-functional. Since the LK-AA mutant shows that the GEF

activity is not required for SLP-76 movement, persistence, or calcium flux, the loss of the enzymatic activity in the L213A and L278Q mutants cannot explain their lack of function. Therefore, the global organization of the GEF domains may be altered as a result of these mutations. However, these effects are most likely to be restricted to the DH, PH, and C1 domains, as the L213A mutant is able to enter SLP-76 MC (Figure 39) and also becomes phosphorylated following TCR stimulation (Figure 42).

I next measured the effect of the Vav1 GEF on upregulation of CD69. The L213A mutant failed to mediate increases in CD69 and the L278Q mutant was only able to weakly induce CD69 expression (Figure 43). However, the LK-AA mutant displays an intermediate phenotype. This result is unexpected, as CD69 responses are thought to correspond to Vav1 GEF activity [Cao, Janssen et al. 2002; Castellanos, Munoz et al. 1997; Reynolds, de Bettignies et al. 2004]. The presence of high intracellular calcium in this mutant suggests that PLCγ1 is being activated and generating second messengers. The upregulation of CD69 in this case could reflect an alternate pathway in which DAG generated by PLCγ1 activates ERK and AP-1.

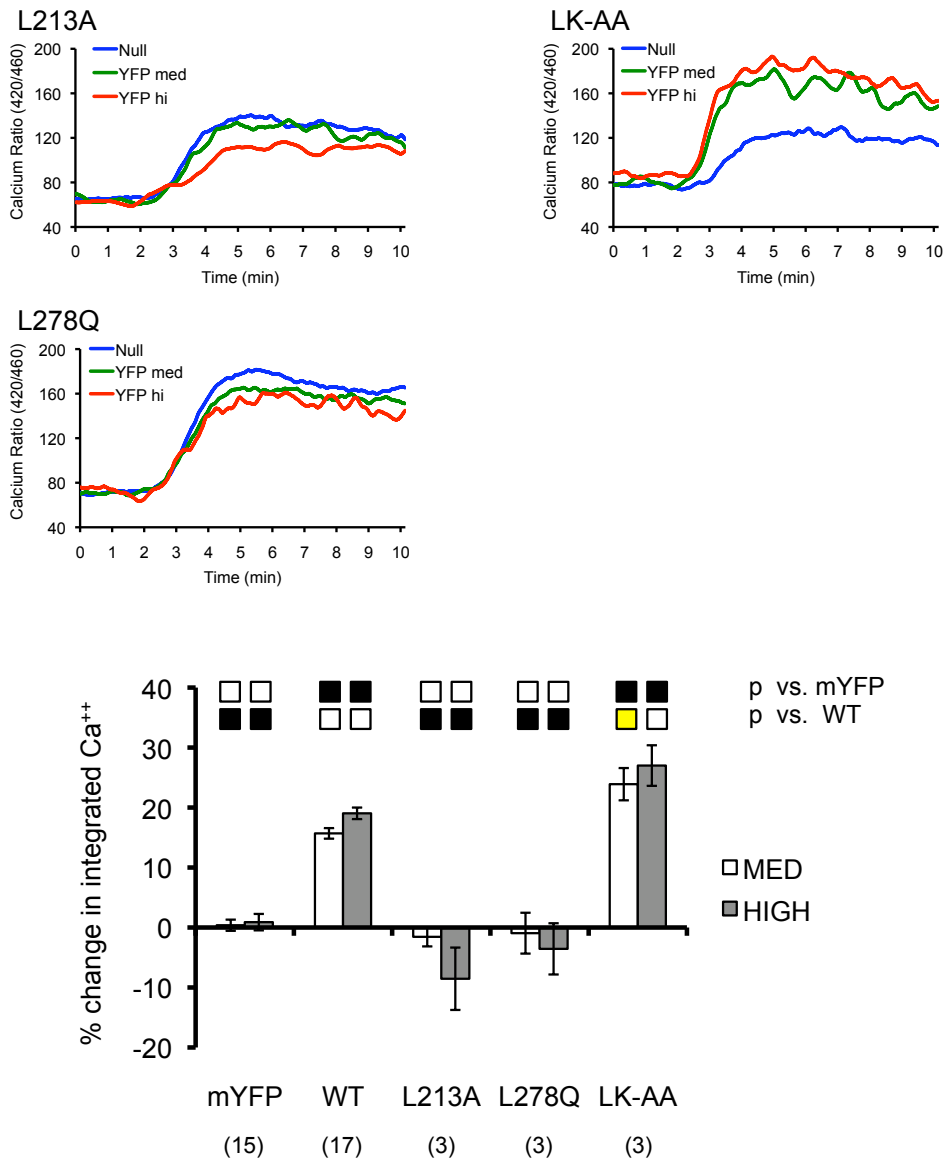

Figure 41: Vav1 GEF activity is not required to mediate calcium flux

Intracellular calcium flux was measured in J.Vav1 cells transiently transfected with plasmids encoding the indicated Vav1 mutant protein fused to mYFP. **Top**: Calcium flux was measured in tightly gated populations of cells expressing moderate and high levels of fusion protein compared to untransfected cells (mYFP-null) from the same sample. One representative of three experiments are shown. **Bottom**: The percent change in integrated calcium responses is shown for populations of cells expressing medium and high levels of fusion protein relative to untransfected, mYFP-null cells from the same sample. The mean value is shown ± SEM. Replicates are listed in parenthesis below each sample. Black boxes indicate significant differences versus the indicated null or WT control, using a cutoff of p = 0.05. Yellow boxes also indicate statistical significance, but are used to emphasize responses greater than wild-type.

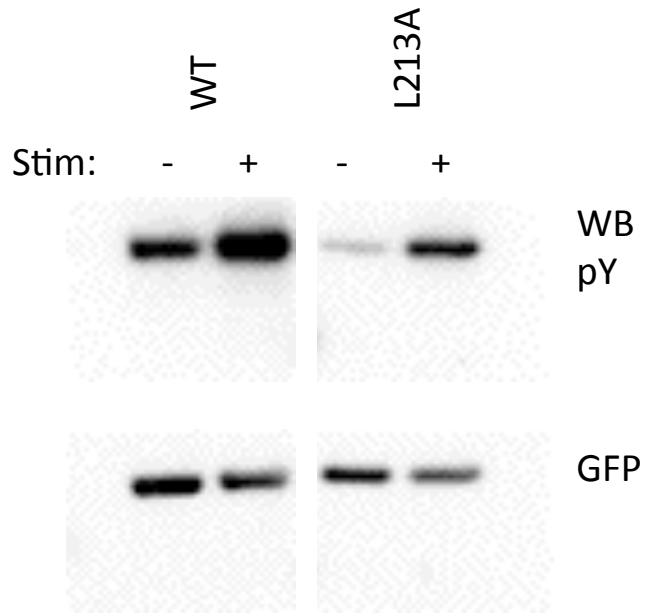

Figure 42: GEF activity is not required for Vav1 phosphorylation

The indicated Vav1 mutants were expressed as mYFP fusion proteins in Jurkat T cells. Following stimulation with C305 anti-TCR antibody, Vav1 fusion proteins were precipitated from stimulated cell lysate using antibodies specific for GFP. Vav1 phosphorylation was determined by Western blotting with antibodies against phosphotyrosine. One representative of three experiments is shown.

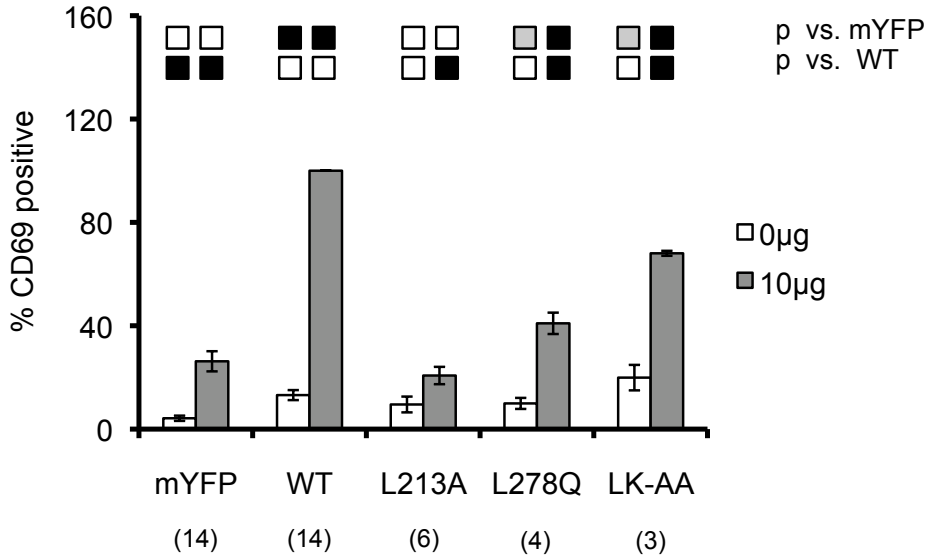

Figure 43: Vav1 GEF activity is required for optimal CD69 upregulation

J.Vav cells were transiently transfected with plasmids encoding the indicated Vav1 constructs fused to mYFP. Cells were stimulated for 16 hours with 10 µg/ml of soluble OKT3. Surface expression of CD69 was then measured by FACS in cell populations expressing tightly gated amounts of mYFP. The fraction of cells expressing CD69 was normalized to the response observed in J.Vav cells reconstituted with WT Vav1.mYFP and is shown ± SEM. Replicates are listed in parenthesis below each sample. Black boxes indicate significant differences versus the indicated null or WT control, using a cutoff of $p = 0.05$. Grey boxes denote trends ($0.1 > p > 0.5$).

7.2.6 Vav1 performs its enzymatic activity within SLP-76 MC

I have shown that Vav1 must be present in SLP-76 MC to become phosphorylated (Section 7.2.2). Since Vav1 phosphorylation potentiates its enzymatic activity toward its target GTPases, I propose that Vav1 selectively binds and activates targets, such as Rac1, within microclusters [Gulbins, Coggeshall et al. 1993; Han, Das et al. 1997]. To test this hypothesis, Vav1.mYFP was expressed with Rac1 conjugated to the fluorescent marker TagRFP-Turbo (Rac1.TagRFP). Indeed, dim clusters of wild-type Rac1 could be observed transiently colocalizing with Vav1 in movies (not shown), but the vast majority of the Rac1 was uniformly distributed (Figure 44). Clusters of Rac1 corresponding to Vav1 clusters were dimly visible for short periods of time, but the vast majority was uniformly distributed. Since Vav1 may bind with higher affinity to GTPases in the inactive state [Ming, Li et al. 2007], I also co-imaged Vav1 and dominant negative (DN) Rac1. Vav1 and DN Rac1 showed a high degree of colocalization and migrated together from the periphery to the center of the contact. This colocalization was not observed in the presence of the LK-AA mutant, suggesting that the LK-AA mutation prevents the Vav1 GEF activity by preventing the association of Vav1 with its target GTPases. Since Vav1 also activates RhoG, a close relative of Rac1, I imaged DN RhoG and Vav1 in JV.SC cells stimulated on anti-TCR antibodies. Similar to Rac1, I found that DN RhoG colocalizes with Vav1-containing microclusters (Figure 45). As would be expected, based on our observations with Rac1, this binding was prevented by deletion of the Vav1 DH and PH domain. These data indicate that the catalytic core of Vav1 selectively binds to its target GTPases within SLP-76 MC, confirming that SLP-76 microclusters are the

‘hotspots’ in which Vav1 performs its enzymatic activity downstream of TCR stimulation.

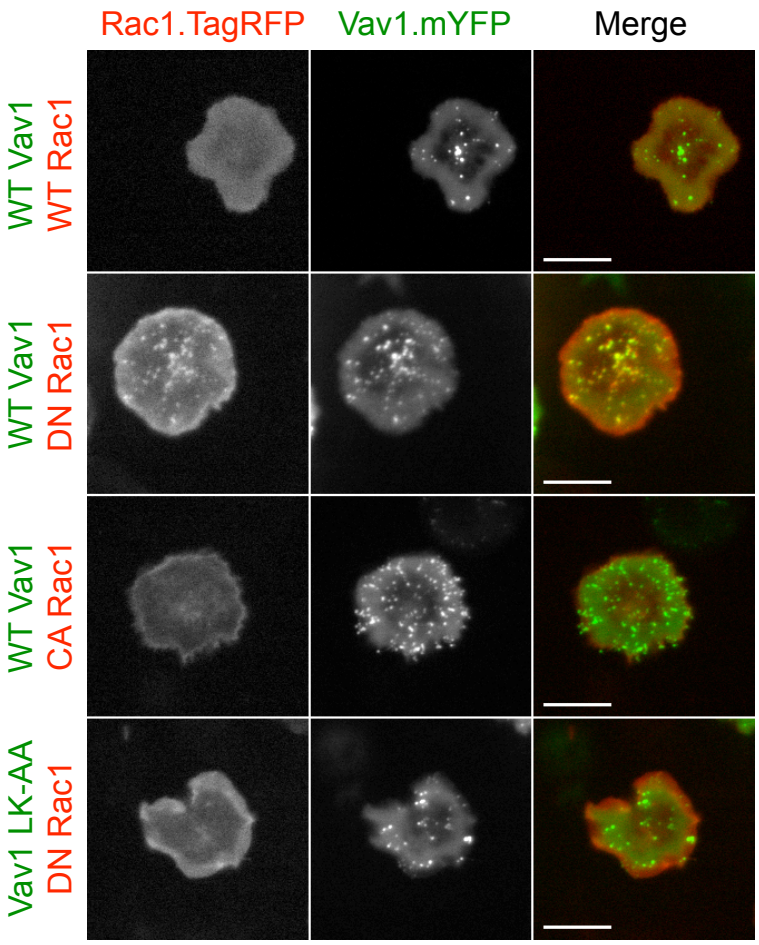

Figure 44: Dominant-negative Rac1 colocalizes with Vav1 within microclusters

JV.SC cells were transiently transfected with plasmids encoding either WT or LK-AA Vav1 and either dominant negative (DN), constitutively active (CA), or wild-type (WT) Rac1, as indicated. The cells were then stimulated on glass coverslips coated with 3 µg/ml OKT3 and imaged for 5 minutes by confocal microscopy. Vav1 constructs are shown in green and Rac constructs are shown in red. One representative of 3 experiments is shown.

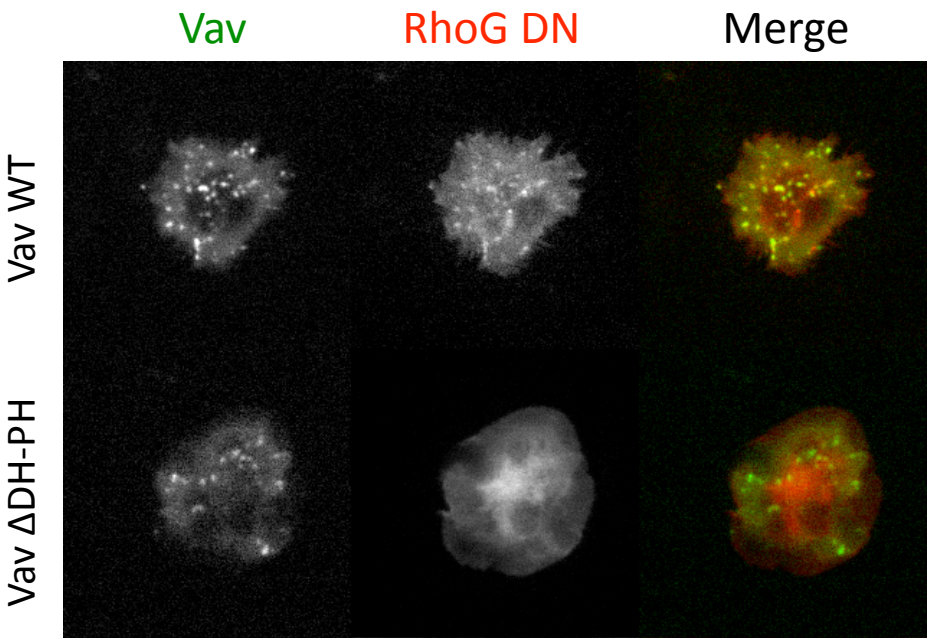

Figure 45: Dominant-negative RhoG colocalizes with Vav1 within microclusters

JV.SC cells were transiently transfected with plasmids encoding dominant negative (DN) RhoG and the indicated Vav1 construct fused to mYFP. The cells were then stimulated on glass coverslips coated with 3 µg/ml OKT3 and imaged for 5 minutes by confocal microscopy. Vav1 constructs are shown in green and RhoG constructs are shown in red. One representative of 2 experiments is shown.

7.2.7 Summary / Discussion II

I propose that one of the functions of SLP-76 MC is to act as an enzymatic hotspot, where effector molecules are recruited to facilitate their activation and their activity on downstream substrates. In support of this model, I found that those mutations that prevented Vav1 from entering microclusters (SH2*, Δ323) also prevented Vav1 from becoming phosphorylated. Vav1 phosphorylation on tyrosines 142, 160, and 174 is required to activate the enzymatic GEF activity. This suggests that the recruitment of Vav1 into SLP-76 MC and its subsequent phosphorylation potentiates the Vav1 GEF activity within these structures. I found that Vav1 colocalizes with various dominant negative (DN) GTPases in SLP-76 MC. These data are consistent with a model in which SLP-76 MC act as platforms for the recruitment and activation of various effector molecules. To further test this model, the activation of GTPases within SLP-76 MC could be measured by FRET with reporter constructs that bind to active GTPases (such as a PAK-CRIB construct). In addition, increased binding of DN GTPases would be expected in Vav1 mutations which promote the 'open,' GTPase-accessible form of the protein (such as the Vav1 Y3F mutation).

Although the Vav1 GEF activity is required for optimal signaling, our imaging data suggest that it is not required for the formation, persistence, or movement of SLP-76 MC. The Vav1 LK-AA mutant, which eliminates the Vav1 GEF activity, restores nearly all parameters of SLP-76 behavior. Interestingly, the GEF-inactivating L213A and L278Q mutations are unable to support SLP-76 MC movement and persistence. In contrast to the LK-AA mutant, these residues are not oriented toward the GTPase-binding surface in

the structure of the folded protein. L213 is oriented toward the hydrophobic core of the DH domain and L278 is oriented away from the DH domain and contacts the C1 domain (Figure 38). Either of these mutations could conceivably impact the proper folding of the DH-PH-C1 domains, thereby eliminating any scaffolding functions they may perform.

I found that the GEF activity of Vav1 is required for the optimal upregulation of surface CD69. This finding is in agreement with previous studies showing that the upregulation of CD69 relies on the activation of Rac1, JNK, and AP-1 [Billadeau 2000; Cao, Janssen et al. 2002; Castellanos, Munoz et al. 1997; Zugaza, Lopez-Lago et al. 2002]. Both the L213A and L278Q mutations prevented CD69 upregulation. However, the LK-AA mutation allowed moderate, but significant, increases in CD69 upregulation. This was surprising since CD69 upregulation normally reflects the activity of the GEF domains. This mutant also increased calcium flux compared to WT Vav1 when expressed at moderate levels, indicative of PLCγ1 activation. I suspect, but have not proven that the residual increase in CD69 could be driven by the diacylglycerol-dependent activation of Erk and AP-1.

Dynamic actin rearrangements are required for the inward movement of SLP-76 MC [Nguyen, Sylvain et al. 2008]. The Vav1 GEF activates several GTPases that are involved in actin cytoskeletal reorganization such as Rac and Cdc42. However, the Vav1 GEF is not required for SLP-76 MC movement. It is possible that Vav1 does not activate the specific GTPase that drive the retrograde actin flows responsible for microcluster movement. Alternatively, Vav1 could act redundantly with another GEF to activate the

relevant GTPases. To distinguish between these possibilities, the activation status of various GTPases could be monitored directly in the presence or absence of Vav1. This could be accomplished by pulling down the activated GTPases using bead-bound PAK constructs.

These data reveal that Vav1 possesses at least two functions within SLP-76 MC: a GEF-independent impact on the structural stability of the microcluster, and the provision of a localized GEF activity responsible for downstream signaling.

7.3 Result III: Scaffolding interactions mediated by the N-terminus of Vav1 contribute to the persistence, function, and cytoskeletal association of SLP-76 MC

7.3.1 Rationale III

The Vav1 Src homology domains in the C-terminus localize to SLP-76 MC, but are insufficient to restore microcluster persistence and movement. I have shown in Section 7.2 that the GEF activity does not contribute to SLP-76 MC persistence, suggesting that scaffolding interactions mediated by the N-terminus are required. In this section, I examine how the remaining N-terminal domains function in increasing microcluster persistence. In addition, association with the cytoskeleton is required for SLP-76 MC formation and movement. Since Vav1 is also required for the inward movement of SLP-76 MC, I examined the role of Vav1 in linking SLP-76 MC to the cytoskeleton.

7.3.2 Vav1 N-terminal domains contribute to MC stability through scaffolding interactions

The Vav1 GEF activity is not required to stabilize SLP-76 MC. However, this does not preclude the possibility that the DH, PH, and C1 domains could mediate protein-protein interactions and perform a scaffolding function to increase microcluster persistence. To determine whether the DH, PH, and C1 domains could perform scaffolding interactions to increase SLP-76 MC persistence, I created deletion mutants in which either the DH and PH domains or the C1 domain were deleted (ΔDH-PH or ΔC1, respectively – Figure 46). The ΔDH-PH and C1 mutant were recruited into long-lived SLP-76 MC which migrated toward the center of the cell:glass contact (Figure 47). Kymographs generated

from these cells revealed that these mutants exerted significant positive effects on the behavior of SLP-76 MC. To quantify SLP-76 MC behavior, individual microcluster paths were manually traced. Quantitative analysis showed that persistence and inward movement were slightly, but significantly, reduced in the ΔDH-PH mutant compared to WT Vav1 (Figure 48). These data indicate that the DH and PH domains could be involved in non-enzymatic scaffolding interactions to increase the persistence of SLP-76 MC.

To further study the effect of these deletions, I assayed T cell activation in J.Vav cells transiently expressing ΔDH-PH Vav1. Cells were stimulated for 16 hours with anti-TCR antibodies and upregulation of CD69 was measured by FACS. As expected, elimination of the GEF cassette completely prevented increases in surface CD69 following TCR stimulation (Figure 50), since upregulation of CD69 normally reflects the Vav1 GEF activity [Cao, Janssen et al. 2002; Castellanos, Munoz et al. 1997; Zugaza, Lopez-Lago et al. 2002]. I also measured calcium flux in cells reconstituted with ΔDH-PH Vav1 and found that this construct augmented calcium responses (Figure 49). This result provides further evidence that Vav1 controls calcium responses via its non-catalytic functions. However, the ΔDH-PH mutant was significantly less effective than wild-type Vav1 or the enzymatically inactive LK-AA mutant. This suggests that the overall topology of the N-terminus or non-catalytic surfaces present within the DH-PH module contribute to Vav1-dependent calcium responses.

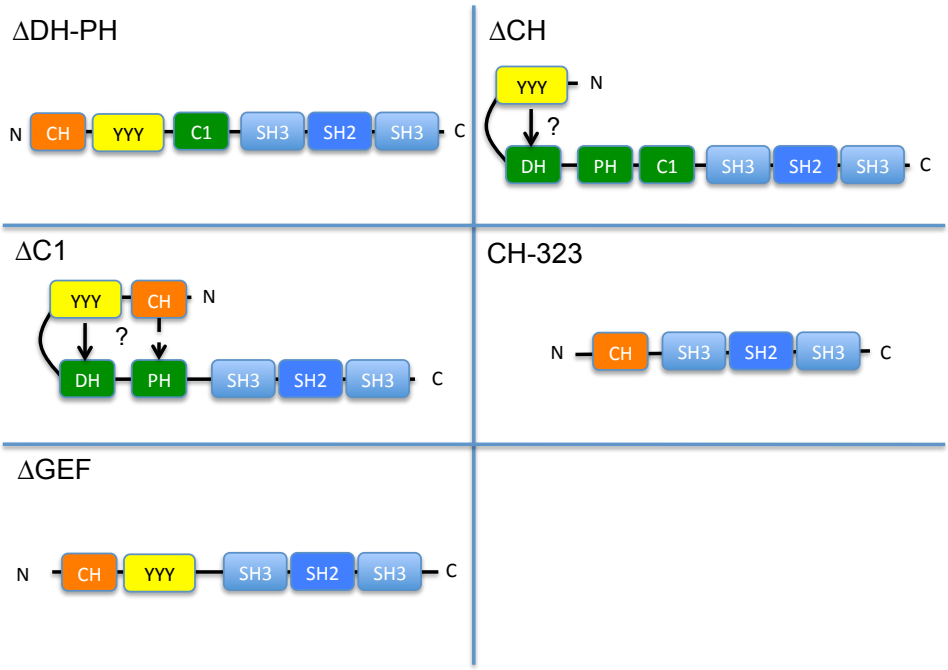

Figure 46: Diagram of Vav1 mutants used in this section

Simplified cartoon diagram of Vav1 mutants used in this section. For each mutant, the predicted effect of each mutation with regards to the open vs. closed conformation of Vav1 is shown. Solid and dashed arrows represent inhibitory folding mediated by the CH domain and N-terminal tyrosines.

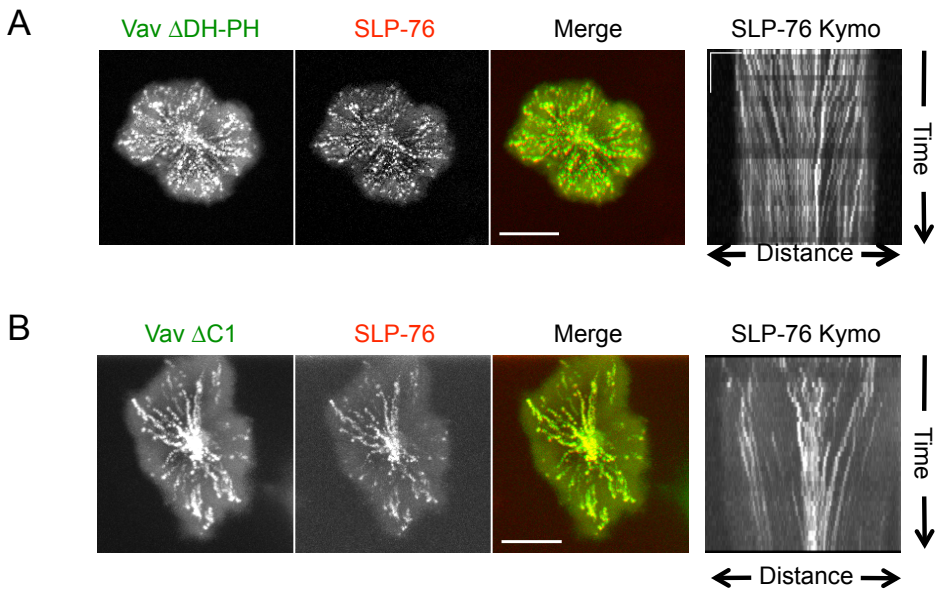

Figure 47: Vav1 enhances SLP-76 MC persistence independent of its GEF domains

JV.SC cells were transiently transfected with plasmids encoding the Vav1 ΔDH-PH (**A**) or ΔC1 (**B**) mutant as an mYFP fusion protein. One day post transfection, cells were imaged on glass coverslips coated with 3 µg/ml OKT3 for 5 minutes. SLP-76.mCFP is shown in red and mYFP constructs are shown in green. In the left panels, one representative MOT image from 3 experiments is shown (for panel B, one representative image from 2 experiments is shown). Scale bars correspond to 10 µm. In the right panels, kymographs were generated from these cells showing the inward movement (x-axis) over time (y-axis) of individual SLP-76 MC. Scale bars correspond to 5 µm and 60 s.

A

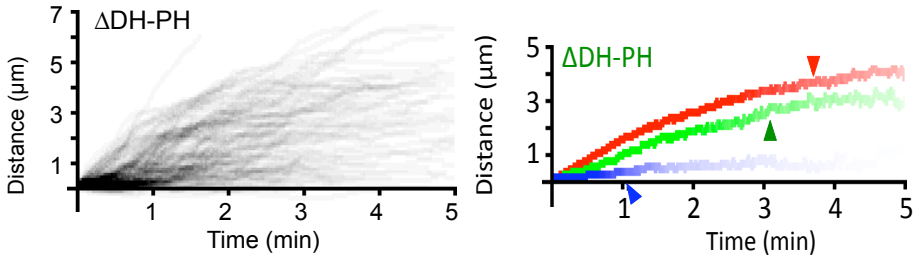

B

	Persistence (sec)	Movement (μm)	Speed (nm/sec)	% SLP in Clusters	Clusters per cell
mYFP	68.57 ± 3.93 ††	0.65 ± 0.03 ††	56.62 ± 2.12 ††	5.90 ± 0.67 ††	10.80 ± 0.84 ††
WT	180.51± 6.95 **	3.34 ± 0.19 **	102.96 ± 3.26 **	43.59 ± 2.83 **	19.15 ± 0.81 **
ΔDH-PH	166.62 ± 13.41 **	2.28 ± 0.34 **,†	82.30 ± 4.72 **,†	28.90 ± 3.58 **,†	17.40 ± 1.66 **

Figure 48: Vav1 DH and PH domains are required for optimal SLP-76 MC movement and persistence

A – Left: Individual SLP-76 MC paths were traced from cells expressing the Vav1 ΔDH-PH mutant. Kymographs from 10 cells across 3 experiments were traced. Of the total SLP-76 MC traced, the graph displays all traces persisting for more than 90 s or moving more then 2 μm. The fraction of microclusters passing these criteria are shown compared to the total number of microclusters traced. **Right**: All microcluster traces acquired from each cell were averaged to yield composite kymographs depicting fractional persistence (line intensity) over time (x-axis) and microcluster movement (y-axis). Arrowheads represent the half-life of SLP-76 MC for each condition. **B –** To obtain mean values for the duration and movement of SLP-76 MC were extracted from individual traces. These mean values are shown ± SEM. Single and double asterisks indicate statistical significance relative to cells expressing mYFP alone, single and double daggers indicate statistical significance relative to cells expressing wild-type Vav1.mYFP ($P < 0.05$ and $P < 0.005$, respectively).

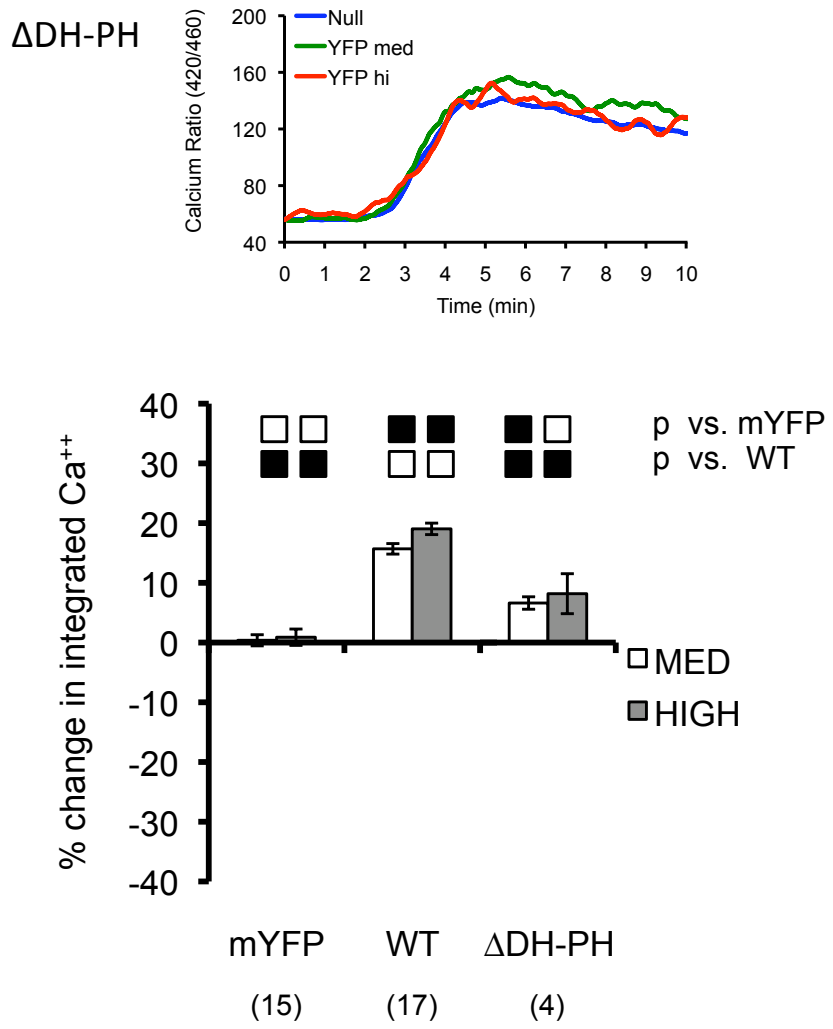

Figure 49: Vav1 ΔDH-PH mutant supports moderate increases in calcium flux

Intracellular calcium flux was measured in J.Vav1 cells transiently transfected with plasmids encoding the indicated Vav1 mutant protein fused to mYFP. **Top**: Calcium flux was measured in tightly gated populations of cells expressing moderate and high levels of fusion protein compared to untransfected cells (mYFP-null) from the same sample. One representative of three experiments are shown. **Bottom**: The mean percent change in integrated calcium responses is shown for populations of cells expressing medium and high levels of fusion protein relative to untransfected, mYFP-null cells from the same sample. Error bars indicate ± SEM. Replicates are listed in parenthesis below each sample. Black boxes indicate significant differences versus the indicated null or WT control, using a cutoff of $p = 0.05$.

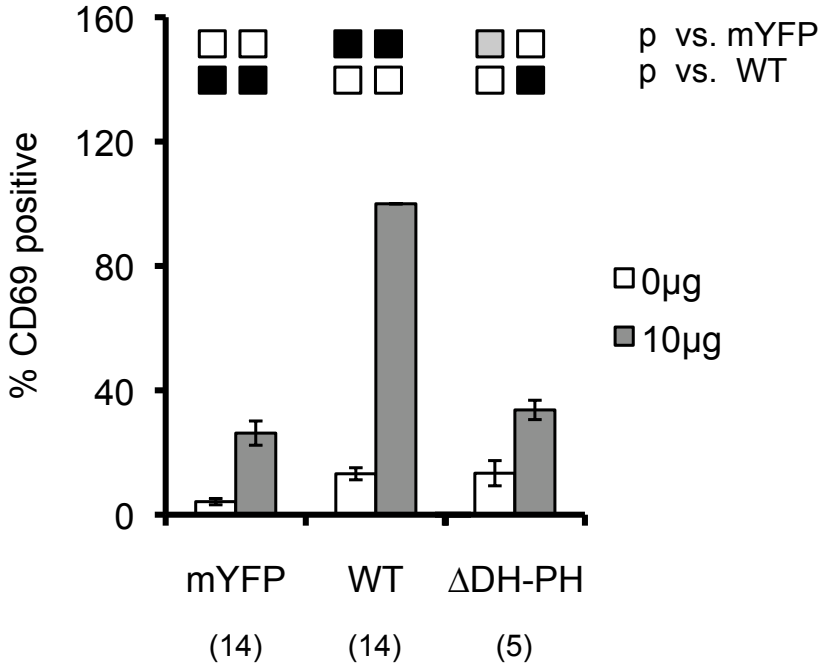

Figure 50: Vav1 DH and PH domains are required to upregulate CD69

J.Vav cells were transiently transfected with plasmids encoding the indicated Vav1 constructs fused to mYFP. Cells were stimulated for 16 hours with 10 µg/ml of soluble OKT3. Surface expression of CD69 was then measured by FACS in cell populations expressing tightly gated amounts of mYFP. The fraction of cells expressing CD69 was normalized to the response observed in J.Vav cells reconstituted with WT Vav1.mYFP and is shown as the mean ± SEM. Replicates are listed in parenthesis below each sample. Black boxes indicate significant differences versus the indicated null or WT control, using a cutoff of $p = 0.05$. Grey boxes are used to denote trends ($0.10 < p < 0.05$).

7.3.3 Vav1 CH plays a role in MC persistence

In the inactive state, the CH domain binds to the DH domain and contributes to the autoinhibition of Vav1 [Yu, Martins et al. 2010]. However, the role of potential scaffolding interactions mediated by this domain have not been addressed with respect to SLP-76 MC movement and persistence. To determine whether the Vav1 CH domain is required for SLP-76 MC persistence, I expressed a Vav1 mutant in which the CH domain was deleted (ΔCH) in JV.SC cells. These cells were stimulated on anti-TCR coated coverglass and imaged by confocal microscopy. SLP-76 and Vav1 ΔCH colocalized in microclusters that formed in the periphery of the cell:glass contact (Figure 51). These microclusters were mobile, as shown by 'streaks' in MOT images and diagonal traces in kymographs. Quantification of individual SLP-76 MC paths revealed Vav1 ΔCH showed intermediate, but significant, increases in almost all aspects of microcluster behavior (Figure 52). These data indicate that the Vav1 plays a role in optimal SLP-76 MC persistence and movement, potentially through scaffolding interactions.

Though Vav1 ΔCH enters mobile SLP-76 MC, this mutant was very rarely observed in the center of the cell:glass contact. To quantitate this observation, the fluorescence intensity of SLP-76 in the center of the contact was compared to the intensity at the periphery of the contact. From these measurements, I derived a 'centralization index' by comparing the average brightness of the cell to the average brightness found within the central region, after correcting for background brightness. A positive score in the resulting centralization index indicates that SLP-76 is enriched in the center of the contact, whereas a negative number indicates that most of the SLP-76 is present in the

periphery of the contact. A score of 0 indicates that the SLP-76 MC were uniformly distributed throughout the contact. These analyses confirmed that SLP-76 MC containing WT Vav1 accumulated in the center of the contact. In contrast, although the SLP-76 MC containing Vav1 ΔCH were mobile, they were excluded from center of the contact (Figure 53). This phenomenon is correlated with significant reductions in the stoichiometry of SLP-76 recruitment into microclusters as well as reductions in microcluster persistence and movement (Figure 52). Thus, in addition to its well-established role in regulating the enzymatic activity of Vav1, the CH domain is also required for the persistence, movement, and accumulation of SLP-76 MC in the center of the contact.

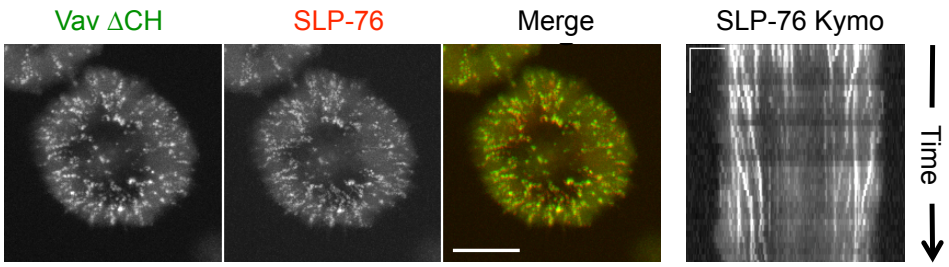

Figure 51: Vav1 CH domain is required for optimal SLP-76 MC persistence and movement

JV.SC cells were transiently transfected with plasmids encoding the indicated Vav1 construct as an mYFP fusion protein. One day post transfection, cells were imaged on glass coverslips coated with 3 µg/ml OKT3 for 5 minutes. SLP-76.mCFP is shown in red and mYFP constructs are shown in green. In the left panels, one representative MOT image from 3 experiments is shown. Scale bars correspond to 10 µm. In the right panels, kymographs were generated from these cells showing the inward movement (x-axis) over time (y-axis) of individual SLP-76 MC. Scale bars correspond to 5 µm and 60 s.

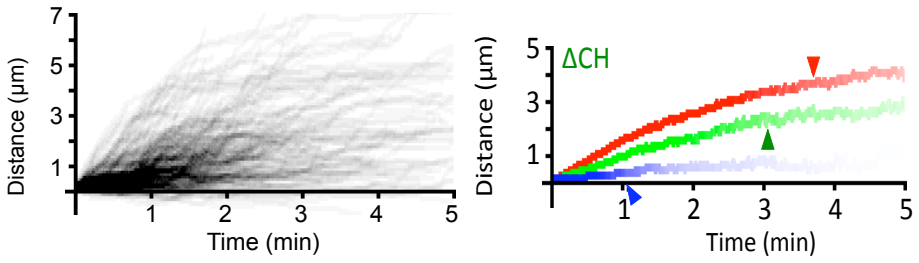

	Persistence (sec)	Movement (µm)	Speed (nm/sec)	% SLP in Clusters	Clusters per cell
mYFP	68.57 ± 3.93 ††	0.65 ± 0.03 ††	56.62 ± 2.12 ††	5.90 ± 0.67 ††	10.80 ± 0.84 ††
WT	180.51± 6.95 **	3.34 ± 0.19 **	102.96 ± 3.26 **	43.59 ± 2.83 **	19.15 ± 0.81 **
ΔCH	153.05 ± 10.09 **,†	2.20 ± 0.23 **,††	90.20 ± 3.85 **,†	23.66 ± 3.49 **,††	20.60 ± 1.41 **

Figure 52: Vav1 CH domain is required for optimal SLP-76 MC persistence and movement

A – Left: Individual SLP-76 MC paths were traced from cells expressing the Vav1 ΔCH mutant. Kymographs from 10 cells across 3 experiments were traced. Of the total SLP-76 MC traced, the graph displays all traces persisting for more than 90 s or moving more then 2 µm. The fraction of microclusters passing these criteria are shown compared to the total number of microclusters traced. **Right**: All microcluster traces acquired from each cell were averaged to yield composite kymographs depicting fractional persistence (line intensity) over time (x-axis) and microcluster movement (y-axis). Arrowheads represent the half-life of SLP-76 MC for each condition. **B –** To obtain mean values for the duration and movement of SLP-76 MC were extracted from individual traces. These mean values are shown ± SEM. Single and double asterisks indicate statistical significance relative to cells expressing mYFP alone, single and double daggers indicate statistical significance relative to cells expressing wild-type Vav1.mYFP ($P < 0.05$ and $P < 0.005$, respectively).

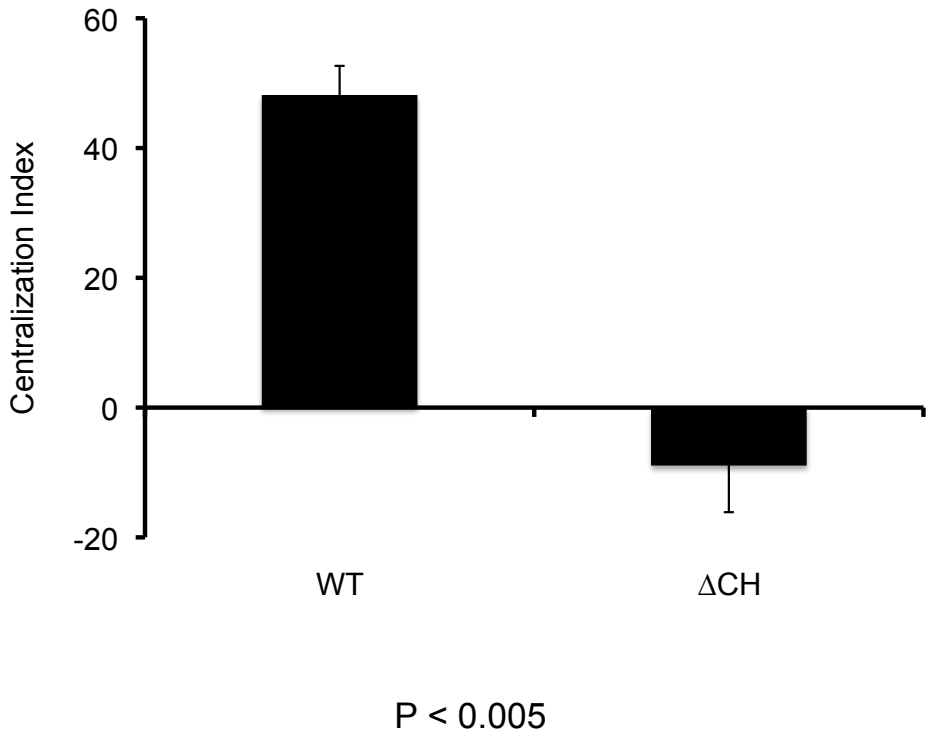

Figure 53: Vav1 CH domain is required for SLP-76 MC centralization

Kymographs generated from Figure 51 were used to determine the degree of SLP-76 MC centralization, expressed as a 'centralization index.' The centralization index was calculated as the average brightness of SLP-76 present in the center of the contact compared to the average brightness of the cell. For each condition, 15 individual cells were analyzed in 3 experiments.

7.3.4 Vav1 CH domain is required for calcium entry, but is dispensable for CD69 upregulation

To determine how the Vav1 CH domain functions in T cell activation, Vav1 ΔCH was transfected into Vav1 deficient cells. Following TCR stimulation, calcium flux was measured by FACS in populations of cells expressing comparable levels of fluorescently tagged chimeras. Consistent with previous studies [Billadeau 2000; Cao, Janssen et al. 2002], I found that the CH domain was required for Vav1-mediated calcium flux (Figure 54). High levels of ΔCH Vav1 caused a strong dominant negative phenotype, which could be explained by the chimera competing out endogenous Vav2 and Vav3.

I next measured upregulation of CD69 in cells reconstituted with the ΔCH mutant. Vav1 ΔCH restored CD69 upregulation to levels comparable to wild-type Vav1 (Figure 55). Interestingly, this mutant did not support levels greater than wild-type Vav1, as the Y3F mutant did, even though both of these mutants increase Vav1 GEF activity [Zugaza, Lopez-Lago et al. 2002]. This could reflect the reduced persistence of ΔCH microclusters, which may reflect reduced activity of microcluster-resident proteins. Alternately, this could reflect the loss of a CH-dependent PLCγ1, ERK, and AP-1 pathway leading to CD69 upregulation.

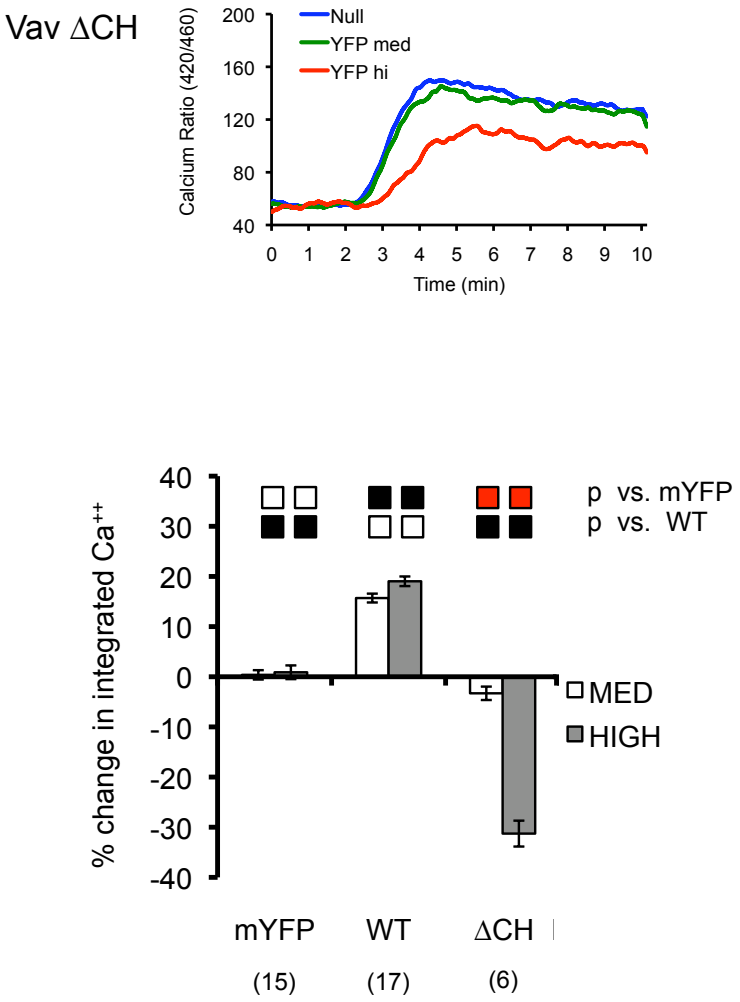

Figure 54: Vav1 CH domain is required for TCR-induced calcium flux

Intracellular calcium flux was measured in J.Vav1 cells transiently transfected with plasmids encoding the indicated Vav1 mutant protein fused to mYFP. **Top**: Calcium flux was measured in tightly gated populations of cells expressing moderate and high levels of fusion protein compared to untransfected cells (mYFP-null) from the same sample. One representative of three experiments are shown. **Bottom**: The mean percent change in integrated calcium responses is shown for populations of cells expressing medium and high levels of fusion protein relative to untransfected, mYFP-null cells from the same sample. Error bars indicate ± SEM. Replicates are listed in parenthesis below each sample. Black boxes indicate significant differences versus the indicated null or WT control, using a cutoff of $p = 0.05$. Red boxes also indicate statistical significance, but are used to emphasize dominant negative effects.

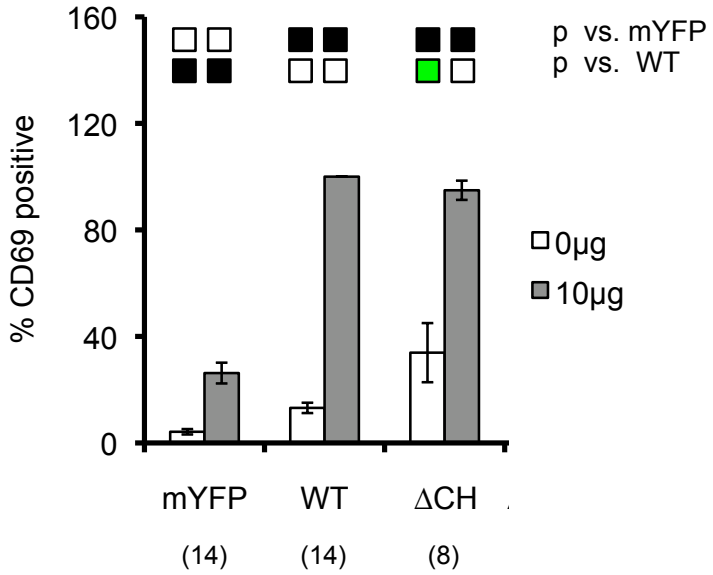

Figure 55: Deletion of Vav1 CH domain increases basal expression of CD69

J.Vav cells were transiently transfected with plasmids encoding the indicated Vav1 constructs fused to mYFP. Cells were stimulated for 16 hours with 10 µg/ml of soluble OKT3. Surface expression of CD69 was then measured by FACS in cell populations expressing tightly gated amounts of mYFP. The fraction of cells expressing CD69 was normalized to the response observed in J.Vav cells reconstituted with WT Vav1.mYFP and is shown ± SEM. Replicates are listed in parenthesis below each sample. Black boxes indicate significant differences versus the indicated null or WT control, using a cutoff of $p = 0.05$. Green boxes also indicate statistical significance, but are used to emphasize responses above wild-type.

7.3.5 The Vav1 CH domain does not influence SLP-76 MC movement via calcium entry

Deletion of the Vav1 CH domain reduces SLP-76 MC persistence and movement (Figure 52). This effect on microcluster persistence could be due to the loss of scaffolding interactions mediated by the CH domain. Alternately, the persistence and movement defects could be indirect consequences of the loss of CH domain-dependent calcium entry (Figure 54). To test whether the effect of the ΔCH mutant is due to the loss of scaffolding interactions or to reduced calcium levels, I measured SLP-76 MC persistence in the presence or absence of extracellular calcium. Cells responding in the absence of extracellular calcium adhered to the stimulatory surface and formed persistent, mobile SLP-76 MC (Figure 56A). The persistence of SLP-76 MC formed in the absence of extracellular calcium was not significantly reduced compared to those formed in the presence of calcium (Figure 56B and C). These data argue that the impact of the Vav1 CH domain on SLP-76 MC persistence is due to scaffolding interactions mediated by this domain and not to the loss of intracellular calcium flux.

Notably, the SLP-76 MC formed in the absence of extracellular calcium moved with greater speed and covered more distance (Figure 56B and C). Because the movement of SLP-76 MC requires dynamic rearrangement of the actin cytoskeleton [Ilani, Vasiliver-Shamis et al. 2009; Nguyen, Sylvain et al. 2008], I hypothesized that the increased SLP-76 movement seen in the absence of extracellular calcium could be caused by an increase in the speed of retrograde actin flow. To test this hypothesis, Jurkat T cells expressing GFP-tagged actin were imaged following stimulation on anti-TCR coated coverslips.

These cells were imaged in the presence of EGTA with or without additional calcium (note that EGTA sequesters extracellular calcium, added calcium is sufficient to overcome this effect and functions as a control). To compare the speed of retrograde actin flow in these two conditions, I generated kymographs from representative cells. Since it was difficult to assess the movement speed by eye, the inward flow of actin in each cell was approximated by placing multiple straight lines. By calculating the average slopes of these lines, I were able to confirm that the speed of retrograde actin flow was increased in the absence of extracellular calcium (Figure 57). Faster-moving objects travel a greater distance (horizontal plane in our kymographs) in the same amount of time (vertical plane in kymographs) than would a slower object. Therefore, the smaller slope observed in the absence of calcium indicates that actin flowed in with greater speed than in the presence of calcium. Using these slopes, our calculations show that retrograde actin flow moves inward at a rate of 188 nm/sec in the presence of EGTA and 119 nm/sec in the presence of calcium. The speed observed in the control sample is comparable to the speed of retrograde actin flow reported elsewhere [Yu, Wu et al. 2010]. Therefore, the increased speed of retrograde actin flow could contribute to the increased SLP-76 MC movement that I observed in the absence of extracellular calcium. Since the reduced entry of calcium observed in the ΔCH mutant is predisposed to cause faster microcluster movement, it is unlikely that this biochemical defect could cause the movement defects observed with the ΔCH mutant.

A

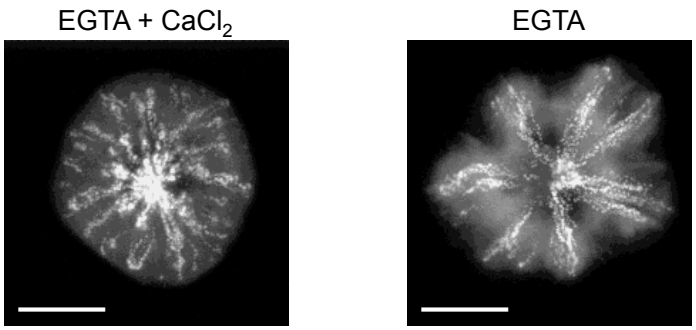

B

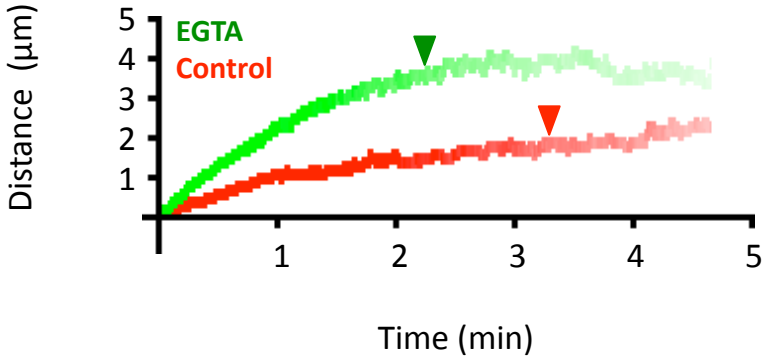

C

	Control	EGTA
Persistence	179.68 ± 14.39	147.76 ± 8.38
Movement	19.98 ± 2.29	32.08 ± 3.95 *
Speed	92.00 ± 8.34	120.60 ± 10.36 *
% SLP in Clusters	43.70 ± 4.67	43.40 ± 5.46
Clusters per cell	20.80 ± 1.60	26.30 ± 3.52

Figure 56: Calcium chelation increases SLP-76 MC movement and speed

A - J14.SY cells were stimulated on glass coverslips coated with 3 µg/ml OKT3 in imaging media containing 2 mM EGTA with or without 2 mM $CaCl_2$. Cells were imaged for 5 minutes by confocal microscopy. MOT projections from cells representative of three experiments are shown. **B –** Kymographs were generated from the imaging experiments shown in panel A. For each condition, the microcluster traces from each cell were averaged to yield composite kymographs depicting fractional persistence (line intensity) over time (x-axis) and microcluster movement (y-axis). Kymographs were generated from 10 cells across 3 experiments. Arrowheads represent the half-life of SLP-76 MC for each condition. **C –** To obtain mean values for the duration and movement of SLP-76 MC were extracted from individual traces. These mean values are shown ± SEM. Asterisks indicate statistical significance relative to cells imaged in the presence of calcium ($P < 0.05$).

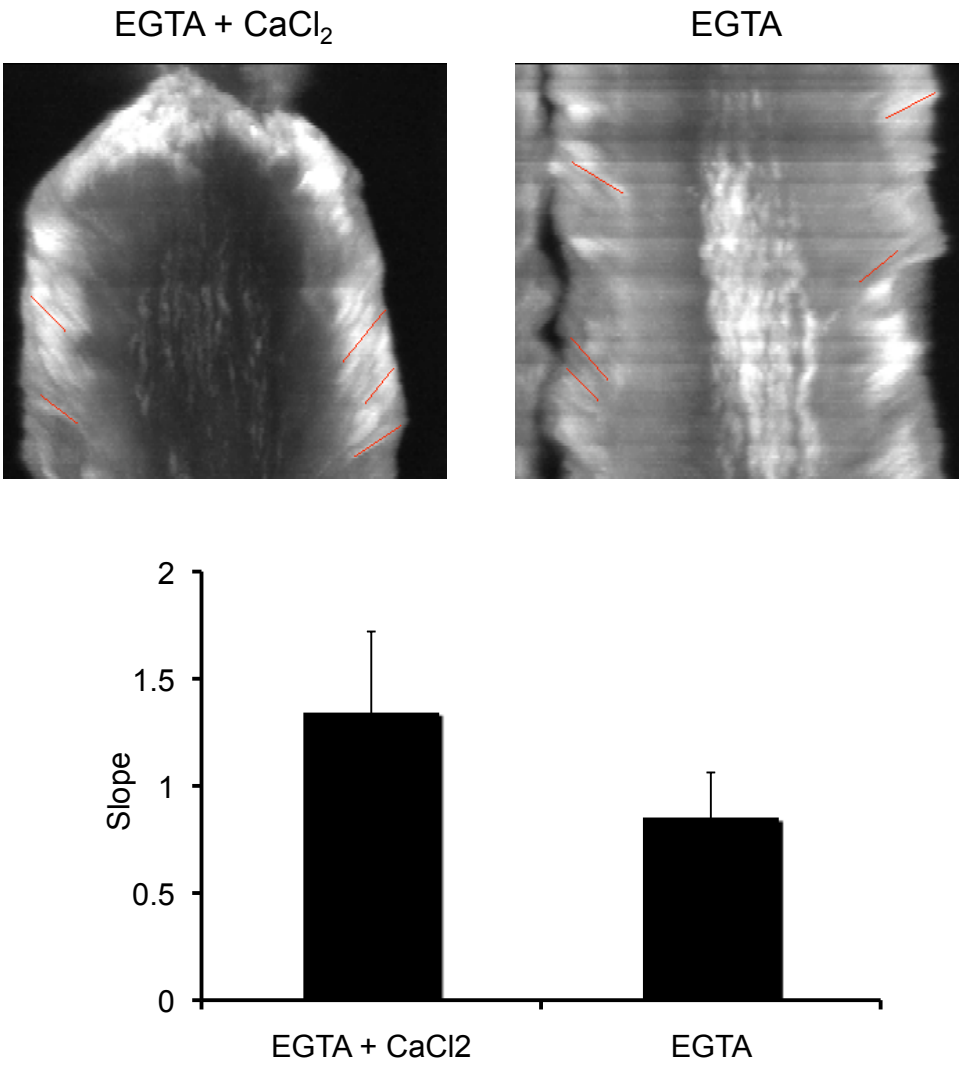

Figure 57: Calcium chelation increases retrograde actin flow

Jurkat T cells expressing EGFP-tagged actin (EGFP.actin) were stimulated on glass coverslips coated with 10 µg/ml of the anti-TCR antibody OKT3. Cells were imaged over 5 minutes in imaging media containing 2 mM EGTA with or without 2 mM $CaCl_2$. Kymographs were generated from representative cells. To measure the speed of retrograde actin flow, the inward movement over time of actin was traced (red lines in top panels). I then measured the slope of the line: lower slope corresponds to faster movement and vice versa. These slopes correspond to movement speeds of 119 nm/sec in the presence of EGTA + $CaCl_2$ and 188 nm/sec in the presence of EGTA.

7.3.6 SLP-76 MC act as attachment sites to stimulatory substrates

Microclusters form within zones of tight adhesion between the T cell and stimulatory surface [Bunnell, Hong et al. 2002]. Therefore, I propose that one of the functions of SLP-76 MC is to act as adhesion sites in T cells upon contacting a stimulatory surface. To visualize the recruitment of SLP-76 MC components and cytoskeletal proteins to a stimulatory surface, I imaged cells expressing fluorescently-tagged fusion proteins of SLP-76, ZAP-70, tubulin, or actin. These cells were stimulated on beads coated with anti-TCR antibodies and VCAM. After adhering and stimulating, the cells were fixed with the reversible crosslinker dithiobis[succinimidylpropionate] (DSP) and imaged by confocal microscopy. I found that SLP-76 and ZAP-70 formed microclusters on the surface of the stimulatory bead. In addition, the microtubule-organizing center (MTOC) polarized toward the stimulatory beads and the cells formed actin-rich extensions around the beads (Figure 58A – top panels). SLP-76, ZAP-70, and actin remained bound to the bead despite physical disruption of the cell by sonication (Figure 58B – bottom panels), showing that these microcluster proteins adhere tightly to beads. I confirmed that these proteins were retained on beads by Western blot, and confirmed the selectivity of their retention by blotting for tubulin (Figure 59B). These data strongly suggest that SLP-76 MC are sites of tight adhesion between stimulatory surfaces and T cells. Therefore, it is plausible that any mutations that negatively impact the stability of the SLP-76 MC would reduce T cell adhesion.

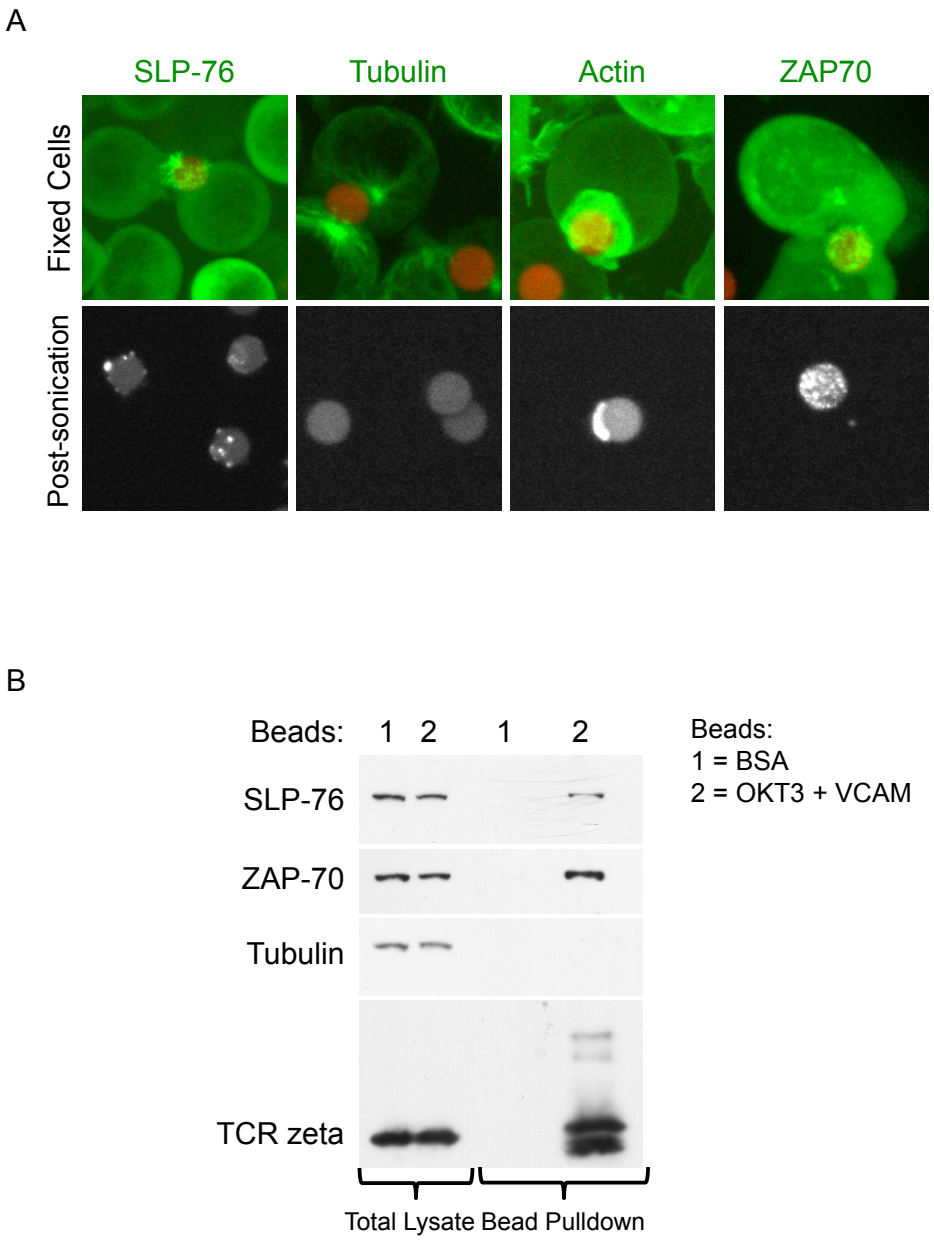

Figure 58 SLP-76 MC adhere to stimulatory surfaces and resist physical disruption

A – Jurkat T cells expressing the indicated proteins fused to either mYFP or GFP (green) were stimulated on OKT3 and VCAM coated beads (red). After 5 minutes, cells were fixed with the reversible crosslinker DSP and imaged by confocal microscopy (top panels). A subset of cells were sonicated to remove the cell body and any weakly-adherent structures. The remaining bead-conjugated material was washed 3x in PBS and imaged. **B –** J14.SY cells were incubated with beads coated with either BSA or OKT3 and VCAM. After 5 minutes, a subset of the cells were lysed in lysis buffer. The remaining cells were fixed, sonicated, and washed. The beads were then boiled in Novex running buffer; protein retention was determined by Western blot.

7.3.7 Vav1 domains required for normal MC speed and directionality

When expressed in JV.SC cells, the Vav1 SH3-SH2-SH3 fragment localizes to SLP-76 MC, but does not support microcluster persistence or movement, indicating that one or more of the N-terminal domains are responsible for these functions. I have shown that the ΔDH-PH mutant displayed mild defects in SLP-76 MC behavior (Figure 48) and the ΔCH mutant produced moderate defects (Figure 52). Neither of these deletions reduced the extent of Vav1 phosphorylation (Figure 59), indicating the phenotypes associated with these domains are decisively caused by the loss of these domains, rather than by the indirect loss of scaffolding interactions or catalytic functions that depend on the phosphorylation of the N-terminal tyrosines of Vav1. Of these deletions, the ΔCH mutant produced greater defects in SLP-76 MC persistence, movement, and centralization. To identify the minimal unit of Vav1 required to support SLP-76 MC movement, I fused the CH domain to the SH3-SH2-SH3 fragment (termed CH-323) and transfected this construct into JV.SC cells. Cells were stimulated on anti-TCR coated coverslips and microcluster behavior was observed by microscopy. Upon contacting the coverslips, microclusters containing SLP-76 and Vav1 CH-323 were formed (Figure 60A). Microcluster persistence appeared to be increased relative to the isolated SH323 fragment. While some microclusters show centralized movement, many microclusters show erratic, non-directional movement (not shown). Also, these SLP-76 MC move at speeds much greater than the inward actin flow, suggesting that they have become uncoupled from the normal, actin-dependent translocation machinery. Due to the non-directional movement of these microclusters, I were unable to capture and analyze them with our standard approach

The CH-323 fragment shows rapid, non-centralizing movement. However, of the domains removed by this mutation, I have deleted the DH, PH, and C1 domains an point mutated the N-terminal tyrosines, all without replicating this defect. This suggests that regions outside of the classical homology domains of Vav1 mediate directed centripetal movement of SLP-76 MC. Potential regions of interest include regions of the N-terminal acidic domain flanking the conserved regulatory tyrosines, and an evolutionarily conserved polybasic region which lies between the C1 domain and the N-terminal SH3 region (Figure 61). There are no known functions for any of these regions. However, the polybasic region shows similarities to the actin-binding motif (KKEK) present in villin [Friederich, Vancompernolle et al. 1992]. To address the potential roles of these regions in the directed movement of SLP-76 MC, I left them intact while simultaneously removing the DH, PH, and C1 domains (ΔGEF mutant). I expressed this construct as an N-terminal fusion protein with mYFP in JV.SC and stimulated these cells on anti-TCR coated coverslips. The Vav1 ΔGEF construct colocalized with SLP-76 MC and displayed moderate defects in microcluster movement and persistence (Figure 60B). This could be a result of the loss of scaffolding interactions mediated by the DH, PH, and C1 domains. Importantly, this mutant did not display the undirected movement characteristic of the CH-323 mutant. Thus, it is plausible that one of these two regions plays a crucial role in the coupling of Vav1 to systems responsible for the directed movement of microclusters.

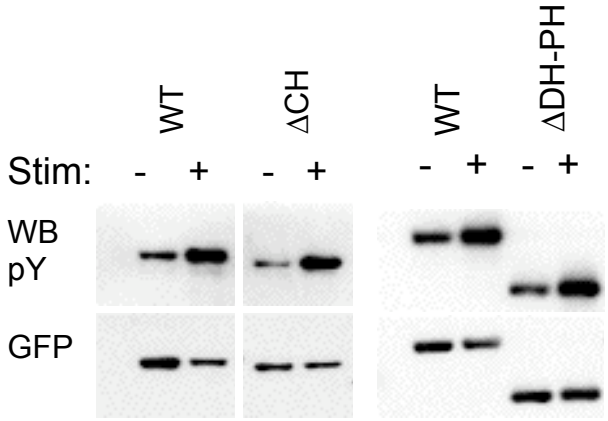

Figure 59: CH, DH, and PH domains are not required for Vav1 phosphorylation

The indicated Vav1 mutants were expressed as mYFP fusion proteins in Jurkat T cells. Following stimulation with C305 anti-TCR antibody, Vav1 fusion proteins were precipitated from stimulated cell lysate using antibodies specific for GFP. Vav1 phosphorylation was determined by Western blotting with antibodies against phosphotyrosine. One representative of three experiments is shown.

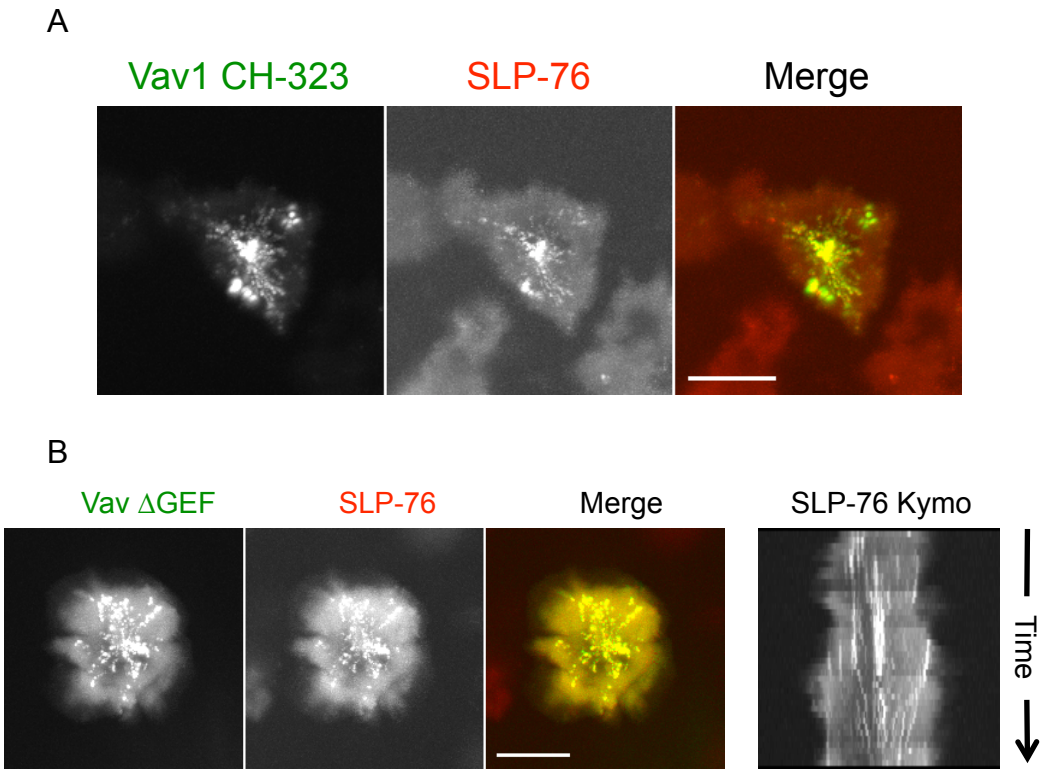

Figure 60: Interactions within the Vav1 N-terminus contribute to SLP-76 MC movement and persistence

JV.SC cells were transiently transfected with plasmids encoding the indicated Vav1 construct as an mYFP fusion protein. One day post transfection, cells were imaged on glass coverslips coated with 3 µg/ml OKT3 for 5 minutes. SLP-76.mCFP is shown in red and mYFP constructs are shown in green. **A –** One representative MOT image from 4 experiments is shown. Kymographs were not generated for this mutant due to a subset of SLP-76 MC that displayed rapid, non-centralized movement. **B -** In the left panels, one representative MOT image from 2 experiments is shown. Scale bars correspond to 10 µm. In the right panels, kymographs were generated from these cells showing the inward movement (x-axis) over time (y-axis) of individual SLP-76 MC.

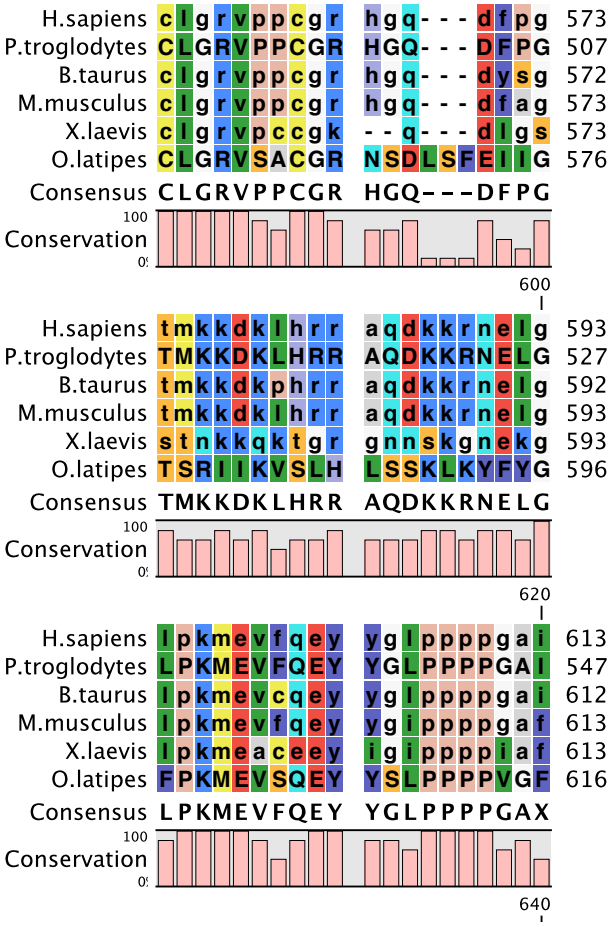

Figure 61: Evolutionary conservation of the Vav1 polybasic region

Homo sapiens Vav1 protein sequence was compared to various other species. The histogram at the bottom shows the degree of conservation across all species examined.

7.3.8 Summary / Discussion III

SLP-76 MC are signaling structures that form in the tight junctions formed between T cells and a stimulatory surface [Bunnell, Hong et al. 2002]. Their formation, persistence, and movement are dependent on the dynamic reorganization of the actin cytoskeleton [Ilani, Vasiliver-Shamis et al. 2009; Nguyen, Sylvain et al. 2008]. I have shown that non-persistent SLP-76 MC can be mobile (see SLP-76 movement and speed in Vav1 N3*C3* mutant – Figure 25), indicating that defects in SLP-76 MC movement are not necessarily secondary effects of mutations that decrease microcluster persistence. I speculate that mutations that affect the movement of SLP-76 MC could affect the association of Vav1 with the actin cytoskeleton or with the translocation machinery.

To determine which N-terminal domains of Vav1 contribute to SLP-76 MC persistence and movement, I created deletion mutants of various N-terminal domains. I found that deletion of the DH and PH domains caused limited defects in the persistence and movement of SLP-76 MC, whereas the GEF-inactivating LK-AA mutation did not significantly alter the properties of SLP-76 MC. Since the complete removal of the DH and PH domains was less severe than the introduction of the GEF-inactivating point mutations L213A and L278Q, these point mutations must affect the folding or structure of adjacent domains that are left intact by the excision of the DH and PH domains. Furthermore, these data suggest that non-catalytic scaffolding interactions mediated by the DH and PH domains contribute to microcluster stability. Alternatively, large-scale deletions could alter the normal spatial organization of the remaining domains, which may impair scaffolding interactions mediated by these domains. One potential caveat of

these mutations is that the deletion of the N-terminal domains could alter the conformation of the remaining C-terminal domains. However, both the ΔDH-PH and ΔCH constructs localized to SLP-76 MC, a function that I have shown requires an intact SH2 domain (Figure 22). Furthermore, these constructs become phosphorylated following TCR signaling (Figure 59) and I have never observed bands in Western blots that would indicate degradation of the protein. These observations suggest that the remaining domains in the ΔDH-PH and ΔCH deletion mutants fold and function normally.

In addition to binding GTPases, the DH domain of Vav1 also binds to the p67phox complex, which regulates NADPH oxidase [Ming, Li et al. 2007]. This interaction enhances the enzymatic activities of both Vav1 and p67phox. It is possible that this interaction could cause Vav1 to shift into an 'open' conformation. The conformational changes induced by Vav1 activation not only increase the accessibility of the DH domain, but are also likely to increase the availability of the CH domain, which is also involved in the autoinhibitory fold [Yu, Martins et al. 2010]. Our data suggest that the Y3F mutation increases calcium flux in a similar manner, by increasing the availability of the CH domain. In addition, experiments performed *in vitro* suggest that the PH domain of Vav1 is capable of binding PIP3 present in the cell membrane [Han, Luby-Phelps et al. 1998]. These observations suggest the involvement of the non-catalytic scaffolding interactions mediated by the DH and PH domains in the stabilization of SLP-76 MC.

I have also shown that the CH domain participates in scaffolding interactions in addition to its well-established role in mediating calcium flux (Figure 52). Based on sequence homology data, the CH domain has been proposed to be an actin-binding domain [Castresana and Saraste 1995]. However, single CH domains such as the one present in Vav1 usually mediate protein-protein interactions, while tandem CH domains are capable of binding actin [Mario Gimona 2002]. Currently, there are two confirmed binding partners for the Vav1 CH domain: calmodulin [Cao 2007], and Ezh2 [Hobert, Jallal et al. 1996]. Ezh2 is a lysine methyltransferase that is involved in actin cytoskeletal reorganization [Su, Dobenecker et al. 2005]. Loss of this interaction could hinder the normal actin dynamics that are required to form persistent, mobile SLP76 MC.

Interestingly, the absence of extracellular calcium increases the movement speed and distance of SLP-76 MC (Figure 57). In the absence of extracellular calcium, I also observed an increase in the speed of retrograde actin flow (Figure 59). This could represent a positive feedback loop, in which productive TCR signaling generates a SLP-76 MC that is competent to transduce signals resulting in intracellular calcium flux. This increased calcium would allow the SLP-76 MC to remain in the periphery, prolonging its tyrosine phosphorylation and allowing continued signaling.

A similar correlation between SLP-76 MC movement and retrograde actin flow has been observed in cells co-stimulated with VCAM. In this study, VCAM costimulation slowed the movement of both SLP-76 MC and the actin cytoskeleton [Nguyen, Sylvain et al. 2008]. However, it is not yet clear whether actin determines SLP-76 speed, or MC

mobility affects rate at which actin can move. Imaging experiments have shown that SLP-76 MC slow down as they approach ZAP-70 containing microclusters, suggesting that they do not freely flow in on actin. Instead, proteins within SLP-76 MC may act as a molecular 'clutch' by binding both mobile actin and immobile receptor components [Hu, Ji et al. 2007]. In this regard, Vav1 may be a key protein in regulating SLP-76 MC movement. It possesses Src homology domains that bind to SLP-76 MC components and may be involved in F-actin binding, either through its CH domain or through its polybasic region, which shares homology with other actin binding proteins.

8 Discussion

In this thesis, I have examined the function of SLP-76 MC by analyzing one of their constituent proteins, Vav1. By analyzing the structure and function of this protein, I have gained insight into the requirements for the formation and persistence of SLP-76 MC following TCR stimulation. In addition, I have shown that Vav1 is required for the translocation of SLP-76 MC, and have characterized the regions of Vav1 that are required for this function.

Of the three Vav family member proteins, Vav1 is the single most important for T cell development, proliferation, and activation following TCR stimulation [Fujikawa, Miletic et al. 2003]. However, other Vav family members are able to partially compensate for the lack of Vav1 and mediate weak calcium flux in the absence of Vav1 [Cao, Janssen et al. 2002]. I observed this phenomenon when measuring calcium flux in the J.Vav cell line (Figure 21). In these Vav1 deficient cells, I also observed the formation of transient SLP-76 MC. Endogenous Vav2 or Vav3 could be involved in formation of these microclusters and in the weak calcium flux that I observed in Vav1 deficient cells. Expression of the Vav1 SH323 fragment reduces calcium flux below that observed in a Vav1 deficient cell. This dominant-negative effect could be due to the entry of the SH323 fragment into the microcluster and the displacement of endogenous Vav2 and Vav3. It would be interesting to see whether Vav2 and Vav3 enter SLP-76 MC following TCR stimulation and whether this localization is required for their function. However,

for the purpose of this thesis, I have focused on addressing the role of Vav1 in SLP-76 MC formation and persistence.

8.1 Microcluster formation: a prerequisite for function

8.1.1 Multivalent interactions contribute to MC stability

SLP-76 MC formed downstream of the TCR contain a variety of adapter and effector molecules. I propose that one of the critical functions of SLP-76 MC is to act as a platform for the efficient recruitment and activation of downstream signaling proteins. Evidence from the Bunnell lab and others suggests that SLP-76 MC persistence is achieved through multivalent interactions among microcluster resident proteins (multivalent interactions among some of the critical SLP-76 MC components is shown in Figure 62). Among the proteins known to be present in SLP-76 MC, it is known that LAT, Gads, SLP-76, SOS, Itk, PLCγ1, and c-Cbl participate in multivalent interactions to increase the persistence of SLP-76 MC [Arudchandran, Brown et al. 2000; Balagopalan, Barr et al. 2007; Braiman, Barda-Saad et al. 2006; Bunnell, Diehn et al. 2000; Bunnell, Singer et al. 2006; Dombroski, Houghtling et al. 2005; Houtman, Yamaguchi et al. 2006; Lin and Weiss 2001; Meuer, Fitzgerald et al. 1983; Reynolds, de Bettignies et al. 2004; Reynolds, Smyth et al. 2002]. I have shown that Vav1 is also recruited into SLP-76 MC and increases their persistence through scaffolding interactions. In the absence of these scaffolding domains, or in the absence of Vav1 recruitment into a SLP-76 MC, stable microclusters do not form and TCR signaling is likewise impaired. Therefore, the formation of a stable, persistent structure is a prerequisite for optimal TCR signaling. The contributions of Vav1 to signaling pathways leading to T cell activation are shown in Figure 63.

Assembly of the signaling complex through multivalent interactions confers a number of benefits to the T cell. First, it allows the rapid assembly of a signaling platform from modular components and the rapid disassembly of the platform upon termination of the signal. This can allow the T cell to discriminate between TCR ligands of varying affinity, as predicted by the kinetic proofreading model. In addition, by participating in multivalent interactions, SLP-76 MC-resident proteins increase their dwell time within the microcluster. This may facilitate their association with upstream activators their downstream targets. Thus, persistent SLP-76 MC may increase the efficacy of signaling by their constituent proteins.

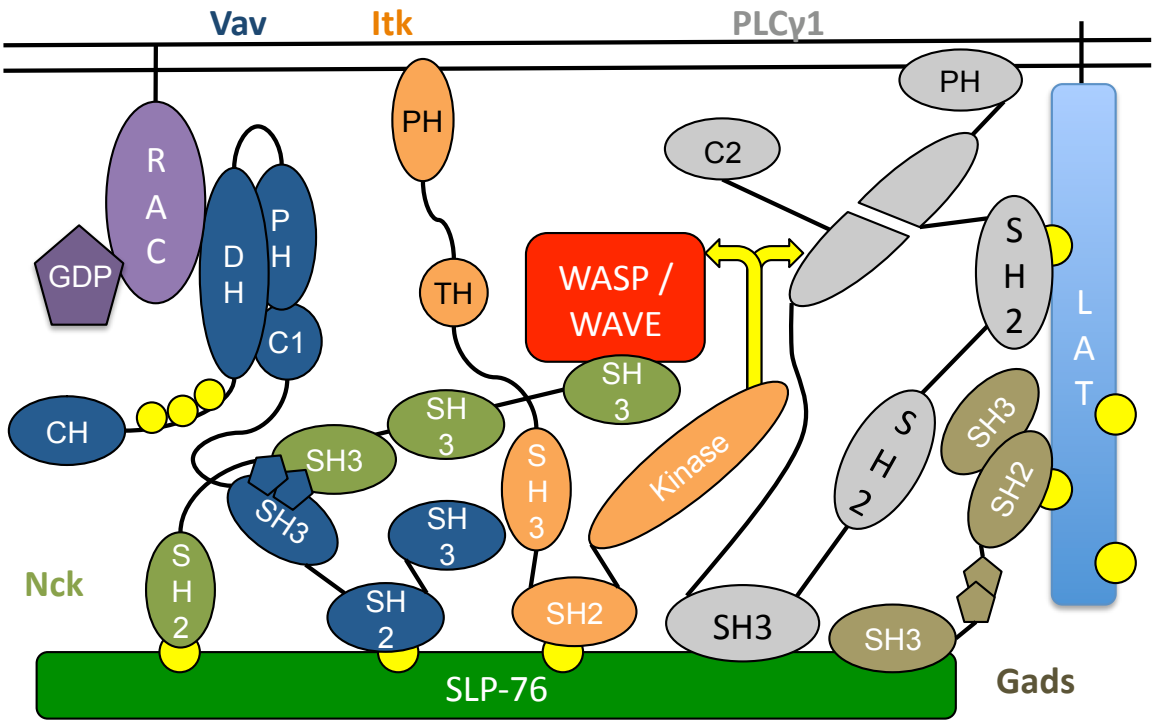

Figure 62: Multivalent interactions within SLP-76 MC

Interactions within the signaling complex are nucleated on the N-terminal tyrosines of SLP-76 (tyrosine phosphorylation is shown by yellow circles). These tyrosines create docking sites for Nck, Vav1, and Itk. These interactions alter the quaternary structure of Itk, activating its kinase activity (yellow arrows) toward PLCγ and the actin regulatory protein WASP. Rac1 activates the actin polymerization mediated by WAVE.

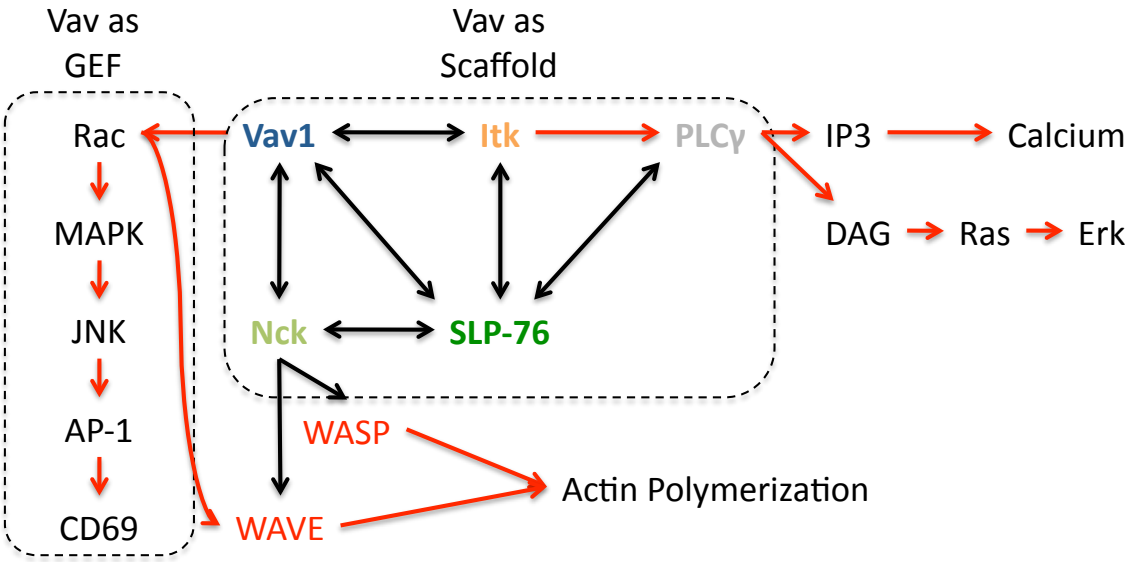

Figure 63: GEF-dependent and GEF-independent functions of Vav1

Involvement of Vav1 in signaling pathways leading to activation of T cells. Known biochemical interactions are shown by black arrows, while activation of downstream effectors is indicated by red arrows. Two functions of Vav1 within the SLP-76 MC (scaffold and enzyme) are indicated by dashed boxes.

8.1.2 Enzymatic activities recruited into SLP-76 MC

Itk/PLCγ1

A variety of effector modules are recruited into SLP-76 MC. One such effector molecule is the kinase Itk, which is required for T cell activation, proliferation, and function. Itk facilitates the localization of Vav1 to the site of antigen contact in a kinase-independent manner [Dombroski, Houghtling et al. 2005]. Itk participates in multiple protein-protein interactions within SLP-76 MC: it binds to SLP-76 tyrosine 145 through its SH2 domain and to Vav1 through an unknown mechanism. However, it is unknown whether the loss of these interactions from the SLP-76 MC results in decreased microcluster persistence, though it is likely given that Vav1 would also be absent from the microcluster in the absence of the scaffolding functions of Itk. Though the kinase activity is not required for these scaffolding interactions, Tec family kinases have been implicated in the activation of PLCγ1 and calcium mobilization [Schaeffer, Debnath et al. 1999], indicating that the enzymatic activity of Itk plays an important role in signal transduction. Activation of PLCγ1 is a critical event in TCR signal transduction, as it results in the generation of DAG and intracellular calcium flux. Since both Itk and PLCγ1 are recruited into SLP-76 MC [Braiman, Barda-Saad et al. 2006], the increased persistence of these signaling structures is likely to facilitate the activation of PLCγ1. However, scaffolding interactions mediated by PLCγ1 are unlikely to be involved in SLP-76 MC persistence, since microcluster persistence is unaffected in PLCγ1 deficient cells [Bunnell, Singer et al. 2006]. Therefore, PLCγ1 represents a purely functional module that is recruited into SLP-76 MC.

MC Ubiquitination and Turnover

Though SLP-76 MC contain many proteins that mediate T cell activation, inhibitory proteins are also recruited into these structures. The ubiquitin ligase c-Cbl, which down-regulates signaling, are also recruited into SLP-76 MC [Balagopalan, Barr et al. 2007]. The enzymatic activity of c-Cbl drives the endocytosis and down-regulation of signaling complexes. As I have discussed in Section 4, down-modulation of the immune response is also critical for the health of the host. Recruiting such inhibitory proteins may be a mechanism to limit the useful lifespan of SLP-76 MC, thereby reducing T cell activation and preventing autoimmune reactions.

GEFs and GTPases

In addition, GEFs such as Vav1 and SOS are also recruited into SLP-76 MC (Figure 12 and [Houtman, Yamaguchi et al. 2006]). Our data show that the GTPases Rac1 and RhoG are recruited into SLP-76 MC, which are the site of Vav1 exchange activity (Figure 45 and 46). Although SOS may also perform its enzymatic activity within microclusters, this has not been experimentally shown. Nevertheless, it is probable that the SLP-76 MC is involved in Ras-dependent Erk signaling [Reynolds, de Bettignies et al. 2004] and Rac-dependent MAPK signaling and cytoskeletal reorganization [Billadeau, Nolz et al. 2007] downstream of Vav1, as Vav1 is required for optimal Ras and Rac signaling. Vav1 also binds the GTPase Dynamin 2 (Dyn2) through its C-terminal SH3 domain. This GTPase is also likely to be recruited into SLP-76 MC, as the association of Vav1 and Dyn2 is required for optimal T cell activation [Gomez, Hamann et al. 2005].

Additional enzymatic activities

Vav1 also binds other enzymes and may recruit them to SLP-76. However, these interactions have not been directly shown. For example, Vav1 binds the lysine methyltransferase Ezh2 through its CH domain [Hobert, Jallal et al. 1996]. While the target of the Ezh2 enzymatic activity in the cytoplasm remains unknown, this protein is required for actin cytoskeletal reorganization and optimal signaling [Su, Dobenecker et al. 2005]. An interesting possibility is that lysine methylation by Ezh2 opposes ubiquitinylation by c-Cbl by modifying lysine residues on LAT such that they are unable to be ubiquitinated [Balagopalan, Barr et al. 2007]. This could prevent the ubiquitin-dependent movement and internalization of SLP-76 MC. In this manner, Ezh2 may prevent the internalization and down-regulation of signaling complexes to promote T cell activation. Vav1 also binds to p67phox through its DH domain [Ming, Li et al. 2007]. p67(phox) is a Rac-dependent mediator of reactive oxygen species (ROS) generation; its interaction with Vav1 enhances its own activity as well as the GEF activity of Vav1. In addition, Vav1 has been implicated in (ROS) generation in macrophages following Toll-like receptor (TLR) stimulation [Miletic, Graham et al. 2007]. ROS generation is also required for optimal T cell signaling [Williams and Kwon 2004], which could rely on the activities of Vav1 and p67(phox) within SLP-76 MC.

8.1.3 Microcluster persistence is required for T cell activation

To date, I have not observed optimal T cell activation in the absence of persistent signaling microclusters. This shows that SLP-76 MC formation and persistence are closely correlated with efficient T cell signaling. However, fully persistent SLP-76 MC may not be required for every step in the TCR signaling cascade. I observed tyrosine

phosphorylation (albeit reduced) in the Vav1 L213A mutant, which reduced SLP-76 MC persistence (Figure 44). However, this same mutant was unable to mediate intracellular calcium flux (Figure 42), one of the later events in SLP-76 MC function. The ΔCH mutant does not support calcium elevations (Figure 54), but nevertheless becomes phosphorylated following TCR stimulation (Figure 59). I can therefore infer that Vav1 phosphorylation temporally precedes calcium flux. Thus short-lived microclusters may support early events in T cell activation, but are unable to mediate optimal TCR signaling, consistent with the kinetic segregation model.

8.2 Microclusters as a hub of enzymatic activity

8.2.1 MC persistence contributes to activation of constituent proteins

Phosphorylation of Vav1 is critical for potentiating its enzymatic activity and for optimal T cell signaling. I found that those mutations that prevent Vav1 from entering SLP-76 MC also prevent its phosphorylation (Figure 33). This is a critical step in mediating Vav1 function, as the Δ323 mutant, which possesses the appropriate effector domains to mediate calcium flux and CD69 upregulation, can perform neither of these functions in the absence of appropriate localization to and phosphorylation within SLP-76 MC. Following TCR stimulation, Vav1 enters SLP-76 MC that form adjacent to ZAP-70-containing TCR microclusters (Figure 14). These data suggest that Vav1 recruitment into SLP-76 MC places it in close proximity to its upstream kinase, facilitating its phosphorylation. In addition, PLCγ1 is phosphorylated within SLP-76 MC [Braiman, Barda-Saad et al. 2006]. These data are consistent with a model in which recruitment to SLP-76 MC facilitates the activation of various effector molecules.

8.2.2 Vav1 performs its enzymatic activity within MC

Since Vav1 phosphorylation alters the structure of Vav1 and permits the accessibility of the DH domain to GTPases, I hypothesized that Vav1 performs its enzymatic activity within SLP-76 MC. I found that Vav1 colocalizes with its target GTPases Rac1 and RhoG within SLP-76 MC (Figure 45 and 46). However, only the dominant-negative forms of these GTPases strongly colocalized with Vav1. One explanation for this result is that Vav1 only has high affinity for the inactive form of the GTPase. Once activated within SLP-76 MC, the GTPase no longer has high affinity for Vav1 and leaves the SLP-76 MC to mediate downstream signaling.

These data are consistent with a model in which the recruitment of effectors into SLP-76 MC precedes and is required for their activation. In a broader context, the data presented in this section indicate that the SLP-76 MC acts as a hub of enzymatic activity. Recruitment into SLP-76 MC facilitates the activation of effectors such as Vav1, which allows them to transduce signals from the TCR.

8.3 Microcluster movement and tethering to cytoskeleton

8.3.1 MC as adhesion sites and the significance of inward movement

Several lines of evidence suggest that the centralized movement of SLP-76 is a mechanism to down-modulate their signaling capability. First, co-ligation of the TCR with the costimulatory molecule VCAM prevents the inward movement of SLP-76 MC and retains them in the periphery of the cell, where they remain highly tyrosine phosphorylated [Nguyen, Sylvain et al. 2008]. Second, following their formation and

translocation, LAT-containing microclusters are internalized and degraded in a c-Cbl-dependent manner [Balagopalan, Barr et al. 2007]. While our imaging system is not amenable to detecting internalization (axial resolution 1-2μm), experiments using Total Internal Reflection Fluorescence (TIRF – axial resolution ~200nm) suggest that SLP-76 MC are internalized as they reach the center of the contact, which could lead to their degradation and loss of signaling capacity [Barr, Balagopalan et al. 2006]. Finally, preventing SLP-76 MC movement with a physical barrier augmented T cell responses [Mossman, Campi et al. 2005].

SLP-76 MC are formed at the tight junction between a T cell and a stimulatory surface [Bunnell, Hong et al. 2002] and contain several proteins required for dynamic rearrangement of the cytoskeleton [Billadeau, Nolz et al. 2007]. In addition, these structures adhere tightly to stimulatory surfaces and resist disruption by physical forces (Figure 58). Therefore, I propose that SLP-76 MC are the sites of tight adhesion between T cells and their targets. In addition, cytoskeletal reorganization initiated by microcluster components may be required for cell spreading to increase TCR ligation or to adhere more tightly to a target cell. When I observe inward movement of SLP-76 MC, these structures are moving away from upstream kinases (Figure 14) and phosphorylation is lost. SLP-76 MC movement requires the inward flow of the actin cytoskeleton [Ilani, Vasiliver-Shamis et al. 2009; Nguyen, Sylvain et al. 2008]; either increasing or decreasing the speed of retrograde actin flow correlates with changes in the speed of SLP-76 MC movement (Figure 57 and [Nguyen, Sylvain et al. 2008]). Since SLP-76 MC associate with receptor-proximal, immobile structures and with the cytoskeleton, they are

uniquely positioned to act as a molecular clutch, distributing forces between the mobile cytoskeleton and the immobile receptor. One prediction from this model is that the retrograde actin flow will be greater in cells with less persistent SLP-76 MC, since these adhesive structures will be unable to resist inward flow.

8.3.2 Requirements and mechanism of MC movement

The centralized movement of SLP-76 MC requires both the actin and microtubule cytoskeletons [Bunnell, Hong et al. 2002; Nguyen, Sylvain et al. 2008]. In addition, the movement of the motor protein myosin II is involved in SLP-76 MC translocation [Ilani, Vasiliver-Shamis et al. 2009]. Therefore, the movement of SLP-76 MC may be dependent upon tethering the microcluster to the cytoskeleton or to cytoskeletal motors. The SLP-76 MC components Vav1 and ADAP bind myosin II and dynein, respectively, potentially providing a direct link from the microcluster to cytoskeletal motors [Combs, Kim et al. 2006; Lee, Choi et al. 2010]. However, the importance of these interactions for SLP-76 MC movement has not been shown. The Vav-myosin interaction seems to be mainly involved in regulation of the Vav1 GEF activity. Alternatively, Vav1 could mediate SLP-76 MC movement directly by tethering to the cytoskeleton, or indirectly by stabilizing actin-binding proteins within the microcluster. One potential mechanism for Vav1 to directly support SLP-76 MC movement could be through cytoskeletal association through its polybasic region (Figure 61), which shares homology with the actin-binding protein villin [Friederich, Vancompernolle et al. 1992]. Other potential links between the SLP-76 MC and the cytoskeleton are shown in Figure 64.

It is not yet clear how SLP-76 MC translocate from the periphery of the contact to the center. Unpublished data from the Bunnell lab shows that myosin II filaments form fibers that connect SLP-76 MC, but that SLP-76 MC also move in along microtubule 'tracks.' Therefore, myosin contractions may provide the force required, while the microtubule filaments guide the direction of movement. SLP-76 MC components may associate with a specific motor protein or complex of proteins that could link them to the cytoskeleton and provide motive force. Alternatively, SLP-76 MC components may bind directly to actin filaments and be carried in along with retrograde actin flow. This retrograde flow may be regulated by the contraction of myosin in the lamellum, which is connected to branched actin networks in the lamellipodium [Cai, Biais et al. 2006; Ponti, Machacek et al. 2004]. Whether motor proteins are directly bound to SLP-76 MC components or not, the speed of retrograde flow influences the speed of microcluster movement (Figure 56-57), supporting the hypothesis that SLP-76 MC are tethered to the cytoskeleton and that the forces generated by inward actin flow and myosin contribute to microcluster movement (Figure 64). When costimulatory signals inhibit SLP-76 MC movement, they also slow retrograde actin flow, though this does not address whether decreased retrograde flow is the cause or symptom of decreased microcluster movement [Nguyen, Sylvain et al. 2008]. To address this issue, I propose observing the speed of retrograde actin flow under conditions of persistent or non-persistent SLP-76 MC. These conditions could be achieved using the existing JV.SC cell line and transiently expressing either mYFP or WT Vav1.mYFP. If SLP-76 MC inhibit inward actin flow by acting as a molecular clutch, then persistent SLP-76 MC should slow the retrograde actin flow. If,

however, SLP-76 MC are completely anchored to the cytoskeleton, their persistence will have no effect on the speed of actin.

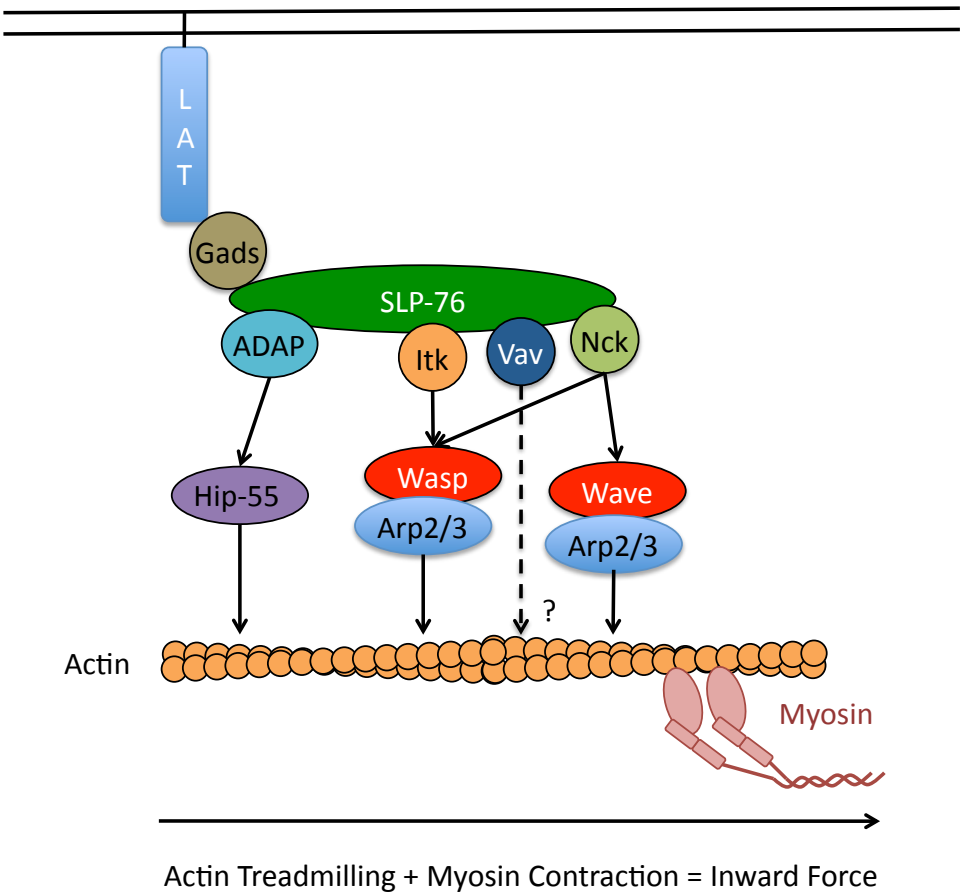

Figure 64: Potential links between SLP-76 MC and the actin cytoskeleton

Itk and Nck bind to the actin regulatory proteins WASP and Wave. The adaptor protein ADAP binds to SLP-76 and to the actin-binding protein Hip-55. Finally, the Vav1 polybasic region (Figure 61) may function as an actin-binding motif and could help tether the microcluster to the actin meshwork. Movement of SLP-76 MC requires dynamic reorganization of the actin cytoskeleton and could be driven by both actin treadmilling and myosin contractions.

8.3.3 Vav1 is required for movement

Vav1 deficient cells form short-lived SLP-76 MC that are also immobile. The defect in SLP-76 MC movement is unlikely to be a secondary defect to the lack of persistence since the N3*C3* mutant, which does not persist, is nevertheless mobile and initially moves comparably to WT Vav1. This suggests that Vav1 drives SLP-76 movement by linking microcluster components (directly or indirectly) to the cytoskeleton or to a motor complex, since dynamic actin rearrangement and the motor protein myosin II are required for SLP-76 MC movement [Ilani, Vasiliver-Shamis et al. 2009; Nguyen, Sylvain et al. 2008; Varma, Campi et al. 2006]. Vav1 binds to several proteins that could mediate the actin rearrangements necessary for SLP-76 MC movement, such as Ezh2, which is required for actin polymerization [Su, Dobenecker et al. 2005] and Dynamin2, which is also required for actin polymerization as well as receptor internalization [Gomez, Hamann et al. 2005]. In addition, the actin-regulatory proteins WASP and WAVE2 may be recruited into SLP-76 MC through their interaction with Nck, which binds to the N-terminal tyrosines of SLP-76 along with Vav1 [Jordan, Sadler et al. 2006]. Although Vav1 binds Rac1, an activator of WAVE2 [Billadeau, Nolz et al. 2007], this interaction is unlikely to drive SLP-76 MC movement, as GEF-inactivating mutations of Vav1 did not perturb the inward movement of microclusters. Instead, our CD69 upregulation data suggest that the Vav1 GEF functions in MAPK pathways to activate transcription factors. Nevertheless, it would be interesting to observe actin dynamics in Vav1 deficient cells using our imaging system, to see whether actin dynamics, specifically at the periphery of the contact, are affected by the absence of Vav1.

9 References

1. Abraham, R. T. and A. Weiss 2004 Jurkat T cells and development of the T-cell receptor signalling paradigm. *Nat Rev Immunol* 4(4): 301-8.
2. Acuto, O., V. Di Bartolo and F. Michel 2008 Tailoring T-cell receptor signals by proximal negative feedback mechanisms. *Nat Rev Immunol* 8(9): 699-712.
3. Aghazadeh, B., W. E. Lowry, X. Y. Huang and M. K. Rosen 2000 Structural basis for relief of autoinhibition of the Dbl homology domain of proto-oncogene Vav by tyrosine phosphorylation. *Cell* 102(5): 625-33.
4. Allen, P. M. and E. R. Unanue 1984 Differential requirements for antigen processing by macrophages for lysozyme-specific T cell hybridomas. *J Immunol* 132(3): 1077-9.
5. Altan-Bonnet, G. and R. N. Germain 2005 Modeling T cell antigen discrimination based on feedback control of digital ERK responses. *PLoS Biol* 3(11): e356.
6. Amarasinghe, G. K. and M. K. Rosen 2005 Acidic region tyrosines provide access points for allosteric activation of the autoinhibited Vav1 Dbl homology domain. *Biochemistry* 44(46): 15257-68.
7. Arudchandran, R., M. J. Brown, M. J. Peirce, J. S. Song, J. Zhang, R. P. Siraganian, U. Blank and J. Rivera 2000 The Src homology 2 domain of Vav is required for its compartmentation to the plasma membrane and activation of c-Jun NH(2)-terminal kinase 1. *J Exp Med* 191(1): 47-60.
8. Astoul, E., C. Edmunds, D. A. Cantrell and S. G. Ward 2001 PI 3-K and T-cell activation: limitations of T-leukemic cell lines as signaling models. *Trends Immunol* 22(9): 490-6.
9. Balagopalan, L., V. A. Barr, C. L. Sommers, M. Barda-Saad, A. Goyal, M. S. Isakowitz and L. E. Samelson 2007 c-Cbl-mediated regulation of LAT-nucleated signaling complexes. *Mol Cell Biol* 27(24): 8622-36.
10. Balamuth, F., D. Leitenberg, J. Unternaehrer, I. Mellman and K. Bottomly 2001 Distinct patterns of membrane microdomain partitioning in Th1 and th2 cells. *Immunity* 15(5): 729-38.
11. Barda-Saad, M., A. Braiman, R. Titerence, S. C. Bunnell, V. A. Barr and L. E. Samelson 2005 Dynamic molecular interactions linking the T cell antigen receptor to the actin cytoskeleton. *Nat Immunol* 6(1): 80-9.
12. Barda-Saad, M., N. Shirasu, M. H. Pauker, N. Hassan, O. Perl, A. Balbo, H. Yamaguchi, J. C. Houtman, E. Appella, P. Schuck and L. E. Samelson 2010 Cooperative interactions at the SLP-76 complex are critical for actin polymerization. *Embo J* 29(14): 2315-28.
13. Barr, V. A., L. Balagopalan, M. Barda-Saad, R. Polishchuk, H. Boukari, S. C. Bunnell, K. M. Bernot, Y. Toda, R. Nossal and L. E. Samelson 2006 T-cell antigen receptor-induced signaling complexes: internalization via a cholesterol-dependent endocytic pathway. *Traffic* 7(9): 1143-62.

14. Beach, D., R. Gonen, Y. Bogin, I. G. Reischl and D. Yablonski 2007 Dual role of SLP-76 in mediating T cell receptor-induced activation of phospholipase C-gamma1. *J Biol Chem* 282(5): 2937-46.
15. Bezman, N. A., L. Lian, C. S. Abrams, L. F. Brass, M. L. Kahn, M. S. Jordan and G. A. Koretzky 2008 Requirements of SLP76 tyrosines in ITAM and integrin receptor signaling and in platelet function in vivo. *J Exp Med* 205(8): 1775-88.
16. Billadeau, D. D. 2000 Specific Subdomains of Vav Differentially Affect T Cell and NK Cell Activation. *J Immunol*(164): 3971-3981.
17. Billadeau, D. D., J. C. Nolz and T. S. Gomez 2007 Regulation of T-cell activation by the cytoskeleton. *Nat Rev Immunol* 7(2): 131-43.
18. Braiman, A., M. Barda-Saad, C. L. Sommers and L. E. Samelson 2006 Recruitment and activation of PLCgamma1 in T cells: a new insight into old domains. *Embo J* 25(4): 774-84.
19. Brossard, C., V. Feuillet, A. Schmitt, C. Randriamampita, M. Romao, G. Raposo and A. Trautmann 2005 Multifocal structure of the T cell - dendritic cell synapse. *Eur J Immunol* 35(6): 1741-53.
20. Bunnell, S. C., M. Diehn, M. B. Yaffe, P. R. Findell, L. C. Cantley and L. J. Berg 2000 Biochemical interactions integrating Itk with the T cell receptor-initiated signaling cascade. *J Biol Chem* 275(3): 2219-30.
21. Bunnell, S. C., D. I. Hong, J. R. Kardon, T. Yamazaki, C. J. McGlade, V. A. Barr and L. E. Samelson 2002 T cell receptor ligation induces the formation of dynamically regulated signaling assemblies. *J Cell Biol* 158(7): 1263-75.
22. Bunnell, S. C., V. Kapoor, R. P. Trible, W. Zhang and L. E. Samelson 2001 Dynamic actin polymerization drives T cell receptor-induced spreading: a role for the signal transduction adaptor LAT. *Immunity* 14(3): 315-29.
23. Bunnell, S. C., A. L. Singer, D. I. Hong, B. H. Jacque, M. S. Jordan, M. C. Seminario, V. A. Barr, G. A. Koretzky and L. E. Samelson 2006 Persistence of cooperatively stabilized signaling clusters drives T-cell activation. *Mol Cell Biol* 26(19): 7155-66.
24. Burroughs, N. J., Z. Lazic and P. A. van der Merwe 2006 Ligand detection and discrimination by spatial relocalization: A kinase-phosphatase segregation model of TCR activation. *Biophys J* 91(5): 1619-29.
25. Bustelo, X. R. 2001 Vav proteins, adaptors and cell signaling. *Oncogene* 20(44): 6372-81.
26. Cai, Y., N. Biais, G. Giannone, M. Tanase, G. Jiang, J. M. Hofman, C. H. Wiggins, P. Silberzan, A. Buguin, B. Ladoux and M. P. Sheetz 2006 Nonmuscle myosin IIA-dependent force inhibits cell spreading and drives F-actin flow. *Biophys J* 91(10): 3907-20.
27. Campi, G., R. Varma and M. L. Dustin 2005 Actin and agonist MHC-peptide complex-dependent T cell receptor microclusters as scaffolds for signaling. *J Exp Med* 202(8): 1031-6.
28. Cao, Y. 2007 The Calponin Homology Domain of Vav1 Associates with Calmodulin and Is Prerequisite to T cell Antigen Receptor-induced Calcium Release in Jurkat T Lymphocytes. *J Biol Chem* 282(32): 23737-23744.

29. Cao, Y., E. M. Janssen, A. W. Duncan, A. Altman, D. D. Billadeau and R. T. Abraham 2002 Pleiotropic defects in TCR signaling in a Vav-1-null Jurkat T-cell line. *Embo J* 21(18): 4809-19.
30. Castellanos, M. C., C. Munoz, M. C. Montoya, E. Lara-Pezzi, M. Lopez-Cabrera and M. O. de Landazuri 1997 Expression of the leukocyte early activation antigen CD69 is regulated by the transcription factor AP-1. *J Immunol* 159(11): 5463-73.
31. Castresana, J. and M. Saraste 1995 Does Vav bind to F-actin through a CH domain? *FEBS Lett* 374(2): 149-51.
32. Chen, I. J., H. L. Chen and M. Demetriou 2007 Lateral compartmentalization of T cell receptor versus CD45 by galectin-N-glycan binding and microfilaments coordinate basal and activation signaling. *J Biol Chem* 282(48): 35361-72.
33. Clements, J. L., B. Yang, S. E. Ross-Barta, S. L. Eliason, R. F. Hrstka, R. A. Williamson and G. A. Koretzky 1998 Requirement for the leukocyte-specific adapter protein SLP-76 for normal T cell development. *Science* 281(5375): 416-9.
34. Combs, J., S. J. Kim, S. Tan, L. A. Ligon, E. L. Holzbaur, J. Kuhn and M. Poenie 2006 Recruitment of dynein to the Jurkat immunological synapse. *Proc Natl Acad Sci U S A* 103(40): 14883-8.
35. Costello, P. S., A. E. Walters, P. J. Mee, M. Turner, L. F. Reynolds, A. Prisco, N. Sarner, R. Zamoyska and V. L. Tybulewicz 1999 The Rho-family GTP exchange factor Vav is a critical transducer of T cell receptor signals to the calcium, ERK, and NF-kappaB pathways. *Proc Natl Acad Sci U S A* 96(6): 3035-40.
36. Crespo, P., K. E. Schuebel, A. A. Ostrom, J. S. Gutkind and X. R. Bustelo 1997 Phosphotyrosine-dependent activation of Rac-1 GDP/GTP exchange by the vav proto-oncogene product. *Nature* 385(6612): 169-72.
37. Davis, M. M., J. J. Boniface, Z. Reich, D. Lyons, J. Hampl, B. Arden and Y. Chien 1998 Ligand recognition by alpha beta T cell receptors. *Annu Rev Immunol* 16: 523-44.
38. Davis, S. J. and P. A. van der Merwe 2006 The kinetic-segregation model: TCR triggering and beyond. *Nat Immunol* 7(8): 803-9.
39. Dittel, B. N., I. Stefanova, R. N. Germain and C. A. Janeway, Jr. 1999 Cross-antagonism of a T cell clone expressing two distinct T cell receptors. *Immunity* 11(3): 289-98.
40. Dombroski, D., R. A. Houghtling, C. M. Labno, P. Precht, A. Takesono, N. J. Caplen, D. D. Billadeau, R. L. Wange, J. K. Burkhardt and P. L. Schwartzberg 2005 Kinase-independent functions for Itk in TCR-induced regulation of Vav and the actin cytoskeleton. *J Immunol* 174(3): 1385-92.
41. Douglass, A. D. and R. D. Vale 2005 Single-molecule microscopy reveals plasma membrane microdomains created by protein-protein networks that exclude or trap signaling molecules in T cells. *Cell* 121(6): 937-50.
42. Dustin, M. L. 2008 Hunter to gatherer and back: immunological synapses and kinapses as variations on the theme of amoeboid locomotion. *Annu Rev Cell Dev Biol* 24: 577-96.
43. Fang, N. and G. A. Koretzky 1999 SLP-76 and Vav function in separate, but overlapping pathways to augment interleukin-2 promoter activity. *J Biol Chem* 274(23): 16206-12.

44. Fischer, K. D., Y. Y. Kong, H. Nishina, K. Tedford, L. E. Marengere, I. Kozieradzki, T. Sasaki, M. Starr, G. Chan, S. Gardener, M. P. Nghiem, D. Bouchard, M. Barbacid, A. Bernstein and J. M. Penninger 1998 Vav is a regulator of cytoskeletal reorganization mediated by the T-cell receptor. *Curr Biol* 8(10): 554-62.
45. Fooksman, D. R., S. Vardhana, G. Vasiliver-Shamis, J. Liese, D. A. Blair, J. Waite, C. Sacristan, G. D. Victora, A. Zanin-Zhorov and M. L. Dustin 2009 Functional anatomy of T cell activation and synapse formation. *Annu Rev Immunol* 28: 79-105.
46. Friederich, E., K. Vancompernolle, C. Huet, M. Goethals, J. Finidori, J. Vandekerckhove and D. Louvard 1992 An actin-binding site containing a conserved motif of charged amino acid residues is essential for the morphogenic effect of villin. *Cell* 70(1): 81-92.
47. Fujikawa, K., A. V. Miletic, F. W. Alt, R. Faccio, T. Brown, J. Hoog, J. Fredericks, S. Nishi, S. Mildiner, S. L. Moores, J. Brugge, F. S. Rosen and W. Swat 2003 Vav1/2/3-null mice define an essential role for Vav family proteins in lymphocyte development and activation but a differential requirement in MAPK signaling in T and B cells. *J Exp Med* 198(10): 1595-608.
48. George, A. J., J. Stark and C. Chan 2005 Understanding specificity and sensitivity of T-cell recognition. *Trends Immunol* 26(12): 653-9.
49. Gomez, T. S., M. J. Hamann, S. McCarney, D. N. Savoy, C. M. Lubking, M. P. Heldebrant, C. M. Labno, D. J. McKean, M. A. McNiven, J. K. Burkhardt and D. D. Billadeau 2005 Dynamin 2 regulates T cell activation by controlling actin polymerization at the immunological synapse. *Nat Immunol* 6(3): 261-70.
50. Gonen, R., D. Beach, C. Ainey and D. Yablonski 2005 T cell receptor-induced activation of phospholipase C-gamma1 depends on a sequence-independent function of the P-I region of SLP-76. *J Biol Chem* 280(9): 8364-70.
51. Goodnow, C. C., J. Sprent, B. Fazekas de St Groth and C. G. Vinuesa 2005 Cellular and genetic mechanisms of self tolerance and autoimmunity. *Nature* 435(7042): 590-7.
52. Grakoui, A., S. K. Bromley, C. Sumen, M. M. Davis, A. S. Shaw, P. M. Allen and M. L. Dustin 1999 The immunological synapse: a molecular machine controlling T cell activation. *Science* 285(5425): 221-7.
53. Groysman, M., I. Hornstein, A. Alcover and S. Katzav 2002 Vav1 and Ly-GDI two regulators of Rho GTPases, function cooperatively as signal transducers in T cell antigen receptor-induced pathways. *J Biol Chem* 277(51): 50121-30.
54. Groysman, M., C. S. Russek and S. Katzav 2000 Vav, a GDP/GTP nucleotide exchange factor, interacts with GDIs, proteins that inhibit GDP/GTP dissociation. *FEBS Lett* 467(1): 75-80.
55. Gulbins, E., K. M. Coggeshall, G. Baier, S. Katzav, P. Burn and A. Altman 1993 Tyrosine kinase-stimulated guanine nucleotide exchange activity of Vav in T cell activation. *Science* 260(5109): 822-5.
56. Han, J., B. Das, W. Wei, L. Van Aelst, R. D. Mosteller, R. Khosravi-Far, J. K. Westwick, C. J. Der and D. Broek 1997 Lck regulates Vav activation of members of the Rho family of GTPases. *Mol Cell Biol* 17(3): 1346-53.

57. Han, J., K. Luby-Phelps, B. Das, X. Shu, Y. Xia, R. D. Mosteller, U. M. Krishna, J. R. Falck, M. A. White and D. Broek 1998 Role of substrates and products of PI 3-kinase in regulating activation of Rac-related guanosine triphosphatases by Vav. *Science* 279(5350): 558-60.
58. Hobert, O., B. Jallal, J. Schlessinger and A. Ullrich 1994 Novel signaling pathway suggested by SH3 domain-mediated p95vav/heterogeneous ribonucleoprotein K interaction. *J Biol Chem* 269(32): 20225-8.
59. Hobert, O., B. Jallal and A. Ullrich 1996 Interaction of Vav with ENX-1, a putative transcriptional regulator of homeobox gene expression. *Mol Cell Biol* 16(6): 3066-73.
60. Hogquist, K. A., S. C. Jameson, W. R. Heath, J. L. Howard, M. J. Bevan and F. R. Carbone 1994 T cell receptor antagonist peptides induce positive selection. *Cell* 76(1): 17-27.
61. Houtman, J. C., H. Yamaguchi, M. Barda-Saad, A. Braiman, B. Bowden, E. Appella, P. Schuck and L. E. Samelson 2006 Oligomerization of signaling complexes by the multipoint binding of GRB2 to both LAT and SOS1. *Nat Struct Mol Biol* 13(9): 798-805.
62. Hu, K., L. Ji, K. T. Applegate, G. Danuser and C. M. Waterman-Storer 2007 Differential transmission of actin motion within focal adhesions. *Science* 315(5808): 111-5.
63. Huse, M., L. O. Klein, A. T. Girvin, J. M. Faraj, Q. J. Li, M. S. Kuhns and M. M. Davis 2007 Spatial and temporal dynamics of T cell receptor signaling with a photoactivatable agonist. *Immunity* 27(1): 76-88.
64. Ilani, T., G. Vasiliver-Shamis, S. Vardhana, A. Bretscher and M. L. Dustin 2009 T cell antigen receptor signaling and immunological synapse stability require myosin IIA. *Nat Immunol* 10(5): 531-9.
65. Irles, C., A. Symons, F. Michel, T. R. Bakker, P. A. van der Merwe and O. Acuto 2003 CD45 ectodomain controls interaction with GEMs and Lck activity for optimal TCR signaling. *Nat Immunol* 4(2): 189-97.
66. Irvine, D. J., M. A. Purbhoo, M. Krogsgaard and M. M. Davis 2002 Direct observation of ligand recognition by T cells. *Nature* 419(6909): 845-9.
67. Jordan, M. S., J. Sadler, J. E. Austin, L. D. Finkelstein, A. L. Singer, P. L. Schwartzberg and G. A. Koretzky 2006 Functional hierarchy of the N-terminal tyrosines of SLP-76. *J Immunol* 176(4): 2430-8.
68. Jordan, M. S., J. E. Smith, J. C. Burns, J. E. Austin, K. E. Nichols, A. C. Aschenbrenner and G. A. Koretzky 2008 Complementation in trans of altered thymocyte development in mice expressing mutant forms of the adaptor molecule SLP76. *Immunity* 28(3): 359-69.
69. Kaizuka, Y., A. D. Douglass, S. Vardhana, M. L. Dustin and R. D. Vale 2009 The coreceptor CD2 uses plasma membrane microdomains to transduce signals in T cells. *J Cell Biol* 185(3): 521-34.
70. Kaminuma, O., M. Deckert, C. Elly, Y. C. Liu and A. Altman 2001 Vav-Rac1-mediated activation of the c-Jun N-terminal kinase/c-Jun/AP-1 pathway plays a major role in stimulation of the distal NFAT site in the interleukin-2 gene promoter. *Mol Cell Biol* 21(9): 3126-36.

71. Kasri, N. N., K. Torok, A. Galione, C. Garnham, G. Callewaert, L. Missiaen, J. B. Parys and H. De Smedt 2006 Endogenously bound calmodulin is essential for the function of the inositol 1,4,5-trisphosphate receptor. *J Biol Chem* 281(13): 8332-8.
72. Katzav, S., D. Martin-Zanca and M. Barbacid 1989 vav, a novel human oncogene derived from a locus ubiquitously expressed in hematopoietic cells. *Embo J* 8(8): 2283-90.
73. Katzav, S., M. Sutherland, G. Packham, T. Yi and A. Weiss 1994 The protein tyrosine kinase ZAP-70 can associate with the SH2 domain of proto-Vav. *J Biol Chem* 269(51): 32579-85.
74. Krummel, M. F. and M. M. Davis 2002 Dynamics of the immunological synapse: finding, establishing and solidifying a connection. *Curr Opin Immunol* 14(1): 66-74.
75. Krummel, M. F., M. D. Sjaastad, C. Wulfing and M. M. Davis 2000 Differential clustering of CD4 and CD3zeta during T cell recognition. *Science* 289(5483): 1349-52.
76. Kuhne, M. R., G. Ku and A. Weiss 2000 A guanine nucleotide exchange factor-independent function of Vav1 in transcriptional activation. *J Biol Chem* 275(3): 2185-90.
77. Kumar, L., V. Pivniouk, M. A. de la Fuente, D. Laouini and R. S. Geha 2002 Differential role of SLP-76 domains in T cell development and function. *Proc Natl Acad Sci U S A* 99(2): 884-9.
78. Kupfer, A. and G. Dennert 1984 Reorientation of the microtubule-organizing center and the Golgi apparatus in cloned cytotoxic lymphocytes triggered by binding to lysable target cells. *J Immunol* 133(5): 2762-6.
79. Kupfer, A., T. R. Mosmann and H. Kupfer 1991 Polarized expression of cytokines in cell conjugates of helper T cells and splenic B cells. *Proc Natl Acad Sci U S A* 88(3): 775-9.
80. Lazer, G., L. Pe'er, V. Schapira, S. Richard and S. Katzav 2007 The association of Sam68 with Vav1 contributes to tumorigenesis. *Cell Signal* 19(12): 2479-86.
81. Lee, C. S., C. K. Choi, E. Y. Shin, M. A. Schwartz and E. G. Kim 2010 Myosin II directly binds and inhibits Dbl family guanine nucleotide exchange factors: a possible link to Rho family GTPases. *J Cell Biol* 190(4): 663-74.
82. Lee, K. H., A. R. Dinner, C. Tu, G. Campi, S. Raychaudhuri, R. Varma, T. N. Sims, W. R. Burack, H. Wu, J. Wang, O. Kanagawa, M. Markiewicz, P. M. Allen, M. L. Dustin, A. K. Chakraborty and A. S. Shaw 2003 The immunological synapse balances T cell receptor signaling and degradation. *Science* 302(5648): 1218-22.
83. Lee, K. H., A. D. Holdorf, M. L. Dustin, A. C. Chan, P. M. Allen and A. S. Shaw 2002 T cell receptor signaling precedes immunological synapse formation. *Science* 295(5559): 1539-42.
84. Lillemeier, B. F., J. R. Pfeiffer, Z. Surviladze, B. S. Wilson and M. M. Davis 2006 Plasma membrane-associated proteins are clustered into islands attached to the cytoskeleton. *Proc Natl Acad Sci U S A* 103(50): 18992-7.
85. Lin, J. and A. Weiss 2001 Identification of the minimal tyrosine residues required for linker for activation of T cell function. *J Biol Chem* 276(31): 29588-95.

86. Lin, J. and A. Weiss 2003 The tyrosine phosphatase CD148 is excluded from the immunologic synapse and down-regulates prolonged T cell signaling. *J Cell Biol* 162(4): 673-82.
87. Liu, H., M. A. Purbhoo, D. M. Davis and C. E. Rudd 2010 SH2 domain containing leukocyte phosphoprotein of 76-kDa (SLP-76) feedback regulation of ZAP-70 microclustering. *Proc Natl Acad Sci U S A* 107(22): 10166-71.
88. Lopez-Lago, M., H. Lee, C. Cruz, N. Movilla and X. R. Bustelo 2000 Tyrosine phosphorylation mediates both activation and downmodulation of the biological activity of Vav. *Mol Cell Biol* 20(5): 1678-91.
89. Lucas, B., I. Stefanova, K. Yasutomo, N. Dautigny and R. N. Germain 1999 Divergent changes in the sensitivity of maturing T cells to structurally related ligands underlies formation of a useful T cell repertoire. *Immunity* 10(3): 367-76.
90. Macian, F. 2005 NFAT proteins: key regulators of T-cell development and function. *Nat Rev Immunol* 5(6): 472-84.
91. Mario Gimona, K. D.-C., Wolfgang J. Kranewitter, Steven J. Winder 2002 Functional Plasticity of CH Domains. *FEBS Letters* 513(1): 98-106.
92. McKeithan, T. W. 1995 Kinetic proofreading in T-cell receptor signal transduction. *Proc Natl Acad Sci U S A* 92(11): 5042-6.
93. Mempel, T. R., S. E. Henrickson and U. H. Von Andrian 2004 T-cell priming by dendritic cells in lymph nodes occurs in three distinct phases. *Nature* 427(6970): 154-9.
94. Meuer, S. C., K. A. Fitzgerald, R. E. Hussey, J. C. Hodgdon, S. F. Schlossman and E. L. Reinherz 1983 Clonotypic structures involved in antigen-specific human T cell function. Relationship to the T3 molecular complex. *J Exp Med* 157(2): 705-19.
95. Miletic, A. V., D. B. Graham, V. Montgrain, K. Fujikawa, T. Kloeppel, K. Brim, B. Weaver, R. Schreiber, R. Xavier and W. Swat 2007 Vav proteins control MyD88-dependent oxidative burst. *Blood* 109(8): 3360-8.
96. Miletic, A. V., D. B. Graham, K. Sakata-Sogawa, M. Hiroshima, M. J. Hamann, S. Cemerski, T. Kloeppel, D. D. Billadeau, O. Kanagawa, M. Tokunaga and W. Swat 2009 Vav links the T cell antigen receptor to the actin cytoskeleton and T cell activation independently of intrinsic Guanine nucleotide exchange activity. *PLoS One* 4(8): e6599.
97. Miletic, A. V., K. Sakata-Sogawa, M. Hiroshima, M. J. Hamann, T. S. Gomez, N. Ota, T. Kloeppel, O. Kanagawa, M. Tokunaga, D. D. Billadeau and W. Swat 2006 Vav1 acidic region tyrosine 174 is required for the formation of T cell receptor-induced microclusters and is essential in T cell development and activation. *J Biol Chem* 281(50): 38257-65.
98. Miller, M. J., S. H. Wei, M. D. Cahalan and I. Parker 2003 Autonomous T cell trafficking examined in vivo with intravital two-photon microscopy. *Proc Natl Acad Sci U S A* 100(5): 2604-9.
99. Milstein, O., S. Y. Tseng, T. Starr, J. Llodra, A. Nans, M. Liu, M. K. Wild, P. A. van der Merwe, D. L. Stokes, Y. Reisner and M. L. Dustin 2008 Nanoscale increases in CD2-CD48-mediated intermembrane spacing decrease adhesion and reorganize the immunological synapse. *J Biol Chem* 283(49): 34414-22.

100. Ming, W., S. Li, D. D. Billadeau, L. A. Quilliam and M. C. Dinauer 2007 The Rac effector p67phox regulates phagocyte NADPH oxidase by stimulating Vav1 guanine nucleotide exchange activity. *Mol Cell Biol* 27(1): 312-23.
101. Monks, C. R., B. A. Freiberg, H. Kupfer, N. Sciaky and A. Kupfer 1998 Three-dimensional segregation of supramolecular activation clusters in T cells. *Nature* 395(6697): 82-6.
102. Mossman, K. D., G. Campi, J. T. Groves and M. L. Dustin 2005 Altered TCR signaling from geometrically repatterned immunological synapses. *Science* 310(5751): 1191-3.
103. Negishi, I., N. Motoyama, K. Nakayama, S. Senju, S. Hatakeyama, Q. Zhang, A. C. Chan and D. Y. Loh 1995 Essential role for ZAP-70 in both positive and negative selection of thymocytes. *Nature* 376(6539): 435-8.
104. Nguyen, K., N. R. Sylvain and S. C. Bunnell 2008 T cell costimulation via the integrin VLA-4 inhibits the actin-dependent centralization of signaling microclusters containing the adaptor SLP-76. *Immunity* 28(6): 810-21.
105. Nika, K., C. Soldani, M. Salek, W. Paster, A. Gray, R. Etzensperger, L. Fugger, P. Polzella, V. Cerundolo, O. Dushek, T. Hofer, A. Viola and O. Acuto 2010 Constitutively active Lck kinase in T cells drives antigen receptor signal transduction. *Immunity* 32(6): 766-77.
106. Nishida, M., K. Nagata, Y. Hachimori, M. Horiuchi, K. Ogura, V. Mandiyan, J. Schlessinger and F. Inagaki 2001 Novel recognition mode between Vav and Grb2 SH3 domains. *Embo J* 20(12): 2995-3007.
107. Ogura, K., K. Nagata, M. Horiuchi, E. Ebisui, T. Hasuda, S. Yuzawa, M. Nishida, H. Hatanaka and F. Inagaki 2002 Solution structure of N-terminal SH3 domain of Vav and the recognition site for Grb2 C-terminal SH3 domain. *J Biomol NMR* 22(1): 37-46.
108. Palmby, T. R., K. Abe and C. J. Der 2002 Critical role of the pleckstrin homology and cysteine-rich domains in Vav signaling and transforming activity. *J Biol Chem* 277(42): 39350-9.
109. Paul, W. E. and R. A. Seder 1994 Lymphocyte responses and cytokines. *Cell* 76(2): 241-51.
110. Pivniouk, V., E. Tsitsikov, P. Swinton, G. Rathbun, F. W. Alt and R. S. Geha 1998 Impaired viability and profound block in thymocyte development in mice lacking the adaptor protein SLP-76. *Cell* 94(2): 229-38.
111. Ponti, A., M. Machacek, S. L. Gupton, C. M. Waterman-Storer and G. Danuser 2004 Two distinct actin networks drive the protrusion of migrating cells. *Science* 305(5691): 1782-6.
112. Raab, M., A. J. da Silva, P. R. Findell and C. E. Rudd 1997 Regulation of Vav-SLP-76 binding by ZAP-70 and its relevance to TCR zeta/CD3 induction of interleukin-2. *Immunity* 6(2): 155-64.
113. Rabinowitz, J. D., C. Beeson, D. S. Lyons, M. M. Davis and H. M. McConnell 1996 Kinetic discrimination in T-cell activation. *Proc Natl Acad Sci U S A* 93(4): 1401-5.
114. Ramos-Morales, F., F. Romero, F. Schweighoffer, G. Bismuth, J. Camonis, M. Tortolero and S. Fischer 1995 The proline-rich region of Vav binds to Grb2 and Grb3-3. *Oncogene* 11(8): 1665-9.

115. Rapley, J., V. L. Tybulewicz and K. Rittinger 2008 Crucial structural role for the PH and C1 domains of the Vav1 exchange factor. *EMBO Rep* 9(7): 655-61.
116. Reynolds, L. F., C. de Bettignies, T. Norton, A. Beeser, J. Chernoff and V. L. Tybulewicz 2004 Vav1 transduces T cell receptor signals to the activation of the Ras/ERK pathway via LAT, Sos, and RasGRP1. *J Biol Chem* 279(18): 18239-46.
117. Reynolds, L. F., L. A. Smyth, T. Norton, N. Freshney, J. Downward, D. Kioussis and V. L. Tybulewicz 2002 Vav1 transduces T cell receptor signals to the activation of phospholipase C-gamma1 via phosphoinositide 3-kinase-dependent and -independent pathways. *J Exp Med* 195(9): 1103-14.
118. Rossman, K. L., C. J. Der and J. Sondek 2005 GEF means go: turning on RHO GTPases with guanine nucleotide-exchange factors. *Nat Rev Mol Cell Biol* 6(2): 167-80.
119. Rozdzial, M. M., C. M. Pleiman, J. C. Cambier and T. H. Finkel 1998 pp56Lck mediates TCR zeta-chain binding to the microfilament cytoskeleton. *J Immunol* 161(10): 5491-9.
120. Rudd, C. E., A. Taylor and H. Schneider 2009 CD28 and CTLA-4 coreceptor expression and signal transduction. *Immunol Rev* 229(1): 12-26.
121. Saveliev, A., L. Vanes, O. Ksionda, J. Rapley, S. J. Smerdon, K. Rittinger and V. L. Tybulewicz 2009 Function of the nucleotide exchange activity of vav1 in T cell development and activation. *Sci Signal* 2(101): ra83.
122. Schaeffer, E. M., J. Debnath, G. Yap, D. McVicar, X. C. Liao, D. R. Littman, A. Sher, H. E. Varmus, M. J. Lenardo and P. L. Schwartzberg 1999 Requirement for Tec kinases Rlk and Itk in T cell receptor signaling and immunity. *Science* 284(5414): 638-41.
123. Secrist, J. P., L. A. Burns, L. Karnitz, G. A. Koretzky and R. T. Abraham 1993 Stimulatory effects of the protein tyrosine phosphatase inhibitor, pervanadate, on T-cell activation events. *J Biol Chem* 268(8): 5886-93.
124. Seminario, M. C. and S. C. Bunnell 2008 Signal initiation in T-cell receptor microclusters. *Immunol Rev* 221: 90-106.
125. Shan, X., M. J. Czar, S. C. Bunnell, P. Liu, Y. Liu, P. L. Schwartzberg and R. L. Wange 2000 Deficiency of PTEN in Jurkat T cells causes constitutive localization of Itk to the plasma membrane and hyperresponsiveness to CD3 stimulation. *Mol Cell Biol* 20(18): 6945-57.
126. Shaner, N. C., R. E. Campbell, P. A. Steinbach, B. N. Giepmans, A. E. Palmer and R. Y. Tsien 2004 Improved monomeric red, orange and yellow fluorescent proteins derived from Discosoma sp. red fluorescent protein. *Nat Biotechnol* 22(12): 1567-72.
127. Siebenlist, U., K. Brown and E. Claudio 2005 Control of lymphocyte development by nuclear factor-kappaB. *Nat Rev Immunol* 5(6): 435-45.
128. Singer, A. L. and G. A. Koretzky 2002 Control of T cell function by positive and negative regulators. *Science* 296(5573): 1639-40.
129. Sloan-Lancaster, J. and P. M. Allen 1996 Altered peptide ligand-induced partial T cell activation: molecular mechanisms and role in T cell biology. *Annu Rev Immunol* 14: 1-27.

130. Stefanova, I., B. Hemmer, M. Vergelli, R. Martin, W. E. Biddison and R. N. Germain 2003 TCR ligand discrimination is enforced by competing ERK positive and SHP-1 negative feedback pathways. *Nat Immunol* 4(3): 248-54.
131. Stinchcombe, J. C., E. Majorovits, G. Bossi, S. Fuller and G. M. Griffiths 2006 Centrosome polarization delivers secretory granules to the immunological synapse. *Nature* 443(7110): 462-5.
132. Su, I. H., M. W. Dobenecker, E. Dickinson, M. Oser, A. Basavaraj, R. Marqueron, A. Viale, D. Reinberg, C. Wulfing and A. Tarakhovsky 2005 Polycomb group protein ezh2 controls actin polymerization and cell signaling. *Cell* 121(3): 425-36.
133. Treanor, B., D. Depoil, A. Gonzalez-Granja, P. Barral, M. Weber, O. Dushek, A. Bruckbauer and F. D. Batista 2010 The membrane skeleton controls diffusion dynamics and signaling through the B cell receptor. *Immunity* 32(2): 187-99.
134. Tuosto, L., F. Michel and O. Acuto 1996 p95vav associates with tyrosine-phosphorylated SLP-76 in antigen-stimulated T cells. *J Exp Med* 184(3): 1161-6.
135. Tybulewicz, V. L. 2005 Vav-family proteins in T-cell signalling. *Curr Opin Immunol* 17(3): 267-74.
136. Valitutti, S., M. Dessing, K. Aktories, H. Gallati and A. Lanzavecchia 1995 Sustained signaling leading to T cell activation results from prolonged T cell receptor occupancy. Role of T cell actin cytoskeleton. *J Exp Med* 181(2): 577-84.
137. Varma, R., G. Campi, T. Yokosuka, T. Saito and M. L. Dustin 2006 T cell receptor-proximal signals are sustained in peripheral microclusters and terminated in the central supramolecular activation cluster. *Immunity* 25(1): 117-27.
138. Veillette, A., S. Latour and D. Davidson 2002 Negative regulation of immunoreceptor signaling. *Annu Rev Immunol* 20: 669-707.
139. Vicente-Manzanares, M., X. Ma, R. S. Adelstein and A. R. Horwitz 2009 Non-muscle myosin II takes centre stage in cell adhesion and migration. *Nat Rev Mol Cell Biol* 10(11): 778-90.
140. Wakabayashi-Ito, N. and S. Nagata 1994 Characterization of the regulatory elements in the promoter of the human elongation factor-1 alpha gene. *J Biol Chem* 269(47): 29831-7.
141. Wang, X., A. Gjorloff-Wingren, M. Saxena, N. Pathan, J. C. Reed and T. Mustelin 2000 The tumor suppressor PTEN regulates T cell survival and antigen receptor signaling by acting as a phosphatidylinositol 3-phosphatase. *J Immunol* 164(4): 1934-9.
142. Wange, R. L. and L. E. Samelson 1996 Complex complexes: signaling at the TCR. *Immunity* 5(3): 197-205.
143. Whitehead, I. P., Q. T. Lambert, J. A. Glaven, K. Abe, K. L. Rossman, G. M. Mahon, J. M. Trzaskos, R. Kay, S. L. Campbell and C. J. Der 1999 Dependence of Dbl and Dbs transformation on MEK and NF-kappaB activation. *Mol Cell Biol* 19(11): 7759-70.
144. Williams, M. S. and J. Kwon 2004 T cell receptor stimulation, reactive oxygen species, and cell signaling. *Free Radic Biol Med* 37(8): 1144-51.
145. Wu, J., D. G. Motto, G. A. Koretzky and A. Weiss 1996 Vav and SLP-76 interact and functionally cooperate in IL-2 gene activation. *Immunity* 4(6): 593-602.

146. Ye, Z. S. and D. Baltimore 1994 Binding of Vav to Grb2 through dimerization of Src homology 3 domains. *Proc Natl Acad Sci U S A* 91(26): 12629-33.
147. Yokosuka, T. and T. Saito 2009 Dynamic regulation of T-cell costimulation through TCR-CD28 microclusters. *Immunol Rev* 229(1): 27-40.
148. Yokosuka, T., K. Sakata-Sogawa, W. Kobayashi, M. Hiroshima, A. Hashimoto-Tane, M. Tokunaga, M. L. Dustin and T. Saito 2005 Newly generated T cell receptor microclusters initiate and sustain T cell activation by recruitment of Zap70 and SLP-76. *Nat Immunol* 6(12): 1253-62.
149. Yoon, S. Y., W. S. Koh, M. K. Lee, Y. M. Park and M. Y. Han 1997 Dynamin II associates with Grb2 SH3 domain in Ras transformed NIH3T3 cells. *Biochem Biophys Res Commun* 234(3): 539-43.
150. Yu, B., I. R. Martins, P. Li, G. K. Amarasinghe, J. Umetani, M. E. Fernandez-Zapico, D. D. Billadeau, M. Machius, D. R. Tomchick and M. K. Rosen 2010 Structural and energetic mechanisms of cooperative autoinhibition and activation of Vav1. *Cell* 140(2): 246-56.
151. Yu, C. H., H. J. Wu, Y. Kaizuka, R. D. Vale and J. T. Groves 2010 Altered actin centripetal retrograde flow in physically restricted immunological synapses. *PLoS One* 5(7): e11878.
152. Zhang, W., R. P. Trible, M. Zhu, S. K. Liu, C. J. McGlade and L. E. Samelson 2000 Association of Grb2, Gads, and phospholipase C-gamma 1 with phosphorylated LAT tyrosine residues. Effect of LAT tyrosine mutations on T cell angigen receptor-mediated signaling. *J Biol Chem* 275(30): 23355-61.
153. Zugaza, J. L., M. A. Lopez-Lago, M. J. Caloca, M. Dosil, N. Movilla and X. R. Bustelo 2002 Structural determinants for the biological activity of Vav proteins. *J Biol Chem* 277(47): 45377-92.